UNIVERSITÄTSKLINIKUM HAMBURG-EPPENDORF

Klinik für Pädiatrische Hämatologie und Onkologie

Direktor

Prof. Dr. med. Stefan Rutkowski

Mutation analysis of the *DICER1* gene in Pleuropulmonary Blastoma

Dissertation

zur Erlangung des Grades eines Doktors der Medizin

an der Medizinischen Fakultät der Universität Hamburg

vorgelegt von:

Yannic Saathoff

aus Wilhelmshaven

Hamburg 2020

Angenommen von der

Medizinischen Fakultät der Universität Hamburg am: 13.08.2020

Veröffentlicht mit Genehmigung der

Medizinischen Fakultät der Universität Hamburg.

Prüfungsausschuss, der/die Vorsitzende:

Prof. Dr. Reinhard Schneppenheim

Prüfungsausschuss, zweite/r Gutachter/in:

Prof. Dr. Kerstin Kutsche

Table of contents

1 Introduction

1.1 Pleuropulmonary blastoma

The pleuropulmonary blastoma (PPB) is a rare highly aggressive sarcoma which derives from lung parenchyma and pleura and is predominantly found in children under 6 years of age. It was first described in 1988 by Manivel and colleagues in a series of 11 patients in which this tumor was characterized and differentiated from other known tumors like the (adult) pulmonary blastoma. Evidence suggests that the pleuropulmonary blastoma is at least in part associated with familial disease and also other related tumors. Most of the tumors are still thought to be sporadic with an interference of the *DICER1* gene, a gene involved with lung development. Outcome is relatively good but a tumor-progression must be prevented by aggressive therapy.

Notably essential for the collection of data, analysis, and care for the patients was the immediate foundation of the International PPB Registry (IPPBR) which was founded in 1988 and is a collaboration of several US-wide clinics (Stewart et al. 2014).

1.1.1 Epidemiology

As mentioned above, the pleuropulmonary blastoma is an extremely rare tumor although it still makes up 15% of all pulmonary tumors of childhood and is the most common primary pulmonary malignancy in children (Atlas of Neoplastic Pulmonary Disease, Dishop, P. 7). Despite intense studying of the tumor, there is little information about its incidence and number of reported cases vary as cases occur often only in singularity in different hospitals (Miniati et al. 2006, Priest et al. 2007). Furthermore, cases from the past continuously reviewed by experts steadily increase the number of total cases. Therefore, exact numbers concerning the incidence and total number of cases are not available but about 400 cases have been confirmed by the International Pulmonary Blastoma Registry since its inauguration in 1988 (Messinger et al. 2015). The *Children Cancer Registry of the Society of Pediatric Oncology and Hematology* (GPOH) in Kiel, Germany collected 18 tumor samples within a time span of about 30 years. A database of the National Registry of Childhood from the United Kingdom gathered 20 samples during

35 years (Slade et al. 2011). The IPPBR estimates that possibly ten to twenty cases per year occur in the United States (IPPBR, 24.02.2015, 11:28h) in approximately 4 million births and around 30-50 cases of type I and 40-60 of type II and III worldwide per year, maybe even less.

Studies have not shown a gender preference, unpublished data from the International PPB Registry suggest the female to male ratio being close to equal. Of 138 studied patients, 52% were female and almost 48% male (IPPBR, 07.01.2015, 12:16h). Still, as will be discussed in a later chapter, there is in fact a higher chance of females being affected when considering PPB-associated diseases. There is also no hint that specific ethnic groups have a higher incidence rate (Foulkes et al. 2014). The majority of patients is affected before they reach the age of six. Only about 5% are diagnosed later (Priest et al. 1997, Priest et al. 2009). Occurrence of other PPB-related manifestations may be higher though. There is one reported case of a 36-year-old patient with a histologically confirmed type II pleuropulmonary blastoma (Hill et al. 1999).

1.1.2 Etiology and pathophysiology

The mechanisms involving the genesis of the PPB are not fully understood and are still being investigated. It seems relatively clear however, that there is a sporadic form as well as a hereditary one. The latter of which might also appear as a familial tumor syndrome and seems to exert an autosomal dominant pattern of inheritance with a reduced penetrance (IPPBR, 06.01.2015, 15:56h, Seki et al. 2014). Therefore, children of affected individuals have a 50% chance of receiving the mutated gene. Penetrance describes the relationship between genotype and phenotype. A disease with reduced penetrance allows carriers of the affected gene to have a normal or more mildly affected phenotype. PPB has an estimated penetrance of about 15%, meaning that 85% of the cases which have a genetic predisposition will not have a clinical manifestation (Foulkes et al. 2014). However, the other PPB-related disorders may have a higher penetrance, especially those which are clinically less severe. There is currently no evidence-based exact percentage of penetrance, it might be as stated above about 15% or less. The penetrance of ‘silent’ clinical features such as renal cysts or thyroid nodules might be much higher without any

specific percentages being available (Foulkes et al. 2014, Brenneman et al. 2015 (revised 2018)).

Initially, it was thought that the genetic predisposition type would account for about 25% of all PPBs and the sporadic form subsequently for 75% (Priest et al. 1996), but recently the increase of number of cases and analysis suggested that about 38% of PPB cases are hereditary (Priest et al. 2009). Of course, these numbers might still be revised in the course of further studies as the number of analyzed cases increases. There are several families in which two or more family members had a pleuropulmonary blastoma.

So far, evidence has shown that the *DICER1* gene on chromosome 14 is at least in part involved in the genesis of the tumor. Generally, it can be said that the genetic model involves a succession of steps leading to the PPB (Priest et al. 1997, Hill et al. 2009). Yet, it is unknown if other factors might play a pathophysiological role in the process of this tumor. A detailed discussion of the aspect of *DICER1* will follow.

1.1.3 Signs and symptoms

Children with PPB type I (cystic) often present with respiratory symptoms resulting from rupturing lung cysts and therefore pneumothorax or distress from the cysts themselves. Analysis of cases showed that approximately 50% (range from 20 up to 65% depending on the type) of children initially presented with pneumothorax (Messinger et al. 2014, Hill et al. 2008). Types II (cystic and solid) and III (solid) frequently are misdiagnosed as pneumonia due to presentation with fever, dyspnea, and productive or non-productive cough coupled with chest or abdominal pain. Respiratory symptoms may be severe depending on pleural effusion (possibly empyema), anorexia from tumor and/or increased breathing work, malaise, and pneumothorax (IPPBR, 07.01.2015, 12:16h, Hill et al. 2008, Priest et al. 2009, Schultz et al. 2014).

1.1.4 Diagnosis and differential diagnosis

Due to the extreme rarity of this neoplasm the pleuropulmonary blastoma is seldom considered as a possible diagnosis for an affected child. Usually the diagnosis is made

after resection of the cysts or the cyst-tumor conglomerate when viewed at histologically (Miniati et al. 2006). In chest x-ray pneumothorax, mediastinal shift, opacification resulting from pulmonary, pleural, or mediastinal masses may be seen (Manivel et al. 1988, IPBBR, 25.02.215, 12:21h). CT or MRI also show cystic or solid masses. Pleural puncture and following cytology only yield useful hints in case of a tumor rupture (Schultz et al. 2014). Serology delivers no conclusive evidence of a PPB. Results of fine needle aspiration have been mixed and there is no clear reliability in terms of diagnosis as the tumor tissue is sometimes very heterogeneous and might contain parts of complete necrosis (IPPBR, 25.02.2015, 12:19h, Priest et al. 2009). Cytological examination of pleural fluids is often negative as well (Schultz et al, 2014).

Definite diagnosis is only possible through microscopic evaluation and the criteria given below. Fitting patient age, location of the tumor in the lung and other findings like cystic nephroma which is the most common associated finding related to PPB (Boman et al. 2006, Slade et al. 2011) could further give hints to the diagnosis. The following table gives an overview over the median age at diagnosis:

	Overall	**Type I**	**Type II**	**Type III**
Published Registry Series N=50				
Age Range (months)	0-147	0-28	15-64	31-147
Median Age (months)	38	**10**	**34**	**44**
Unpublished Registry Series N=128				
Age Range (months)	0-431	0-32	6-431	15-147
Median Age (months)		**10**	**36**	**44**

Table 1.1: Age of diagnosis of PPB. www.ppbregistry.org 07.01.2015, 12:16h, Priest et al. 1997.

A conclusion drawn from data presented in table 1.1 could be that solid pleuropulmonary blastoma (type III) is an exception in children that are younger than one and a half years and in children who are older than seven years (Schultz et al. 2014). This is also supported by the fact that about 94% of PPB cases were diagnosed in children under 72 months

(Priest et al. 2009). Still, a diagnosis has to be made as early as possible because of the huge impact of the progression of the disease. Progression to malignant disease from cysts might take about 2-5 years. PPB type II and III development ranges from a few weeks until 8 years (IPPBR, 07.01.2015, 12:15h). Staging involves thoracic and abdominal CT, head MRI, and bone scan.

Differential diagnosis especially in imaging studies but also in gross and clinical manifestation are other first and foremost pulmonary malformations. These include congenital pulmonary adenomatoid malformation (CPAM, previously named CCAM - congenital cystic adenomatoid malformation), fetal lung interstitial tumor (FLIT), bronchogenic cysts, bronchial atresia, congenital lobar emphysema, bronchopulmonary sequestration, hybrid lung malformations and congenital diaphragmatic hernia (Miniati et al. 2006, Ali Khan et al. 2014, Atlas of Neoplastic Pulmonary Disease, Dishop, P. 7). In patients younger than 18 months with solid tumors, malignancies like fetal lung interstitial tumor and congenital peribronchial myofibroblastic tumor are more likely (Schultz et al. 2014, Dishop et al. 2010). Especially differentiation between CPAM type 4 and PPB cystic lesions has proven difficult as they even might be the same entity or should at least prompt a cautions study to avoid overlooking of a PPB with negative effect on the prognosis of the patient (MacSweeney et al. 2003, Hill and Dehner, 2004). Radiological screening in risk-patients with *DICER1*-mutations is possible and has successfully been done previously (Foulkes et al. 2014).

Further screening and other possible novel diagnostic methods are to be found in the discussion.

1.1.5 Histopathology and PPB types

The pleuropulmonary blastoma is a high-grade embryonal rhabdomyosarcoma which can originate from the pleura, the lung or both simultaneously (Priest et al. 1996, Online Mendelian Inheritance in Man (OMIM) #601200, Schultz et al. 2014). The blastoma aspect of the tumor refers to the similarity of the tumorous tissue to tissue in fetal and embryonic development, especially in the first trimester. It can be seen as the pulmonary equivalent of other pediatric tumors like Wilms Tumor (WT), hepatoblastoma, embryonal

rhabdomyosarcoma or others and develops during fetal lung development (Hill et al. 2009, Priest et al. 2009). It is made up of mesenchymal cells as a phenotype having a low level of differentiation. Additionally, it shows epithelial tissue, which is histopathological not abnormal and seems to be trapped within the mesenchymal tumor tissue (Manivel et al. 1988, Priest et al. 1996, Hill et al. 2009). The mesenchymal neoplastic tissue forms a so called 'cambium' layer beneath the non-malignant epithelium in the cyst walls, giving it a distinct appearance among pediatric tumors (Priest et al. 1996, IPPBR, 07.01.2015, 12:15h).

Immunohistochemical staining shows a lack of DICER1 in epithelial cells, mesenchymal cells however appear to contain DICER1. Vimentin and desmin are often positive (Schultz et al. 2014). As stated above, there are four types of PPB which are largely based on the gross manifestation of the tumor. These appear to progress from one to another in a chronological order in the sense of a biological continuum beginning from lung cysts. This makes up an important general concept of PPB and this progression reflects in the types of this intrathoracic tumor (IPPBR, 07.01.2015, 12:15h, Atlas of Neoplastic Pulmonary Disease, Dishop, P. 7, Priest et al. 2009): **Type I** has cystic components entirely while **type II** consists of cystic parts as well as solid tumor tissue. **Type III** does not have any cystic aspects macroscopically and is completely solid. Still type III might show cyst-like spaces which result from tissue degradation and necrosis within the tumor. In addition to these three types, a fourth type evolved in 2006 as the IPPBR reviewed more and more PPB cases. **Type Ir** has a very similar appearance to type I and is characterized by a regression of the cysts or genetically pre-determined cysts and no malignant cells. This type has an estimated 8% chance for abnormal development. It is found in family members of affected patients from childhood to adulthood. Types II and III do not regress.

Four microscopic findings determine a solid tumor as a type II and III PPB (Schultz et al. 2014), which are in short:

1. Embryonal rhabdomyosarcoma tissue with specifically formed cells on a myxoid blue background
2. Blastemal pattern with cells having very little cytoplasm
3. Cartilaginous differentiation (fetal and high-grade malignant nodules)
4. Spindle cell sarcoma

Confirming the theorem of the succession of the PPB types, the median age of diagnosis increases with type accordingly. The median age for diagnosis of type I pleuropulmonary blastoma was 10 months, while for type II it was 34 months and for type III 44 months. In some cases, the pulmonary cysts were surveilled by imaging studies and consequently tumors containing solid aspects were detected after a certain amount of time. It is estimated, that about 10% of type I develop into types II and subsequently into III (IPPBR, 07.01.2015, 12:15h, Priest et al. 2006).

As documented in case reviews, the lung cysts can be uni-, bilateral and multifocal as well, having a correlating pattern to the localization of the PPBs themselves. Until 2009 about 66% of all registered PPB cases lung cysts were either known at or prior to diagnosis (Priest et al. 2009, IPPBR 07.01.2015, 12:15h). Unpublished data from the IPPBR shows that in a study of 134 cases 54% the tumor was found in the right lung, in 37% the children had the PPB in the left lung and the remaining 9% had bilateral PPB or a unilateral PPB and cysts found contralateral (IPPBR, 07.01.2015, 12:16h). Multifocal lesions are possible as well.

In adults, there is a similar tumor called the pulmonary blastoma but this tumor differs from the PPB in the existence of malignant epithelial cells giving it a biphasic appearance compared to pleuropulmonary blastoma which does not have malignant epithelial cells (Priest et al. 1996, Online Mendelian Inheritance in Man (OMIM) #601200, IPPBR, 25.02.2015, 12:15h). Besides the histopathological aspect, the differentiation should be facilitated by consideration of the patient age, supported possibly by a patient history of smoking. However, note that single cases have been reported in which adults were found to have a PPB. Exceptional is especially a case of a 36-year-old male being diagnosed with PPB. Several PPB-associated pathologies are found in children but some also in adults like ovarian tumors or goiter (Foulkes et al. 2011).

1.1.6 Therapy

Being a highly aggressive sarcoma and having documented the biological progression of the different lesions (development from type I to type II and III) a rapid and radical treatment is required. Undoubtedly, early-as-possible surgery with complete excision is

the treatment of choice, preferably thoracotomy but thorascopic approaches might be taken as well. Type I PPBs might receive adjuvant chemotherapy while types II and III will always have a subsequent intensive chemotherapy decreasing the chance of recurrence and improving the outcome of the patients (Miniati et al. 2006, Ferrari et al. 2007). In a survey of 18 patients with type I PPB without adjuvant chemotherapy, in contrast to 14 cases being treated with chemotherapy after surgery, 8 patients of the first group had recurrent disease and 5 passed away. In the second group, no recurrences occurred and all patients were free from detectable disease. Whether complete resection for type I is enough or a lobectomy is required has not been established yet. Radiation therapy is recommended for cases in which a clear-cut surgical margin could not be achieved (Miniati et al. 2006). Current recommendations from the International PPB Registry are summarized in table 1.2 below:

<table>
<tr><th></th><th>Surgery</th><th>Chemotherapy</th><th>Radiation</th><th>Comment</th></tr>
<tr><td>Type I</td><td>yes</td><td>Recommended adjuvant:
VAC
• Vincristine
• Actinomycin D
• Cyclophosphamide</td><td>no recommendation</td><td rowspan="3">Surveillance</td></tr>
<tr><td>Type II</td><td>yes

Possibly 2nd or 3rd look surgery after partial resection.</td><td rowspan="2">(Neo-) adjuvant: IVADo
• Ifosfamide
• Vincristine
• Actinomycin D
• Doxorubicin</td><td rowspan="2">Strongly recommended for residual disease.</td></tr>
<tr><td>Type III</td><td>yes</td></tr>
</table>

Table 1.2: Summary of the therapeutic approach as recommended by the IPPBR.

In case of intraoperative in situ spillage of necrotic tumor material, intrathoracic chemotherapy with cisplatin might be used. Recurrent PPB is treated individually. Stem cell therapy has been used with a success rate of about 50% in a few cases using high-

dose chemotherapy and autologous stem cell rescue and might be a promising approach for metastatic and/or recurrent disease (IPPBBR, 25.02.2015, 12:18h).

Particularly the existence of type I PPB raises the question of cyst management in pediatric patients. Since fine needle aspiration and imaging studies cannot positively confirm or rule out a type I PPB lung cyst, cautious monitoring of the patients might be necessary although it puts patient and family under a lot of psychological stress. Invasiveness of punctures, drawing of blood and side effects of imaging studies must be weighted with the rarity of the PPB and incomplete penetrance of genomic alterations.

Generally, it is of course preferable to surgically remove cysts but risky and unnecessary surgery should be avoided in any case, especially considering that a lobectomy might be necessary. A further indication for surgery is PPB family history in any relatives' history, bilaterality of lesions but also PPB-associated other diseases might be an indication for a removal of the cysts. This of course requires an initial detailed family history. Cases are relatively clear for symptomatic patients having for instance pneumothorax, but asymptomatic lung cysts present a dilemma. After all, each case has to be judged and decided individually by each institution itself. All circumstances, including family history, types and localization of cysts (multilocular cyst removal might not be achievable for instance) and risk profile of the patient, as well as the rarity of the disease, have to be considered when choosing on observation, surgery or other diagnostic and therapeutic means (Priest et al. 2009, Miniati et al. 2006, Foulkes et al. 2014). For instance, in a study group of 175 fetuses with lung lesions, not one had a pleuropulmonary blastoma (Adzick et al. 2003).

Also, the treating physicians should be alert for future events in the family or the patients connected to PPB. A case of an 18-month-old girl that was being screened for cystic nephroma, a PPB-related disease that was found in two of her siblings at 27-months and 31-months respectively, visualizes this aspect. Her screening included chest x-ray which showed no abnormality. The girl presented few months later with pulmonary symptoms and was found to have a large intrapulmonary tumor that caused almost complete atelectasis of the right lung. The patient had surgery and chemotherapy but developed multiple liver metastases and succumbed 9 months later (Delahunt et al. 1993).

1.1.7 Prognosis and complications

Complications result from the tumor masses like rupture and pneumothorax, paralysis or superior vena cava syndrome caused by the tumor or its metastases.

Prognosis is relatively good considering its aggressiveness and correlates to the types I – III (IPPBR, 07.01.2015, 12:16h, Miniati et al. 2006). Recurrence of progressed types of PPB severely worsens the prognosis for the patients. No different outcomes for sporadic and familial diseases have been documented at this point (Foulkes et al. 2014).

Recurrence/event free survival was 76% for type I and 50% and 31% for types II and III respectively, while overall survival for type I is 88% and for type II and III 59% and 45% respectively, based on unpublished data from the International PPB registry. A correlation between the type of PPB, patient age and outcome has been established also reinforcing the notion of the tumor progression.

Metastasis can occur intra- and extrathoracic and is at least in part caused by hematogenous spread. Altogether, metastasis usually occurs within the first two years from diagnosis. The most common sites are the central nervous system (CNS), as well as contra- and ipsilateral lung, diaphragm, liver and bone but there are also reports of iris, ovary or adrenal metastasis. Overall analysis from published cases show that approximately 15% of patients have spreading to the brain, 6% to the bone and 4% to the lung. Mediastinal and hilar lymph nodes can be affected as well (IPPBR, 07.01.2015, 12:16h).

While being rather rare in type I -especially at the time of diagnosis-, cerebral metastasis occurs very often in type II and III being at rates of 11% and 54% respectively. This is very high, particularly in contrast to other pediatric tumors. As a conclusion, MR imaging should be done at a short interval (e.g. 3 months) for about 36 months after the initial diagnosis to be able to detect metastasis and be able to initiate a change in treatment (Priest et al. 2009). Most metastasis occurs within the first 24 months. To this point, there is no data regarding the risk for other malignancies occurring later in life but there are ongoing IPPBR-investigations regarding this issue.

1.2 DICER1

1.2.1 Nomenclature, localization and structure

This chapter will give an overview over *DICER1* nomenclature, its localization in the human genome, the molecular structure as well as the history in relation to the pleuropulmonary blastoma.

DICER1 is the human gene while *Dicer1* describes the *DICER1* in mice. It is the gene localized on chromosome 14q32.13 and encodes for the DICER1 protein, a ~218-kd ribonuclease III endonuclease involved in mRNA regulation (Hill et al. 2009, Foulkes et al. 2014). The gene is composed of 27 exons, of which 26 are coding and one -the first- is non-coding. It has a length of 1922 amino acids and lies in gene region 14:95,086,227-95,158,262. There are several regions in the gene coding for specific domains in the tertiary structure of the final protein. These domains are DExD/H (DExD/H box helicase domain),

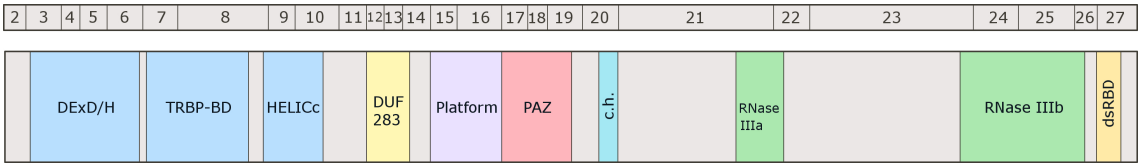

Figure 1.1: *DICER1* exons and domains. The upper bar designates the exons while the lower bar shows the *DICER1* domains with respect to their location on the gene.

TRBP-BD (transactivation response RNA-binding protein binding domain), HELICc (helicase conserved carboxy-terminal domain), DUF283 (Domain of unknown function), Platform, PAZ8 (Piwi/Argonaute/Zwille), connector helix, RNase IIIa, RNase IIIb and dsRBD (DsRNA-binding domain). PAZ seems to be very important for the function of DICER1 as it serves as a molecular ruler and determines where the 5p and 3p arms of miRNA will be cleaved from the so-called hairpin sequence (Zhang et al. 2004, Wilson et al. 2013, Rio Frio et al. 2011, Online Mendelian Inheritance in Man (OMIM), #606241).

DICER1 was first described in 2001 by Bernstein and colleagues. The DICER1 protein has with some imagination an “L”-like tertiary structure and is divided in a head, a body and an arm region. At its head, the PAZ domain and Platform domain are located while further down at the bottom, between body and arm the RNase IIIa and IIIb domains are

found. At the head region the binding site for dsRNA (3' and 5' moieties) is located (Foulkes et al. 2014, Wang et al. 2009, Lau et al. 2012). Both of the RNase III domains dimerize intramolecularly to form the catalytic center. It was shown that a functioning DICER1 protein requires Mn^{2+}/Mg^{2+}-ions which are placed between the dsRNA substrate and the RNase III domains by residues from the catalytic center (Zhang et al. 2004, Foulkes et al. 2014).

DICER1 was chosen initially as a candidate for the genesis of pleuropulmonary blastoma by Hill and colleagues only in 2009 during a larger analysis of possible gene candidates related to this rare condition. A family-based genome-wide linkage analysis on four families which showed history of PPB, revealed a 7-Mb interval of interest. This interval consisted of 72 genes and included *DICER1*. It was considered a suitable candidate because of its role in lung development. It was previously seen in mice that missing *Dicer1* in lung epithelium resulted in a significant malformation of lungs (for example cysts, abnormal branching) that even is similar to early forms of PPB (Harris et al. 2006). Further analysis (genomic sequencing) of 11 families in total revealed that *DICER1* was in fact at least in part involved with this neoplastic condition. Normally, DICER1 should be present in lung epithelium at any time (Hill et al. 2009).

1.2.2 Molecular function, miRNA biogenesis and RNA interference (RNAi)

In the eukaryotic cell nucleus, the genes are transcribed by a RNA Polymerase II to single stranded heterogeneous nuclear RNA (hnRNA) which is a precursor to the messenger RNA (mRNA). MRNA is then transported into the cell cytoplasm to be processed by ribosomes into large chains of amino acids (translation) which fold into the final proteins. This pathway can be inhibited by micro RNA (miRNA) and small interfering RNA (siRNA) in a process called RNA interference or RNAi. *DICER1* codes for an RNase III endonuclease that cleaves and processes small RNA which then negatively regulates mRNA and therefore gene expression. Both miRNA and siRNA are examples of small RNA.

Usually, miRNA is coded in the introns of the genome and reversely transcribed from RNA Polymerase II in the cell nucleus. The single-stranded RNA products are longer

precursors which are called *primary-miRNA* or pri-miRNA. They are up to 10000nt in length and have an extensive hairpin loop structure. The ribonuclease III DROSHA and a binding protein coded by *DGCR8* (DiGeorge Syndrome Critical Region Gene 8, PASHA*)* compose the so-called *microprocessor*, a protein complex which cleaves the hairpins from their precursors resulting in approximately 60 – 70nt long so called *preliminary-miRNA* or pre-miRNA. Pre-miRNA is transported from the nucleus to the cytoplasm by exportin 5 (XPO5) (Yi et al. 2003, Bohnsack et al. 2004). Now, RNase III endonuclease DICER1 measures the length of miRNA with the help of cofactor TRBP (transactivation response RNA-binding protein) and then cleaves the remaining hair-pin loop from the pre-miRNA leaving 18 – 22nt double-stranded mature miRNA (Slade et al. 2011, Bernstein et al. 2001).

The resulting strands can also be designated as miRNA and miRNA✭ (star strand or inert carrier strand) (Heravi-Moussavi et al. 2012). The result from the DICER1-cleavage are a 5p and a 3p (p for prime) arm from the pre-miRNA, which are still connected and therefore double-stranded (called miRNA duplex) and the loop from the hairpin region of the preliminary-miRNA (Pugh et al. 2014). The RNase IIIa domain is responsible for the cleaving of miRNA✭ and the RNase IIIb domain for the cleaving the miRNA strand.

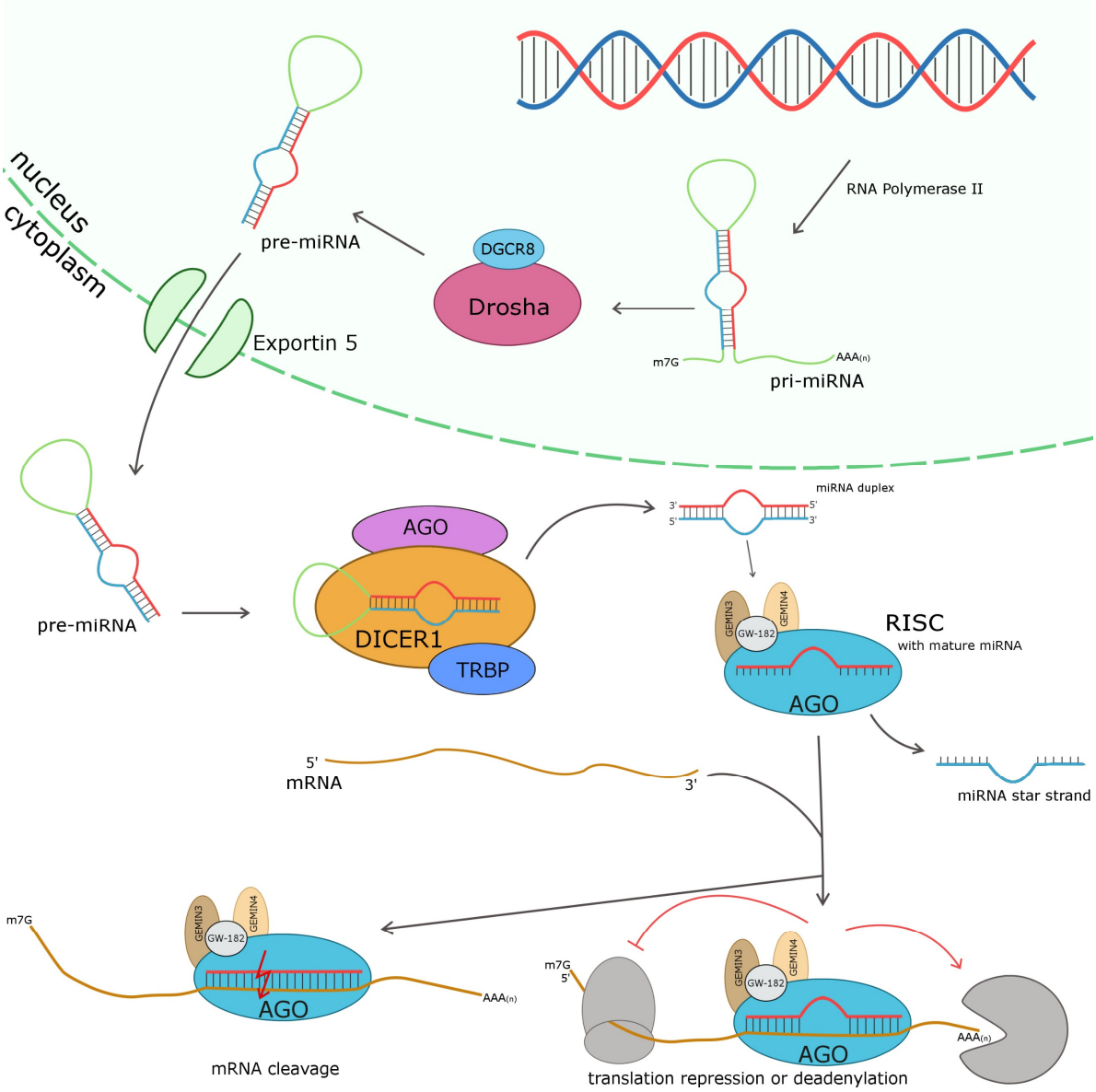

Figure 1.2: miRNA biogenesis pathway and RNAi. *Modified after Filipowicz et al. 2008, Rassow et al. Duale Reihe Biochemie, P. 465, Bahubeshi et al, 2011.*

RNA Polymerase II reversely transcribes the *primary-miRNA,* which is then processed by the *microprocessor* (consisting of DROSHA and DGCR8) into *preliminary-miRNA*. The protein Exportin-5 (XPO5) transports this *pre-miRNA* in to the cytoplasm. DICER1, a RNase III endonuclease, measures the length of miRNA and cleaves the hairpin-loop from the double-stranded miRNA duplex. DICER1 facilitates the RISC-loading of the miRNA. The duplex strand is cleaved into a mature miRNA strand and a miRNA star strand by the multiprotein complex *RISC* (AGO, GEMIN3, GEMIN4, GW-182). The mature miRNA-loaded RISC then negatively regulates mRNA by mRNA cleavage, translation repression or deadenylation.

Binding to a protein from the Argonaute protein family along with other cofactors (GEMIN3, GEMIN4, GW-182), the miRNA forms the multiprotein complex *RISC,* the

RNA-induced silencing complex. Binding of small RNAs to Argonaute is called *RISC loading* and is facilitated by DICER1 (Maniataki et al. 2005, Foulkes et al. 2014). *RISC* now separates both miRNA strands into the mature miRNA and the miRNA star strand. Loaded RISC now is driven by imperfect base pairing of miRNA to complementary strands to repression of translation or a deadenylation of mRNA leading to a degradation of mRNA (Bahubeshi et al. 2011, Rassow et al. Duale Reihe Biochemie, P. 465, Foulkes et al. 2014, Bartel, 2009).

DICER1 also cleaves a second type of small RNA, the so-called long dsRNA into small interfering RNAs (siRNAs). Long double-stranded RNAs result from transcription of inverted repeats or bidirectional transcription of RNA. In this case it is called endogenous RNA. Exogenous long dsRNAs result from virus RNA or transposons that enter the cell or are introduced experimentally. When siRNA is loaded to RISC it requires perfect complementary base pairing to mRNA and then cleaves the mRNA through the help of Argonaute2 (Ago2) (Rassow et al. Duale Reihe Biochemie, P. 465, Foulkes et al. 2014, Lee et al. 2004).

Alternatively, instead of being cleaved by DICER1, some miRNAs can also be sliced by Argonaute2 (Bahubeshi et al. 2011). Approximately 60% of the human genes are regulated by miRNA. Each miRNA is not responsible for one but for an average of 200 genes (Friedman et al. 2009, Carthew, 2006, Slade et al. 2011, Rassow et al. Duale Reihe Biochemie, P. 464). Therefore, a miRNA is not specific for just one mRNA but a wide variety. About 900 different miRNAs have been identified and their rage of actions include areas like metabolism, cell proliferation, morphogenesis and others. Changes in miRNA have been implicated with various tumors.

Besides the participation in RNAi DICER1 has also shown to be involved in other cellular processes like chromatin-regulation, genome stability or alternative splicing (Wu et al. 2013). DICER1 expression itself seems to be regulated by the let-7 family miRNAs (Tokumaru et al. 2008).

1.2.3 DROSHA

DROSHA is also a ribonuclease III and is involved with biogenesis of miRNA. It was discovered 2003 by Lee and colleagues and has a connection to DICER1 because it is part of the microprocessor complex (with DGCR8/Pasha). It processes pri-miRNA to pre-miRNA and this pre-miRNA subsequently is transported from nucleus to cytoplasm to be cleaved by DICER1. This makes DROSHA also an important element in RNAi processes and therefore normal development (IPPBR, 06.01.2015, 15:56h, Alvarez-Garcia et al. 2005).

1.2.4 Phenotypes associated with *DICER1* and PPB

1.2.4.1 *DICER1*-Syndrome

Family members of patients with PPB show an increase of certain benign and malignant diseases. Patients themselves also have a greater risk of other manifestations. Due to this fact, initially the term PPPB Family tumor and dysplasia syndrome (PPPBFTDS) was used. Because this disease is not limited to PPB, a lot of other diseases can occur and PPB is not always present, the term *DICER1*-Syndrome was first coined in 2011 by Slade and colleagues. It was more commonly used in the recent past due to its more fitting description of the underlining pathology of the disease. Unlike other common tumor suppressor genes or oncogenes, *DICER1* was not known to be associated with neoplasms before. A survey of more than 800 patients with different tumors showed that *DICER1* alterations are generally not seen in most tumors (only 19 out of 823 showed *DICER1* mutations) (Slade et al. 2011). This is also confirmed by the striking low incidence of *DICER1* mutations in any of the available databases like the 1000 Genomes Project (www.internationalgenome.org), Cancer Genome Atlas consortium (www.cancergenome.nih.gov) or Catalogue of Somatic Mutations in Cancer (COSMIC, www.cancer.sanger.ac.uk/cosmic) as well as a general low prevalence of *DICER1* germline mutations (Heravi-Moussavi et al. 2012).

The most common association appears to be the cystic nephroma (CN) which is like pleuropulmonary blastoma rare. It affects kidneys of young children in their first approximately 5-6 years of life with a benign tumorous cystic mass which can make

partial or total nephrectomy necessary (Boman et al. 2006, Slade et al. 2011). Cystic nephroma can affect adults as well (Stamatiou et al. 2011).

Wilms tumor (nephroblastoma) does also have a relation with *DICER1*. It normally occurs in children between two and four years old and is the most common renal tumor in children. A number of tumor suppressor genes which facilitate the development of Wilms Tumor have already been established e.g. *WT1*, *WT2*, *p53*. Gonadal tumors like the ovarian Sertoli-Leydig cell tumor and thyroidal manifestations like nodular adenomatous hyperplasia which presents as multinodular goiter (MNG) or carcinomas are common clinical phenotypes of the *DICER1*-Syndrome. Notably, ovarian tumors and thyroid involvement do usually not occur as early in life as PPB. Females seem to be more often affected than males, especially in the case of multinodular goiter (Foulkes et al. 2014). This may be attributed in part to the occurrence of gender-specific tumors like cervical and ovarian tumors. Foulkes and colleagues estimated in 2014 that approximately 80% of male and 50% of female carriers are clinically unaffected albeit having a *DICER1* alteration.

Another extremely rare tumor was shown to have *DICER1* alterations: the pituitary tumor. In a study nine out of ten patients had mutations in the *DICER1* gene (de Kock et al. 2014).

In relatives and PPB patients, numerous cardiac abnormalities have been documented like bicuspid pulmonary valve, patent ductus arteriosus, TGA (transposition of the great arteries) and atrial septal defects (Foulkes et al. 2011). There are also mice studies which showed similar changes and implicated *DICER1* in cardiac development (Saxena et al. 2010). Interestingly, there does not seem to be a connection to testicular germ cell carcinomas (including seminomas and non-seminomas) to *DICER1* (Sabbaghian et al. 2013).

A synopsis for the severity as well as the possible spectrum of this cancer predisposition syndrome shows a case published in 2014 by Schultz and colleagues: A 5-year-old girl was diagnosed with type II pleuropulmonary blastoma and treated with surgical removal and chemotherapy. About three years later the girl clinically presented with thyroid nodules. Thyroidectomy was performed and pathological evaluation showed a follicular variant of a papillary carcinoma. At 13 years of age she presented with lower abdominal

pain and examination showed a left inguinal hernia and multiple peritoneal cysts around ligamentum rotundum dextrum et sinistrum. After surgical repair the girl presented six months later with nasal congestion and pelvic pain which had been recurring. Diagnostics revealed multiple sinonasal polyps in both sinuses. Histologic section showed that the polyps contained parts which were consistent with nasal chondromesenchymal hamartoma (NCMH). The pelvic pain resulted from a new large left ovarian mass which was ultimately found to be a Sertoli-Leydig cell tumor (SLCT). During surgery the patient again showed bilateral inguinal hernias as well as peritoneal cysts. Her family history was positive for PPB.

1.2.4.2 Phenotypes

There is vast phenotypic variation among affected patients. As already outlined, the clinical penetrance for PPB is relatively low. Table 1.3 gives an overview of clinical manifestations of *DICER1* mutations, conditions in bold are more common. Note that this table is not complete as for example other (embryonal) rhabdomyosarcomas or neuroendocrine tumors have been reported and are not shown in the list.

Of these associations, pleuropulmonary blastoma seems to be the most serious manifestation of the *DICER1*-Syndrome (Foulkes et al. 2011) although in other diseases deaths are associated too. Due to the rareness of PPB and *DICER1* mutations, it cannot be ruled out that in single cases with *DICER1* alterations any additional disease is just a random event and/or a result from radio-chemotherapy.

***DICER1* – clinical associations**	
CNS	Pineoblastoma Pituitary blastoma Medulloblastoma Neuroblastoma
Thyroid gland	**Multinodular goiter** (MNG) Thyroid carcinoma
Respiratory tract	**Pleuropulmonary Blastoma** (PPB) Lung cysts

	Pulmonary sequestration
Kidney	**Cystic Nephroma** Wilms tumor Anaplastic sarcoma of the kidney
Gastrointestinal tract	Juvenile hamartomatous intestinal polyps Intestinal intussusception
Reproductive tract	**Sertoli-Leydig cell tumor** of ovary (SLCT) **Cervical embryonal rhabdomyosarcoma** (cERMS) Ovarian embryonal rhabdomyosarcoma Primitive neuroectodermal tumor (PNET) of cervix
Other	Eye: Ciliary body medulloepithelioma (CBME) Phthisis bulbi Nasal chondromesenchymal hamartoma (NCMH) Embryonal rhabdomyosarcoma of the bladder Transposition of the great arteries Various leukemias Macrocephaly

Table 1.3: Clinical phenotypes of *DICER1* mutations. Bold terms are more frequent associations. IPPBR 04.12.18 13:21h, Foulkes et al. 2014, Slade et al. 2011, Schultz et al. 2018: Foulkes et al, 2011.

Not all manifestations are strictly indicative of the rare *DICER1*-Syndrome but certain phenotypes like PPB, cystic nephroma, Sertoli-Leydig cell tumors of the ovary or NCMH –especially in combination– should prompt a thorough family history and *DICER1* sequencing for mutations. Some phenotypes like Wilms tumor are also caused by other genetic predisposition syndromes like WAGR-Syndrome (**W**ilms tumor, **a**niridia, (uro-) **g**enital abnormalities and mental **r**etardation) or Denys-Drash-Syndrome. Most conditions suggestive of *DICER1*-Syndrome occur early in life and chance of additional disease decreases with adulthood.

In 1996 Priest and colleagues noted that approximately 25% of PPB patients presented with a family history of dysplastic or neoplastic disease (Priest et al. 1996). Data released

2009 showed affected family members in 14% of cases. Newer assessments have an increased ratio of 35 – 40% for manifestations that are possibly related to *DICER1* and PPB (Bahubeshi et al. 2010, Schultz et al. 2014). The IPPBR reported that in nine families there were two or even more patients with PPB (Priest et al. 2009).

1.2.5 Genetics of *DICER1*-Syndrome

Several mutations and subsequent hypotheses regarding the mechanism of *DICER1*-Syndrome have been reported in the recent past. A detailed outline will follow in the discussion after the presentation of the results from this thesis.

1.3 Study design and leading question

The pleuropulmonary blastoma (PPB) is a rare tumor that can occur during childhood. Very few cases are reported each year and knowledge about PPB is scarce and not as abundant as for other more common tumors. It usually appears in children younger than six years old and is attributed at least in part to a change in the *DICER1* gene, which is located on chromosome 14. Several mutations and few deletions in the *DICER1* gene have previously been described. Being such a rare entity any further scientific information about this tumor is helpful to increase the understanding of this malignancy. Furthermore, there are some tumors and diseases that appear to be linked to the PPB like for example cystic nephroma, ovary cancer or multinodular goiter.

This project examines the collection of tumor specimens gathered over nearly 30 years in the Children Cancer Registry of the Society of Pediatric Oncology and Hematology (GPOH) Kiel, Germany. Due to the rarity of the PPB it is paramount that as much information as possible is gathered from the material available. A number of mutations causing PPB have already been determined. This thesis tries to identify *DICER1* mutations via PCR and Sanger sequencing in patients and sometimes family members of individuals with a pleuropulmonary blastoma. Additionally, a newer method called MLPA – multiplex ligation-dependent probe amplification was used to screen for large

deletions, duplications or rearrangements. The practicability of the MLPA method for a clinical use was also evaluated.

The underlying questions are what changes can be found in the germline as well the tumor itself to understand what causes pleuropulmonary blastoma and its associated diseases. Ultimately, a correct diagnosis of PPB and its causes is the foundation for an improved diagnostic procedure and genetic counseling of patients and family. A thorough understanding of the mechanisms and associated conditions can lead to possible anchor points of a future treatment.

2 Patients, methods and material

2.1 Patients, material and storage

In total, there were 18 patients with histologically confirmed pleuropulmonary blastoma. There were 12 patients with sometimes several blocks of paraffin embedded tumor and 6 patients in which DNA already had been extracted in tubes. The material was collected over a time span of 28 years from 1986 to 2014. The material was collected in the Children Cancer Registry of the Society of Pediatric Oncology and Hematology (GPOH) in Kiel, Germany. There was limited information regarding the patients: Usually, the year the tumor was registered in the GPOH (supposedly the year of first diagnosis), date of birth and gender are known. There was often no knowledge on additional disease, family history or outcome. Also, no information on the particular aspects of previous storage e.g. percentage of formalin used or temperatures were available. In two patients additional data and material were available. In one male patient (no. 12) blood, paraffin embedded tissue of a papillary thyroid carcinoma and blood from both parents were available. In one female patient (no. 18), blood from the patient, her parents and her twin sister were available as well. Of the 18 patients, 10 were female and 8 male. Blood samples were provided by two separate clinics.

Several normal control patients were used including a positive control which was provided by N. Sabbaghian, Montreal, Quebec, Canada.

Overview of patients:

Patient number	PPB year	DoB	Gender	Material	Additional information
1.	1986	09/1983	Female	**DNA**	
2.	1993	01/1987	Male	**DNA**	
3.	1993	06/1985	Male	**DNA**	
4.	1994	01/1988	Male	**FFPE**	
5.	1994	12/1984	Female	**FFPE**	
6.	1995	07/1988	Male	**DNA**	

7.	1997	01/1991	Female	**FFPE**	
8.	1997	08/1990	Female	**FFPE**	
9.	1999	04/1992	Female	**FFPE**	
10.	2001	12/1993	Female	**DNA**	
11.	2001	12/1989	Male	**FFPE**	
12.	2003	02/2001	Male	**DNA**	PPB type II
12.a	2003			**FFPE**	PPB type II
12.b	2014			**FFPE**	Papillary thyroid carcinoma
12.c	2014				Blood
13.	2005	01/1998	Female	**FFPE**	
14.	2007	11/1999	Female	**FFPE**	
15.	2012	12/2007	Female	**FFPE**	
16.	2012	07/2009	Male	**FFPE**	
17.	2012	07/2008	Male	**FFPE**	
18.a	2014	04/2012	Female	**FFPE**	
18.b	2014				Blood

Table 2.1: List of patients. DoB = Date of Birth; FFPE = Formalin-fixed paraffin embedded tissue.

Overview of relatives:

Patient number	Year	Additional information
19.	2014	Father of Pt. 12; history of seminoma. Material: Blood.
20.	2014	Mother of Pt. 12. Material: Blood.
21.	2015	Twin sister of Pt. 18. Material: Blood.
22.	2015	Mother of Pt. 18. Material: Blood.
23.	2015	Father of Pt. 18. Material: Blood.

Table 2.2: List of relatives.

Formalin-fixed Paraffin-Embedded tissue (FFPE) as well as already isolated DNA were used. FFPE blocks were stored at room temperature. DNA vials were stored at 4°C in between experiments. MLPA, PCR and sequencing components were stored at -20 to -24°C except BigDye® Terminator 5x Sequencing Buffer Mix V1.1, V3.1 which was stored at 4°C.

2.2 Tumor dissection, preparation and purification

For 12 of the 18 patients FFPE blocks were available. Additionally, patient no. 12 had a second FFPE block for his PPB and a separate thyroid carcinoma as a FFPE. The tumor blocks were used when there was no DNA vial in the first place or if the DNA concentration in the vial was too low. Sometimes, additional DNA material was needed in cases in which experiments were not successful and the original DNA was depleted.

Tumor preparation largely depends on the tissue that is embedded in the paraffin blocks. These areas determine which parts can be sliced off the tumor block. Three different procedures were used for this thesis. First dissection using a microtome, second manual preparation and third a selection of areas by a pediatric pathologist which then were dissected from the tumor block.

The first method was done by laboratory assistants of the pathology department of the Universitätsklinikum Hamburg-Eppendorf. Several 5-10µm slices were taken off the tumor blocks. For the second method sterile scalpels were used and slices in various degrees of thickness were taken off the areas of the paraffin block containing tissue. Slices were then contained in vials. The third method was done for the second PPB tumor block and the papillary thyroid carcinoma of patient 12 exclusively.

QIAamp® DNA FFPE Tissue Kit and Deparaffinization Solution (Qiagen, Hilden, Germany) was used for further preparation. The slices from the tumor blocks are placed in microcentrifuge tubes and 160 – 320µl Deparaffinization Solution is added depending on the number of slices contained in the tube. Thorough vortexing and short centrifuging follows and afterwards the tube is placed on a preheated thermo block at 56°C for 3 minutes. After cooling down at 15-25°C 180µl Buffer ATL is added. The substances are

mixed by vortexing and afterwards again centrifuged at 10000rpm for 60 seconds. Now, 20µl proteinase K is added to the clear phase and mixed by pipetting up and down. The sample is stored at 56°C for 1 hour to completely dissolve and afterwards heated at 90°C in a thermo block for 1 hour to reverse formaldehyde change of nucleic acids. Followed by short centrifuging the clear phase is then mixed with 200µl of Buffer AL and 200µl of ethanol (96-100%) by vortexing to achieve a homogeneous solution.

The entire content of the tube is then transferred to a specific QIAamp MinElute column sitting on a collecting tube. The column is then centrifuged at 8000 rpm (6000 x g) for 60 seconds. Now, the spin column is placed on a clean 2 ml collection tube and the previous tube with the filtrate is discarded. In the next step 500µl Buffer AW1 is added and the column is centrifuged at 8000 rpm (6000 x g) for 1 minute. The filtrate containing tube is again discarded and replaced with a new clean one. 500µl AW 2 is added and succeeded again by 8000 rpm (6000 x g) centrifugation for 1 minute. After disposing the collection tube with the filtrate once more the column is centrifuged at 14000rpm (20000 x g) for 3 minutes (membrane drying). Finally, 20 – 100µl Buffer ATE is placed in the center of the previously dried membrane and after an incubation period of 1 minute at room temperature, the tube is centrifuged for another minute at 14000rpm (20000 x g).

This procedure ultimately yields an amount of DNA within the buffer. The exact amount is not known until measured for example with a photometer or e.g. with Qubit® (see below).

Basis for the entire procedure is the SOP “DNA Säulenaufbereitung” 2.11.7 of the Universitätsklinikum Hamburg-Eppendorf, Klinik und Poliklinik für Pädiatrische Hämatologie und Onkologie, Version 03 last updated 10.04.2012 as well as the manual from QIAGEN, QIAamp DNA FFPE Tissue Handbook 06/2012.

2.3 DNA extraction

Using EDTA blood, genomic DNA was extracted from nucleated leukocytes by a four-step method (Miller et al. 1988). Basis for the procedure was the ‘spin protocol’ of the QIAamp® DNA Blood Mini Kit from Qiagen, Hilden, Germany.

In the initial step 20µl QIAGEN Protease are added to 200µl sample EDTA blood. In case of larger sample volumes the amount of protease has to be increased accordingly. Afterwards 200µl Buffer AL is added and the tube is vortexed for 15 seconds. The tube is then stored at 56°C for 10 minutes for the lysis phase and shortly centrifuged to remove drops adhering to the lid. 200µl ethanol (96-100%) are added to the tube, followed by vortexing and centrifuging. The mixture is now pipetted in a QIAamp Mini spin column and centrifuged at 8000rpm for 1 minute after which the filtrate is discarded. This is the binding step in which the lysate is bound in the column. In two separate steps 500µl Buffer AW1 and AW2 are added and the spin column is centrifuged for 1 min at 8000 rpm (AW1) and for 3 min at 14000 rpm (AW2) respectively. After both steps the filtrate from the collection tube is discarded. Finally, in the elution step the QIAamp Mini spin column in placed in a clean tube and 200µl Buffer AE is added to the spin column and incubated for 1 minute. Afterwards the tube is centrifuged for 1 minute at 8000rpm yielding the extracted DNA.

2.4 DNA purification

In cases of insufficient PCR or MLPA results, a DNA purification was done using the Cycle-pure Kit and protocol from peqlab, Radnor, Pennsylvania, USA. The DNA mix is mixed with a buffer, put on a filter and is separated via centrifugation from salts, oligonucleotides and polymerases. The latter are unable to bind to a membrane in the filter so they are separated from the DNA. The necessary components are:

MicroSpin PerfectBind DNA Columns
MCP Buffer
DNA Elution Buffer

First, each 50µl of PCR product is mixed with 500µl of MCP Buffer and vortexed shortly. The mixture is carefully placed on the filter (spin-column) over the collecting tube and centrifuged for 2 minutes. The liquid is discarded and the spin-column is placed in a new tube and 10 – 20µl DNA elution buffer is added. After a short incubation period of up to 5 minutes and a 1-minute centrifugation, the yielded material is the purified DNA.

2.5 DNA measurement

To assess concentrations of certain DNA volumes and dilutions Qubit® dsDNA BR Assay Kit by life technologies (Eugene, Oregon, USA) as well as Qubit® 2.0 Fluorometer Invitrogen™, Thermo Fisher Scientific (Waltham, Massachusetts, United States) were used. The following reagents are required:

Genomic DNA, 2µl per sample
Qubit® Buffer
Qubit® Reagent
Qubit® Standard #1, #2

Depending on the number of samples that are to be measured, a Qubit master mix is prepared, for which 199µl of the Qubit® Buffer is mixed with 1µl of the Qubit® Reagent per sample. The reagent needs to be stored protected from light at all times and the prepared Qubit® master mix needs to be vortexed. Two standards (#1 and #2) are prepared using a concentration of 0ng/µl and 100ng/µl respectively. 10µl of the standards are mixed with 190µl of the Qubit® master mix. 198µl of the master mix is then pipetted together with 2µl of the DNA in question. All vials (standards and DNA) are vortexed afterwards and incubated for 2 minutes. In the following step, the vials can be measured using the Qubit® 2.0 Fluorometer. Next the standards are set, first the standard #1 with 0ng/µl then standard #2 with 100ng/µl. Broad range DNA is selected for the configuration settings. The yielded concentration is then the basis for future dilutions and procedures.

2.6 DNA dilution

If necessary, the DNA was diluted for the MLPA or PCR procedures to the required amount. TE Buffer (Invitrogen, Life Technologies, Eugene, Oregon, USA) was used.

2.7 Whole Genome Amplification (WGA)

GenomePlex® Complete Whole Genome Amplification (WGA) Kit, WGA2 from Sigma-Aldrich (Saint Louis, Missouri, USA) was used. Based on random fragmentation

and addition of so-called Library sequences as well as primers fusing at the end of the fragments, WGA aims at the increase of DNA material by the means of PCR. An approximate 500-fold amplification of the product is targeted. A minimum quantity of 10ng is needed, which in turn can yield >10µg of WGA product. As sources, whole blood, formalin fixed tissues, cultured cells and others may be used.

The entire procedure was done according to the technical bulletin provided by the supplier. WGA required reagents are:

1. Fragmentation Buffer
2. Library Preparation Buffer
3. Library Stabilization Solution
4. Library Preparation Enzyme
5. Amplification Master Mix
6. WGA DNA Polymerase
7. Water, Molecular Biology Reagent
8. Control Human Genomic DNA

Three general steps make up the WGA procedure: Fragmentation, OmniPlex library generation and PCR amplification. From the respective patient samples, a 10ng solution was prepared with a concentration of 1ng/µL. The recommended ideal amount of 100 ng of fixed tissue DNA was not available for the samples due to lack of material. Generally, a fragment size of at least 200 bp is required in case fixed tissue or degraded DNA is used for WGA. A positive control is always used along the procedure. The resulting fragments range from 100 – 1000 base pairs with a mean of 400 bp.

Fragmentation

1µl of fragmentation buffer is added to 10µl of DNA sample. The multiwell or the tube is placed in the thermocycler at 95°C for exactly 4 minutes. It is important that there is no deviation from the time schedule because any change can alter the results significantly. After the 4 minutes, the samples are cooled immediately on ice.

Library Preparation

2µl of Preparation Buffer as well as 1µl Stabilization Solution are given to each sample. The mixtures are vortexed, centrifuged and heated in a thermocycler at 95°C for 2 minutes. After being cooled down, each tube receives 1µl of Library Preparation Enzyme and is mixed thoroughly. The designed program for the thermal cycler is used:

1. 16°C – 20 minutes
2. 24°C – 20 minutes
3. 37°C – 20 minutes
4. 75°C – 5 minutes
5. 4°C – pause

Amplification

Continuing from the Library Preparation a master mix is prepared containing 7.5µl Amplification Master Mix, 47.5µl of dH_2O, Molecular Biology Reagent and 5µl WGA DNA Polymerase. The tubes have to be mixed afterwards and centrifuged. The last step is the amplification via a thermocycler program:

1. 95°C – 3 minutes (Initial denaturation)
2. 94°C – 15 seconds (Denaturation)
3. 65°C – 5 minutes (Annealing/Extension)

The last two steps are repeated 14 times until the cycler rests at 4°C. The samples are now ready for further processing and are stored at about -20°C. Further analyses are for instance agarose gel electrophoresis or sequencing.
WGA was used to increase the amount of genomic DNA of patients 1, 2, 3, 7 and 11.

2.8 Polymerase chain reaction (PCR)

Polymerase chain reaction is a wide-spread method to dramatically increase the quantity of a specific region of interest of DNA. It is made up of three steps which are repeated in a varying number. Required for a successful PCR are: DNA in a sufficient amount (template), polymerase, two primers and nucleotides. The three essential steps are

denaturation, annealing and DNA-synthesis. Annealing is basically the hybridization of the primers. The primers (oligonucleotides) are synthetic and are designed to bind complementary to a specific location on the DNA. In the first step, denaturation, the double-stranded DNA is divided into two single strands, this is done at 95°C. Annealing temperature depends on the primer used for the PCR, ranging between 40 – 70°C. Their length, base pair composition and GC-content determine the specific temperature that is necessary for successful hybridization. Subsequently, elongation or DNA-synthesis occurs by a heat-resistant polymerase. The polymerase can for example be derived from *Thermus aquaticus*, in which case is it called Taq-Polymerase or *Pyrococccus furiosus* (Pfu-Polymerase). Both are thermophile bacteria. During DNA-synthesis the polymerase adds from the abundant desoxyribonucleotide-triphosphates (dATP, dGTP, dCTP, dTTP) to the 3' end of the primers. Elongation usually requires a temperature of approximately 70 - 72°C and has the advantage of the polymerase not being degraded during the initial denaturation of the PCR. After elongation, new double-strands are the resulted products which in the next loop have to be split again via denaturation at 95°C, being followed again by annealing and synthesis. This cycle is repeated about 20 – 40 times. For tumor samples the PCR was set to 40 loops.

The typical *DICER1* PCR setting used for this project:

95°C – 5 minutes	Initial denaturation
95°C – 40 seconds 55°C – 30 seconds 72°C – 60 seconds	40 loops
72°C – 5 minutes	
15°C – pause	

The substrates per well for *DICER1* that were used are the following:

- 25µl DreamTaq Green PCR Master Mix (Thermo Fisher scientific, Waltham, Massachusetts, USA)
- 21µl dH_2O
- 2µl Primer
- 2µl Genomic DNA

TP53-PCR had the following configurations:

95°C – 5 minutes		Initial denaturation
95°C – 40 seconds 68°C – 30 seconds 72°C – 90 seconds	⌐ | ⌙	35 loops
15°C – pause		

The substrates per well for *TP53* were the following:

- 25µl GoTaq® G2 Green Master Mix (Promega Corporation, Madison, Wisconsin, USA)
- 20µl dH_2O
- 2µl Primer
- 2µl $MgCl^2$
- 1µl DNA

2.8.1 *DICER1* and *TP53* exons and primers

DICER1 and *TP53* were analyzed. Initially, a primer mix has to be made. This was done for PCR by using 5µl of each sense and anti-sense primer and mixing it with 90µl dH_2O. Primer mixes are vortexed prior to use. As stated before, *DICER1* has 27 exons, of which exon 21 and 23 are especially large and where therefore divided into two parts to be able to cover all intron-exon-boundaries. Due to their small size and their short respective introns, exons 16 and 17 as well as exons 25 and 26 could be amplified in one part, respectively. However, they were also available as single PCR-amplicons, except exon 26. The complete list of exons including the sense and anti-sense primers are listed in table 8.3.1 and 8.3.2. *TP53* has 11 exons. The primers for *DICER1* were taken from the publication of Hill et al. 2009, while the *TP53* primers were manually designed.

PCR-primer vary in their specific annealing temperature. For *DICER1*, the annealing temperature was 55°C. The separate exons 16 and 17 had an annealing temperature of 65°C and exon 25 of 52°C. *TP53* had an annealing temperature of 68°C except exon 10, which required a temperature of 52°C.

2.9 Direct blood PCR

In one case, only a very small amount of blood from the patient was available (patient 18a). This was not enough to isolate DNA from the sample. Therefore, PCR was done directly from the blood of the patient, using Phusion Blood Direct PCR Kit (Thermo Fisher Scientific, Waltham, Massachusetts, USA):

- 25µl 2x Blood Buffer
- 5µl Primer Mix
- 1µl Phusion Taq Polymerase II
- 3µl Blood
- 16µl dH_2O

The program for the thermal cycler was:

95°C – 5 minutes

98°C – 1 second
55°C – 5 seconds
72°C – 15 seconds
] 40 loops

72°C – 2 minutes

Due to the sensitivity of the direct blood PCR, a negative control always has to be run along the PCR.

2.10 Agarose gel electrophoresis

Usually, after a PCR is finished, the yielded PCR-product is verified by agarose-gel electrophoresis, which should show a specific band of specific length correlating with the expected PCR product. In electrophoresis, charged PCR products migrate according to the electric current from anode to cathode because of their negative charge and are separated by their length and the resulting migration-velocity. Migration also depends on the molecular weight of the DNA, the concentration of the agarose gel, the buffers used, the amount of electric current and the length of the products. Also, as a useful effect,

unspecific products, as well as the primers are separated from the desired products. First an agarose gel has to be prepared and cast in a casting mold. Depending on the number of samples used and the resulting number of slots needed 100ml, 200ml or 300ml gels can be cast.

1.2g Agarose (Biozym Scientific GmbH, Hessisch Oldendorf, Germany) and 100ml modified TAE (TRIS-Acetate-EDTA-Buffer) Buffer are used. 10ml, 20ml or 30ml of distilled H_2O are added to account for any loss of fluid during the following heating. Both are mixed in a beaker and put in a microwave for a duration of approximately 4-8 minutes. Afterwards the beaker is weighted and if needed, distilled H_2O is added again to level the amount of fluid to the desired amount. The solution is cooled under continuous stirring and 5µl of Roti®-Safe-GelStain (Carl Roth GmbH, Karlsruhe, Germany) or 10µl of Ethidium-Bromide (5µg/ml) / 100ml are added. After waiting for a short moment, the solution is cast in the mold. After it is polymerized, it can be used for electrophoresis in the electrophoresis chamber which is filled with TAE Buffer.

Depending on the size of the slots, between 10-45µl of PCR product are used. No Loading Buffer III was needed due to the usage of a pre-mix dye in the PCR, except for the direct blood PCR of patient 18. Additionally, a GeneRuler DNA Ladder Mix (Thermo Fisher Scientific, Waltham, Massachusetts, USA) is used to produce predictable bands at known base pair lengths which are used for orientation. The samples run on the gel at 100 – 160 volts for about 30 – 45 minutes. Afterwards, the gel is taken from the electrophoresis chamber and viewed at under UV-light (UV-Transilluminator, 60-ECM-20.M, Peqlab GmbH, Germany).

The PCR products from the direct blood PCR were cut out from the gel under UV-light and further processed. Specific PCR-bands could be extracted using a DNA Gel extraction kit (Merck Millipore, Massachusetts, United States). The pieces from the agarose gel are transferred to an ultrafree-DA unit. With the cap closed, the tube is centrifuged for 10 minutes at 5000 x g. After centrifugation, the extracted DNA is found in the collecting tube and can be further processed.

2.10.1 Gel Documentation Imaging System

Results seen under the UV-Transilluminator can also be documented through a photo documentation system using Gel Documentation Imaging (E-Box VX2, Vilber Lourmat Deutschland GmbH, Eberhardzell, Germany).

2.11 Restriction digestion

Instead of manually extracting the electrophoresis-bands for the sequencing, a restriction digestion can be performed. The restriction digestion is done using the PCR-product samples. 10µl of these samples are mixed with 3.8µl of dH_2O, 0.4µl Exonuclease I (Thermo Fisher Scientific, Waltham, Massachusetts, USA) 0.8µl Fast-AP, thermosensitive Alkaline Phosphatase (Thermo Fisher Scientific, Waltham, Massachusetts, USA). The multiwell or tubes are placed in a thermal cycler and kept initially at 37°C for 15 minutes and then at 85°C for 15 minutes. Exonuclease I degrades the remaining primers from the PCR while the alkaline phosphatase dephosphorylates the remaining dNTP.

2.12 Sanger sequencing

The aim of Sanger sequencing is the identification of the succession of the bases in the part of the genome analyzed. Possible mutations, deletions or insertions may be seen in this analysis. This method was developed in 1977 by Sanger and colleagues. The genomic sequence of interest has to be known in order to serve as a reference for the analyzed gene segment. In the first step, dsDNA is denatured into single-strands which act as templates for the sequencing. The principle is based on an in-vitro replication of DNA using a primer that anneals to the DNA strand in question which allows a heat-resistant polymerase to synthesize a complementary strand. DNTPs are added as in the PCR but fluorescently marked ddNTPs (didesoxynucleotides, also called terminators) are also present in a much lower concentration. By chance, these ddNTPs are built in to the newly synthesized strands and cause a stop of synthesis because there is no free 3'-OH-group

for the addition of another dNTP. This statistically generates strands of different size, at each end having a fluorescently marked ddNTP. These markings are detected in the next step by a laser in the detection chamber during capillary electrophoresis as the different products run along the capillary in a polymer. A respective base is assigned to each of the four different ddNTPs. A succession of these bases makes up the genomic sequence of the targeted DNA, which then can be computational analyzed and compared to a normal genomic sequence.

Between sequencing and capillary electrophoresis, a DyeEx removal (Merck Millipore, Massachusetts, United States) has to be done to remove an excess of DyeTerminators.

Primer mixes for sequencing are made up of 45µl dH_2O and 5µl of either sense or anti-sense primer. The mix has to be vortexed each time before use. 4µl from the restriction digestion step are now mixed with 11µl dH_2O, 1µl BigDye® Terminator V3.1 Ready Reaction Mix (Thermo Fisher Scientific Waltham, Massachusetts, USA), 3µl BigDye® Terminator 5x Sequencing Buffer Mix V1.1, V3.1 (Thermo Fisher Scientific Waltham, Massachusetts, USA) and 1.5µl Primer. Importantly, every strand is now mixed with just one primer (either sense or anti-sense).

Mutation screening was carried out by sequencing forward and reverse DNA strands.

The tubes are placed in a thermocycler using the following program for *DICER1* samples:

95°C – 5 minutes

95°C – 30 seconds
55°C – 30 seconds
60°C – 4 minutes
] 80 – 90 loops

10°C – pause

For *TP53* samples an annealing temperature of 60°C was used having 60 cycles.

The NCBI Reference sequence used was NM_177438.2.

2.13 MLPA - Multiplex Ligation-dependent Probe Amplification

2.13.1 Principle and purpose

Multiplex ligation-dependent probe amplification (MLPA) is a semi-quantitative method which allows to identify deletions as well as duplications in a targeted gene. It was first described in 2002 by Schouten and colleagues and one of the first applications was the examination of alterations in the *BRCA1* gene (Hogervorst et al. 2003). Nowadays, it is a commonly used method to examine large-scale variations on the genomic level (Stuppia et al, 2012). The general principle is the placement of a probe with high accuracy on a single DNA strand. It will then be amplified to be later analyzed in terms of quantity. MLPA is not designed to identify small point mutations. It also will not detect most inversions and translocations.

In the first MLPA step, dsDNA is heated so the DNA denatures and will split in single strands. Two short hybridizing sequences, which are complementary to the gene-DNA in question, are added and will dock on their respective counterpart. The sequences are designed in a way that they will be placed very close to each other. Each has a forward and reverse primer attached respectively, as well as an optional stuffer sequence between those two parts. Left and right part are named LPO and RPO for Left/Right Probe Oligonucleotide, respectively. When the hybridizing sequences bind adjacent to the single stranded target sequence, they will be fused in the middle via a ligase. Only high-fidelity binding of the sequences will allow hybridizing and therefore ligation. Consequently, the two fused portions will be called MLPA probe and are ready to be amplified by means of PCR. Importantly, only complete i.e. ligated probes will be amplified by PCR. During the PCR, one of the primers is fluorescently marked (FAM), allowing a detection by capillary electrophoresis. Finally, the results are analyzed with a specific software (e.g. SeqPilot) and interpreted using reference samples.

The basis for the usage of this method were the MRC-Holland (Amsterdam, Netherlands) MLPA General Protocol (MDP-005), last revised on 22.09.2014, the Standard Operating Procedure (SOP) for MLPA of the Universitätsklinikum Hamburg-Eppendorf, Klinik und Poliklinik für Pädiatrische Hämatologie und Onkologie, Version 01, updated on

20.10.2014 as well as the MRC-Holland 'Designing synthetic MLPA probes', version 12 (last update 13.01.2012) and version 14 (19.12.2014).

2.13.2 Components

The main MLPA components, excluding the *DICER1* specific probes, are the following:

MLPA Component	Ingredient
SALSA MLPA P200 Human reference probemix (human)	Contains selected reference probes for human DNA and are intended to be used with synthetic human DNA probes. Also contains controls which are found in other SALSA MLPA probemixes.
SALSA MLPA Buffer	KCl, Tris-HCl, EDTA, PEG-6000, oligonucleotide
SALSA Ligase-65 Enzyme	Glycerol, EDTA, Beta-Mercaptoethanol, KCl, Tris-HCl, non-ionic detergent, Ligase-65 enzyme (bacterial origin)
Ligase-65 Buffer A	Coenzyme NAD (also bacterial origin)
Ligase-65 Buffer B	Tris-HCl, MgCl2, non-ionic detergent
SALSA Polymerase	Glycerol, non-ionic detergents, EDTA, DTT, KCl, Tris-HCl, Polymerase enzyme (bacterial origin)
SALSA PCR primers	Synthetic oligonucleotides incl. dNTPs – FAM, fluorescent dye; Tris-HCl, KCl, EDTA, nonionic detergent

Table 2.3: MLPA components from a regular kit.

2.13.3 *DICER1*-Kit

Currently, no *DICER1* MLPA kit is available through MRC-Holland, meaning that a synthetic probemix covering all the 27 exons of the *DICER1* gene had to be designed manually. Previously, Sabbaghian et al. 2014 used MLPA to analyze germline *DICER1* genes in patients. In preparation for this project the authors of this paper were contacted

and made their information on their synthetic *DICER1* MLPA assay available which was developed in cooperation with MRC-Holland. These data mark the basis for the custom *DICER1* set used here.

There are distinct differences between a commercially available and a synthetic MLPA assay. For instance, the minimum and maximum number of probes is limited. At least 5 probes should be used but MRC-Holland does not recommend using more than 11 probes. *DICER1* consists of 27 exons, meaning that there would be at least 3 mixes to distribute the exons equally to the respective mixes. There are also restrictions e.g. on where to place the probes due to the GC content or the first nucleotide, which is found after the LPO primer binding sequence. For synthetic probes for human genes MRC-Holland recommends the use of P200 or P300 Human DNA Reference probemixes; P200 was utilized for this MLPA assay. The following LPO and RPO primer sequences were used at the 5' and 3' ends of left hybridizing sequences (LHS) and right hybridizing sequences (RHS) respectively (Sabbaghian et al. 2014):

LPO – forward primer sequence: GGGTTCCCTAAGGGTTGGA

RPO – reverse primer sequence: TCTAGATTGGATCTTGCTGGCAC

Also, the use of stuffer sequences in synthetic probes is not recommended by MRC Holland. The length of every probe should be unique i.e. the total length consisting of LPO plus RPO, while the differences between the different probes should at least be 4nt in order to guarantee a sufficient separation on an ABI sequencer. LPO and RPO themselves should at least be 41nt long. The minimum total length is 88nt when the P200 probemix is used, while the maximum length is 168nt. Shorter probes would cause a mixing with the Q fragments described later. In commercially available kits the length range is approximately 130 – 500nt. MRC recommends to use synthetics probes from Integrated DNA Technologies, IDT (Coralville, Iowa, USA): www.idtdna.com. Allele ID version 7.7 from PREMIER Biosoft (Palo Alto, CA, USA) was used as a software to design the custom probes (MRC protocol Version 14 Page 3).

2.13.4 Probes

DICER1 has 27 exons. Exon 1 is not coding. Exons 21 and 23 are relatively large and were split, resulting in two probes for each exon leading to 28 probes in total. The LHS and RHS can be found in in the tables in chapter 8.3.3. Having three mixes means therefore each patient requires three separate set-ups for a MLPA to analyze the complete gene. Therefore, each patient has three sets starting with 5µl of DNA. Mix I contains probes for exons 2, 3, 4, 7, 8, 10, 20, 21a, 27. Mix II covers exons 5, 6, 9, 11, 12, 13, 14, 18, 21b, 23a and Mix III exons 15, 16, 17, 19, 22, 23b, 24, 25, 26.

2.13.5 Control fragments

Several fragments are included in the MLPA to ensure the quality of the MLPA. So called Q-fragments are an indicator for a low amount of DNA, i.e. less than 10ng or problems during the ligation process. These Q-fragments are four fragments varying in length between 64 – 82nt and will show as high peaks in case in one of those problems. Two D-fragments are smaller peaks in later analysis when problems during denaturation occur. They hybridize to high GC-content areas which are called CpG-islands and are difficult to denature. Incomplete denaturation is of special note because it can cause false-positive deletions in the MLPA. For Q- and D-fragments there is a 92nt benchmark probe which allows an interpretation of peak height and configuration of the control fragments. Additionally, the mix also contains X and Y fragments for gender control.

2.13.6 Procedure

One cycle of MLPA takes approximately two days. On the first day denaturation and hybridization take place. The procedure starts with 5µl DNA having a total concentration of 50 – 250ng, ideally 50 – 100ng. After a denaturation period of 5 minutes at 98°C, the wells or tubes are removed from the thermocycler and centrifuged shortly to remove any condensate from the cap of the tubes. Afterwards 1.5µl SALSA MLPA Buffer, 1µl SALSA MLPA P200 reference probe mix and variably 0.5µl of *DICER1* Probe Mix I, II or III are added to each well or tube for the hybridization reaction. This is done by creating

a hybridization master mix for each *DICER1* Probe Mix I, II or III. Then subsequently 3µl of the mix are added to the tube. Mixing is done by pipetting up and down or by vortexing. SALSA MLPA Buffer, SALSA MLPA P200 reference Mix as well as the *DICER1* Probe Mix should be thoroughly vortexed before use.

After adding the 3µl, the tubes will be centrifuged once more and placed in the thermocycler. One minute at 95°C ensures complete separation of the strands and the following step at 60°C will take 16-20 hours allowing the hybridization sequences to bind to the single stranded DNA. The next day ligation master mixes are prepared using 25µl dH_2O, 3µl Ligase-65 Buffer A, 3µl Ligase-65 Buffer B and 1µl SALSA Ligase-65 enzyme per well. SALSA Ligase-65 enzyme must be kept at approximately -22°C before and after preparation. It is important that the tubes are kept in the thermocycler during the preparation (60°C) as well as the adding of the 32µl per well, which is done at 54°C. The program continues for 15 minutes at 54°C, afterwards at 98°C for 5 minutes to inactivate the ligase-65 enzyme. The program pauses at 20°C and the tubes will be taken from the cycler and be stored at room temperature. Following this step 7.5µl dH_2O, 2µl SALSA PCR Primer mix and 0.5µl SALSA Polymerase are added through a Polymerase master mix. The primers need to be vortexed and stored protected from light before being added to the mix. The Polymerase is kept at approximately -22°C until used for the mix and then warmed for about 10 seconds to reduce viscosity. Subsequently, 10µl from the Polymerase master mix are added to each tube manually or by use of the repeating pipette, in the latter case gently swiveling the tubes afterwards. The tubes are then centrifuged briefly again and placed in the thermocycler for the polymerase chain reaction. The PCR products can be stored for about a week at 4°C, for longer periods of time a much lower storing temperature is needed.

A summary of the procedure including the thermocycler configuration can be described as the following:

1. Denaturation (day 1)
    a. 98°C - 5 min
    b. 25°C - pause
2. Hybridization (day 1)
    a. 95°C - 1 min
    b. 60°C - pause (16-20h)

3. Ligation (day 2)
    a. 54°C - pause
    b. 54°C - 15 min
    c. 98°C - 5 min
    d. 20°C - pause
4. PCR (day 2)
    a. 35 cycles:
        (1) 95°C - 30 sec
        (2) 60°C - 30 sec
        (3) 72°C - 1min
    b. 72°C - 20 min
    c. 15°C - pause

Further preparation for the capillary electrophoresis involves a two time 1:10 dilution of the *DICER1* MLPA PCR products. This is done by mixing 2µl PCR product with 18µl dH_2O. Afterwards, 2µl of the diluted PCR product are added to 17.75µl formamide plus 0.25µl LIZ® (Thermo Fisher Scientific, Massachusetts, USA) and stored in a fridge. The mix is heated for 3 minutes at 86°C for a separation of the strands and afterwards cooled at 4°C for 2 minutes. Formamide prevents the realignment of the strands. The ABI sequencer then separates the products by length by an electronic potential, causing the products to migrate along the capillary, and measures in the detection chamber the colors of the fluorescent dyes at a specific wavelength. The LIZ® standard marks standard length products so different lengths can be recognized.

2.13.7 MLPA data analysis

An electropherogram is obtained from the previous step and analyzed with a computer software, for example Sequence Pilot (SeqPilot) Version 4.1.2 Build 513 which was used in this case. The files from the ABI are loaded into the software and are at first presented as peak patterns in which the peaks present different relative heights. Absolute fluorescence which is obtained from capillary electrophoresis is not directly used for the analysis. First the peaks within the probe itself (reference probes) are compared (*intrasample* normalization) but also to other samples which should have a normal copy

variant number (normal diploid controls – *intersample* normalization, see below). This means that the relative height of a peak is of interest and not its absolute height.

According to the control fragments there will be four peaks in case there was not enough DNA present in the tube. Also, two D-fragment peaks would present as low compared to the 92nt benchmark probe in case of a problem with denaturation during the MLPA process.

A technical validation occurs to check for any misalignments or other possible errors in the electropherogram.

2.13.8 Presentation and interpretation of results

A completed sample is then compared with normal controls. The controls can be chosen manually and are expected to have a normal gene dose (*intersample* normalization). These normal controls form a compare group which reflect the normal number of copy number variants. The amount of gene dose is represented by a vertical bar which for the sample is colored green and for the controls blue. The blue control bar also shows the standard deviation between the controls. Additionally, a value for the difference in gene dose is given below this illustration and is also depicted as a bar deviating from a mean line which marks 100% and therefore a normal amount of gene dose. An extension of the bar to the top marks a gain of gene dose (up to 200%), while a deviation to the bottom visualizes a decline of gene dose (up to 0%). Summarizing, this means that a bar in the illustration pointing to the bottom shows a deletion and a bar going upwards represents a duplication. Each probe is visualized and labeled for the respective exon and gene it stands for. An example of MLPA results can be seen in figure 3.12.

More reliable results are obtained if the standard deviation of the reference samples is low, i.e. <10%. The same applies if decreased or increased signals are found for adjacent exons. The comparison between the sample and the controls finishes with the medical validation within the software.

2.14 OncoScan® Assay (not part of this thesis)

This procedure was done by the laboratory of human genetics of the university Kiel. It is a DNA microarray in which immobilized unique sequences of single stranded DNA are placed on a chip. Patients and control DNA are fluorescently marked with different colors and are placed on the chip where they will complementarily bind to their respective counterparts. Afterwards a camera scans the fluorescence and a quantitative comparison between the gene doses is made. Small mosaicisms or balanced mutations cannot be detected.

3 Results

3.1 Polymerase chain reaction and Sanger sequencing

In four patients (14, 16, 17, 18) a complete sequencing and PCR of the inspected area of the somatic PPB DNA was possible. In patients 11, 13 and 16 large portions of the *DICER1* gene could be analyzed. In patient 8 PCR and Sanger sequencing was successful in a total of seven exons. Mostly due to poor quality or sometimes low quantity of the DNA or tumor material, very few or, as for patients 9 and 12, no successful analysis of *DICER1* was possible. Six patients showed at least one, out of which three patients had two mutations. Mutations were found in the tumor DNA of patients 7, 13, 14, 16, 17 and 18 and are summarized in table 3.1.

Patient	Exon	Mutation	Predicted AA change	Origin
7	**16**	c.2437-1G > A	Splice site	ND*
13	**25**	c.5428G > T	p.Asp1810Tyr	ND
14	**23**	c.4399dupA	p.Ile1467Asnfs*10	ND*
16	**24**	c.5299delC	p.His1767Metfs*71	ND
	25	c.5438A > G	p.Glu1813Gly	ND
17	**17**	c.2782C > T	p.Gln928*	ND*
	25	c.5425G > A	p.Gly1809Arg	ND
18	**10**	c.1510-1G > A	Splice site	Germline*
	25	c.5438A > G	p.Glu1813Gly	Somatic

Table 3.1: Overview of the somatic and germline mutations found in *DICER1* gene in pleuropulmonary blastoma DNA. ND = not determined. * = previously not described mutations. AA = amino acid.

Most of the mutations were point mutations and specifically substitutions, in which one base is replaced by another. When this replacement leads to a change in the amino acid that is translated, it is called a *missense*-mutation. The sequencing also showed duplications as well as deletions. In these cases, at least one base is duplicated or deleted and results in a frame shift, provided the change is not a multiple of three. Furthermore, two splice-site-mutations were found.

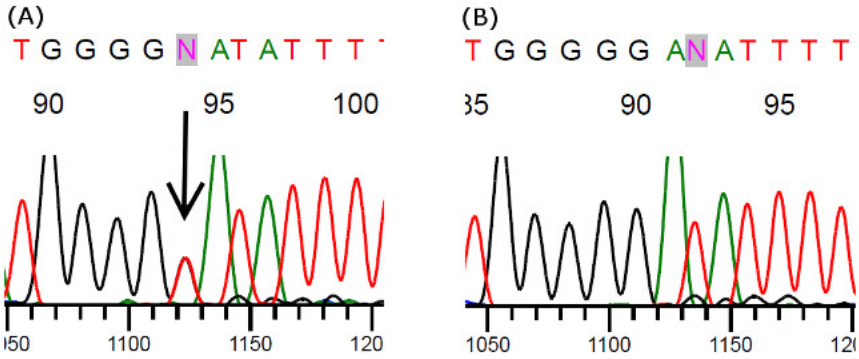

Figure 3.1: *DICER1* sequencing of exon 25 in patient 13 at mutation site c.5428 G > T, SN.
(A) Shows the substitution of guanine to thymine while (B) shows the wild type. In this graphic representation, the red peak of thymine in (A) is exactly overlying the black peak of guanine, which is why the black peak is not visible although it is present. A single peak would indicate homozygosity. Note that the automatically designated nucleotide "N" in the wild type (B) is not correct and is caused by background noise. SN represents the sequencing in sense direction.

In **patient 13** c.5428 G > T designates that at nucleotide position 5428 guanine (G) was replaced by thymine (T) resulting in an amino acid change from aspartic acid (D) to tyrosine (Y) at position 1810 in exon 25. This is due to the change of the codon GAT to TAT (figure 3.1). This mutation was heterozygous and is a so called *transversion* because a purine (in this case guanine) was replaced by a pyrimidine (in this case thymine). Using PolyPhen-2 (Polymorphism Phenotyping v2, http://genetics.bwh.harvard.edu/pph2, Adzhubei et al. 2010), which is a tool to predict the functional effects of an amino acid substitution, the mutation was predicted to be *probably damaging* with a score of 1.00. This means, that a negative alteration of the function of DICER1 is very likely. Since no corresponding DNA from peripheral leukocytes was available, it is not possible to determine if the mutation is of somatic or germline origin.

Analogously in **patient 16**, the change of adenine to guanine at position 5438 leads to a codon change from GAG to GGG and a predicted change from glutamic acid (E) to glycine (G) in position 1813 in exon 25 (figure 3.2). This on the other hand is a *transition* because a purine is replaced with a purine, namely adenine to guanine. The predicted consequence using PolyPhen-2 shows a probably damaging effect on the functionality of the enzyme with a score of 1.00 (see also chapter 4.3.1). This same point mutation was also found in **patient 18**. Both mutations were heterozygous in patients 16 and 18. Since

the mutation in patient 18 was only found in the tumor DNA and not in the DNA extracted from blood it is of somatic origin. Due to lack of additional material this differentiation was not possible for patient 16.

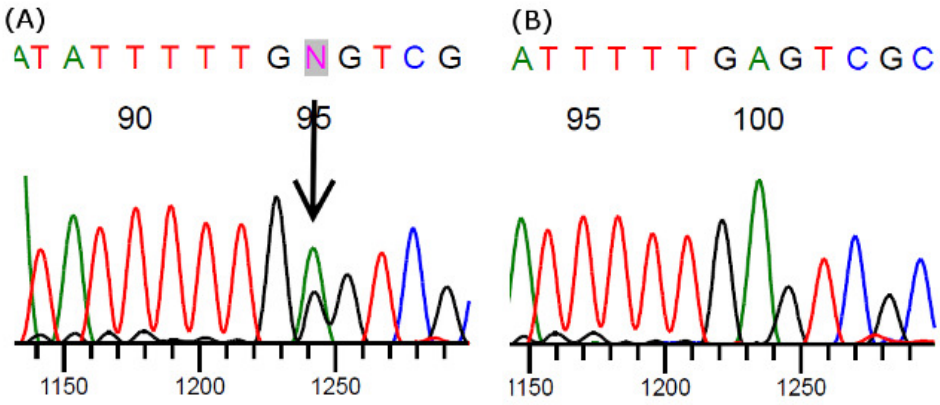

Figure 3.2: Sequencing of exon 25 of *DICER1* in patient 18 at mutation site 5438A > G, SN.
Sequencing shows a heterozygous substitution mutation (A) compared to the wild type sequence (B). Adenine is replaced by guanine and results in p.Glu1813Gly. SN represents the sequencing in sense direction. The same mutation was found in **patient 16**.

A substitution mutation at position 5425 from guanine to adenine leads to an amino acid change of glycine to arginine at amino acid position 1809 in exon 25 of **patient 17** due to the codon change from GGG (Gly, G, Glycine) to AGG (Arg, R, Arginine). This change also resulted in a probably damaging effect on the protein with a score of 1.00 according to the PolyPhen-2 tool. This mutation was heterozygous as well. A second mutation was found in this patient: The change of cytosine to thymine at DNA position 2782 of exon 17 in patient 17 results in a change of codon CAA (Glutamine, Gln, Q) to TAA which is a stop codon that leads to a termination of translation (*nonsense*-mutation, figure 3.3). A premature stop codon has severe effects and will probably result in *nonsense mediated decay* of mRNA and hence lack of translation into a protein. A differentiation between somatic and germline origin was not possible.

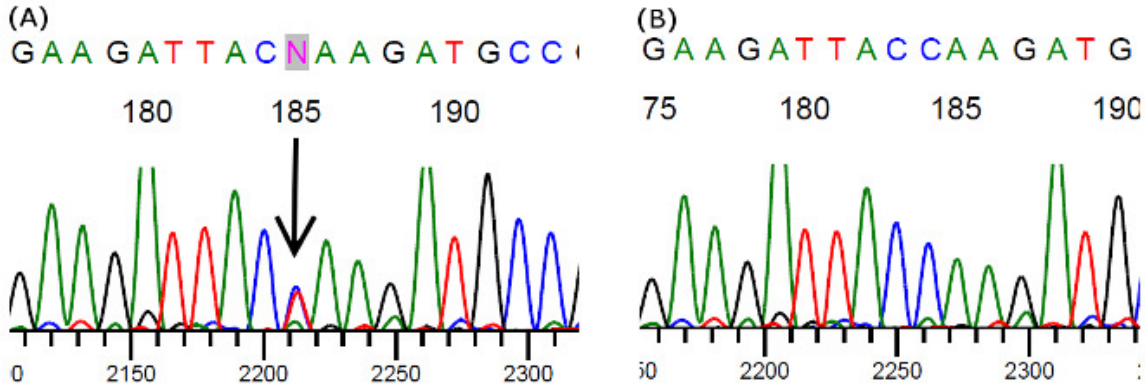

Figure 3.3: *DICER1* sequencing of exon 17 in patient 17 at mutation site c.2782C > T leading to p.Gln 928*, SN.

The sequencing shows a thymine instead of a cytosine leading to a codon change of CAA (glutamine) to TAA (A) compared to the wild type (B), which is a stop codon. This is a nonsense-mutation and leads to an incomplete and hence dysfunctional or -most likely- nonfunctional or not translated protein (loss-of-function mutation). SN represents the sequencing in sense direction.

In exon 23, adenine at position 4399 is duplicated (**patient 14**). This results in a frame shift and a new stop codon after 10 altered amino acids, which will probably also result in nonsense mediated decay of mRNA and hence a null allele (figure 3.4).

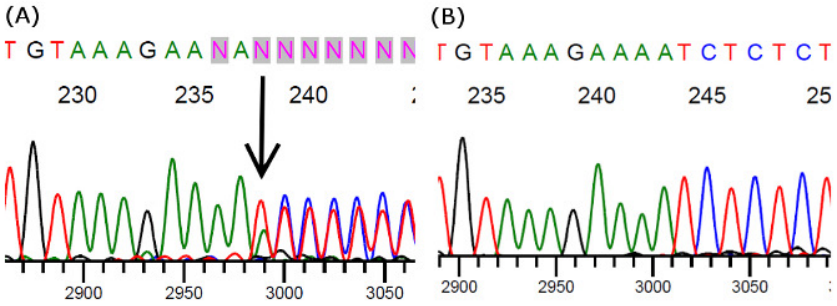

Figure 3.4: Sequencing of exon 23 of *DICER1* in patient 14 at mutation site c.4399dupA, SN.

Sequencing shows a duplication of adenine in position 4399 compared to the wild type (B). This leads to a frame shift mutation p.Ile1467Asnfs*10. SN represents the sequencing in sense direction.

Similarly, a deletion at position 5299 of cytosine results in a frame shift of CAT to ATG and a new stop codon after 71 altered amino acids which will probably also result in nonsense mediated decay of the mRNA (figure 3.5, **patient 16**).

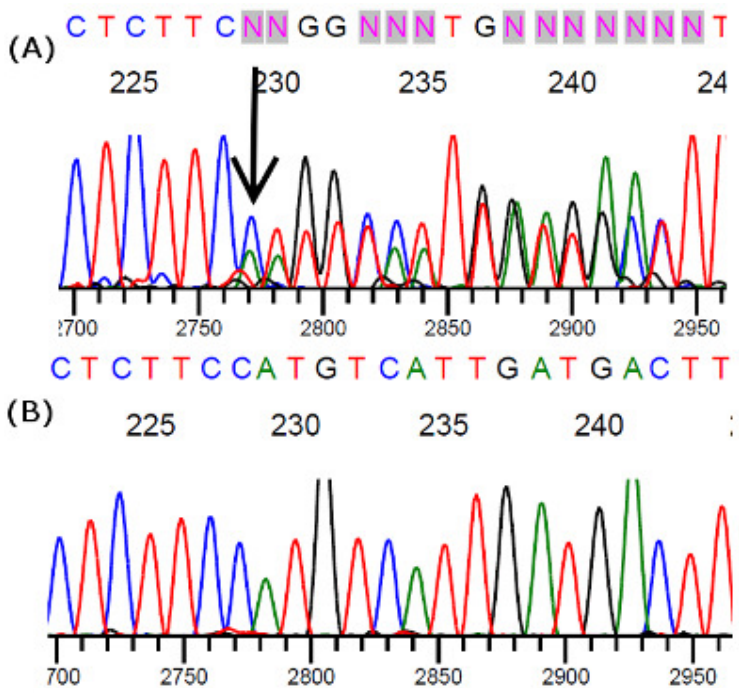

Figure 3.5: Sequencing of exon 24 of *DICER1* in patient 16 at mutation site c.5299delC, SN. Sequencing shows a deletion of cytosine compared to the wild type sequence (B). The consequence is a frame shift mutation (p.His1767Metfs*71) leading to a changed reading frame and a premature stop codon after 71 amino acids probably resulting in nonsense mediated decay of mRNA. SN represents the sequencing in sense direction.

Patient 18: Position 1510-1 designates the last nucleotide of intron 9. The mutation results in a change of guanine to adenine and therefore is a splice site mutation of exon 10 (figure 3.6). The mutation is heterozygous. Splice site mutations can have different effects. There may be a new splice site which could be either in intron 9 or exon 10. In both cases the reading frame may be altered (in-frame or out-of-frame shift). This could result in a premature stop codon. Another possibility is an exon skipping of the entire exon 10. In this thesis, no additional RNA analysis was performed. Therefore, no in vitro simulation of the effect of the splice site mutation was done. Instead, the tool *Human Splicing Finder V3.1* (http://www.umd.be/HSF3/index.html, Desmet et al. 2009) was used for the mutation c.1510-1G > A. The tool predicted, that the acceptor splice site of exon 10 could be affected and predicted a new intronic cryptic acceptor site.

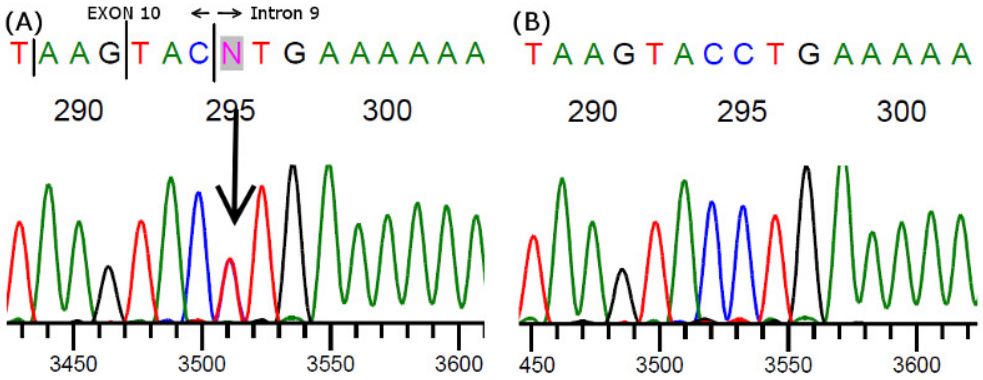

Figure 3.6: Sequencing of exon 10 of *DICER1* in patient 18 at splice site mutation c.1510-1G > A, ASN. The change of guanine to adenine at the last nucleotide of intron 9 results in a splice site mutation. The *predicted* effect is a broken acceptor splice site of exon 10. ASN represents sequencing in antisense direction.

A second heterozygous splice site mutation was found in **patient 7** at the last nucleotide of intron 15, where guanine was replaced by adenine (figure 3.7). The Human Splicing Finder V3.1 predicted that the substitution mutation could lead to a broken wild type acceptor site and most probably affects the splicing process. Due to the lack of genomic DNA from the patient it was not possible to differentiate between somatic and germline origin.

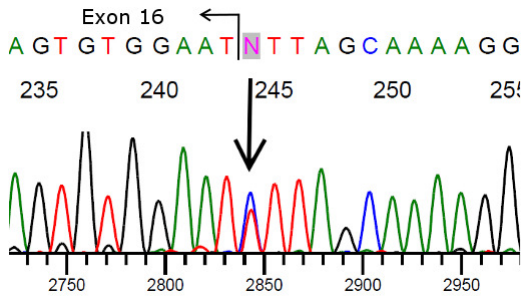

Figure 3.7: Patient 7, exon 16 of *DICER1* – Sequencing at splice site mutation c.2437-1G > A, ASN.
A variant of the last nucleotide of intron 15 eliminates wild type acceptor site.

All of the mutations described above were reproduced by repeated PCR and Sanger sequencing. In patient 7 the mutation was confirmed by sense and antisense sequencing.

The following table (3.2) gives an overview of the results from both methods, PCR and Sanger sequencing, including the mutations. In the patients shown in this table, the

majority of tests were successful. Because there was no genomic DNA available, a determination between a germline mutation and a somatic origin often could not be made.

Patient	11	13	14	15	16	17	18a
Exon							
2	✓	✓	✓	✓	✓	✓	✓
3	✓	✓	✓	✓	✓	✓	✓
4	✓	✓	✓	✓	✓	✓	✓
5	x	✓	✓	x	✓	✓	✓
6	✓	✓	✓	✓	✓	✓	✓
7	✓	✓	✓	✓	✓	✓	✓
8	x	✓	✓	x	✓	✓	✓
9	+ / –	x	✓	x	✓	✓	✓
10	x	x	✓	x	✓	✓	✓
11	✓	– / +	✓	✓	✓	✓	✓
12	x	x	– / +	x	✓	✓	✓
13	– / +	✓	✓	x	✓	✓	✓
14	✓	✓	✓	✓	✓	✓	✓
15	x	+ / –	✓	x	✓	✓	✓
16	✓	✓	✓	✓	✓	✓	✓
17	x	x	✓	x	✓	✓	✓
18	x	x	✓	x	✓	✓	✓
19	x	✓	✓	x	✓	✓	✓
20	x	x	✓	x	✓	✓	✓
21-1	x	✓	✓	x	✓	✓	✓
21-2	✓	✓	✓	✓	✓	✓	✓
22	✓	✓	✓	– / +	✓	✓	✓
23-1	✓	✓	✓	✓	✓	✓	✓
23-2	✓	✓	✓	+ / –	✓	✓	✓
24	✓	✓	✓	✓	✓	✓	✓
25/26	✓	✓	✓	✓	✓	✓	✓
27	✓	✓	✓	✓	✓	✓	✓

Table 3.2: *DICER1* PCR and Sanger sequencing results of patients 11, 13-18a.
X = PCR and Sanger sequencing failed; ✓ = both methods successful; light grey background = mutation; – / + = PCR failed / Sanger sequencing successful; + / – = PCR successful / Sanger sequencing failed.

Summarizing, there were only four patients in which a complete sequencing of all coding exons of *DICER1* was possible: patients 14, 16, 17 and 18a.

In the other PPB cases, it became clear that due to either low quantity or poor quality the methods used were not as successful as in patients 11 and 13 – 18a. The agarose gel electrophoresis showed that there was often no usable PCR product to use for Sanger sequencing.

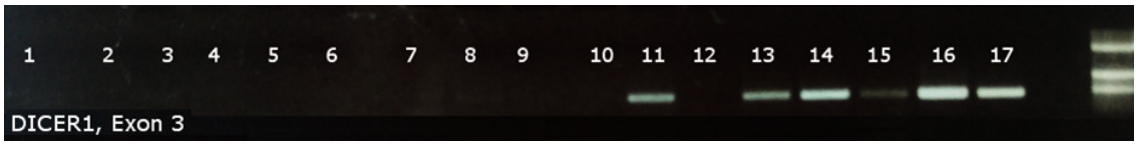

Figure 3.8: Agarose gel electrophoresis of PCR-amplified products of exon 3 of *DICER1* of patients 1 - 17. Not labeled on the far right: molecular weight marker.

One example from agarose gel electrophoresis after PCR showing almost all patients reinforces these findings (figure 3.8). The figure shows that for exon 3 of *DICER1* there was virtually no PCR product in the agarose gel electrophoresis for patients 1 – 10 and 12. Patients 11 and 13 – 17 on the other hand show a clear, well-defined band. The band of patient 15 is the weakest of those bands. As expected, there were several exons of patient 15 that were not successfully sequenced due to the poor quality of the DNA. Also, the use of more DNA in patient 15 could not improve the sequencing results of the previously unsuccessful exons. On the right of the figure the molecular weight marker can be seen.

Also, additional preparation of the FFPE with gaining of new genomic DNA and Whole Genome Amplification (WGA) was performed in several patients. To increase the probability of successful analysis larger amounts of DNA were used for PCR reactions. Ultimately, the entire genetic DNA which was available for patients 1 – 10 was used up.

Patient	1	2	3	4	5	6	7	8	10
Exon									
16	x	x	✓	x	✓	x	✓	x	x
17	x	x	x	x	x	x	x	x	x
24	✓	✓	✓	✓	✓	✓	✓	✓	✓
25	✓	✓	✓	x	x	✓	✓	✓	✓
26	✓	✓	✓	x	x	✓	✓	✓	✓

Table 3.3: Sequencing results of *DICER1* exons 16, 17, 24, 25 and 26 in Patients 1 – 8 and 10. Because most *DICER1* mutations in PPB patients were found in exons 24 and 25, they were sequenced in all the patients. X = Sanger sequencing failed; ✓ = Sanger sequencing successful; light grey background = mutation.

Most of the mutations found in this thesis were in exon 25. In the published literature, the majority of mutations were described in exon 24 and 25. For this reason, those exons were screened preferably to increase the chance of finding mutations in the rest of the patients (table 3.3). Further sequencing results are depicted in table 3.4.

Patient	Successful sequenced *DICER1* exons	Unsuccessful sequenced *DICER1* exons
3	3, 4, 6, 16, 21-2, 22, 24 – 26	2, 5, 7, 8, 10, 17, 19 – 21-1
4	2, 24	3 – 23-2, 25 – 27
5	2, 3, 16, 24	4 – 15, 17 – 23-2, 25 – 27
6	23-2 – 27	10, 16, 17
8	2 – 7, 9, 21-2 – 23-1, 24 – 26	8, 10 – 21-1, 23-2, 27

Table 3.4: Sequencing results of patients 3 – 6 and 8 of *DICER1*.
Most likely due to poor quality of the genomic DNA, sometimes Sanger sequencing was not successful.

There was a mutation in intron 21 (c.4206+9G>T) in patient 3 that, according to the Human Splicing Finder V3.1, has no impact on splicing and according to the *Ensembl Variation database* (http://www.ensembl.org) had a MAF (minor allele frequency) of 0.13 and therefore is a benign single nucleotide variation. No additional mutation was found in patient 3.

3.2 Germline analysis, family members and thyroid carcinoma

3.2.1 Patient 18

Only a very small amount of blood was available from patient 18 which was not sufficient for a routine DNA isolation. For this reason, a direct blood PCR was done which only allowed PCR testing for exon 10 and 25 in which the somatic mutations were found previously. In exon 10, the heterozygous splice site mutation c.1510-1G>A was confirmed while the heterozygous missense mutation in exon 25 of *DICER1* was not identified. In the twin sister and both parents neither the missense nor the splice site mutation were found. This means that the germline splice site mutation in the patient is with a high probability a de novo germline mutation in patient 18. In contrast to the somatic mutation of the PPB (c.5438A > G), the germline mutation is present in all tissues of the patient.

3.2.2 Patient 12

In this patient the sequencing of the genomic DNA isolated from the FFPE was not successful. The patient developed a papillary thyroid carcinoma which was also available as FFPE. Sequencing of all exons and flanking introns showed no mutations. Genomic DNA from peripheral leukocytes of the parents was also available and showed normal sequencing results.

Further testing on this patient was performed and will be laid out in chapters 3.4.2.1 and 3.5.

3.3 TP53

In the literature, a varying degree of *TP53* (or *p53*) mutations were found in PPB specimens. This is why further sequencing was done when sufficient material was available. Sometimes, it was used to test if the sequencing of a different gene was more successful than that of *DICER1*. Sequencing of a control patient was successful and showed no mutations. However, DNA sequencing of the pleuropulmonary blastoma patients was difficult as well. In patients in which some genomic DNA was left, PCR and Sanger sequencing were performed. For comparison, the following figure (3.9) from agarose gel electrophoresis shows control samples as well as two of the healthy family members of a patient:

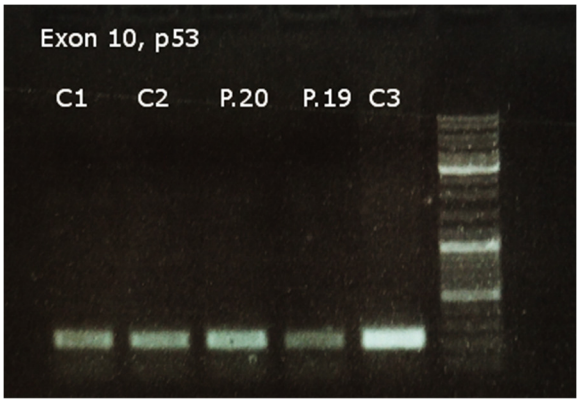

Figure 3.9: Agarose gel electrophoresis of exon 10, *p53*, patients 20 and 19 and controls (C1 - C3). Not labeled on the right: molecular weight marker.

In figure 3.9 all of the bands of exon 10 of *p53* can be seen clearly. In contrast, in the PPB tumor material the results were not as consistent. Not all patients could be tested due to low DNA quantity. Out of those tested, most exons were successfully sequenced in patients 16 and 17.

Figure 3.10 and 3.11 show clearly visible and strong bands by agarose gel electrophoresis particularly for patients 16 and 17 and for exon 11 in patient 4. Additionally, the bands fade out in contrast to the control samples and healthy individuals which is attributed to the poor DNA quality even after prior purification.

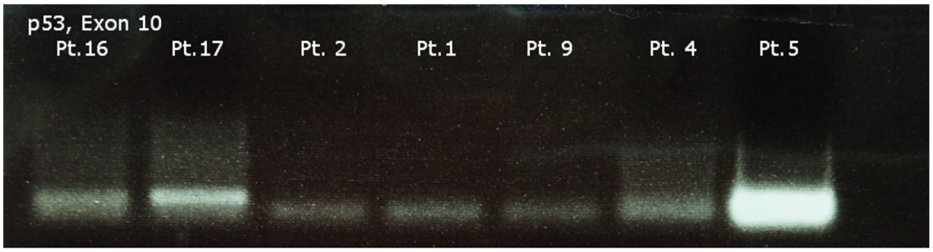

Figure 3.10: Agarose gel electrophoresis of exon 10, *p53* patients 1, 2, 9, 4, 5, 16 and 17.

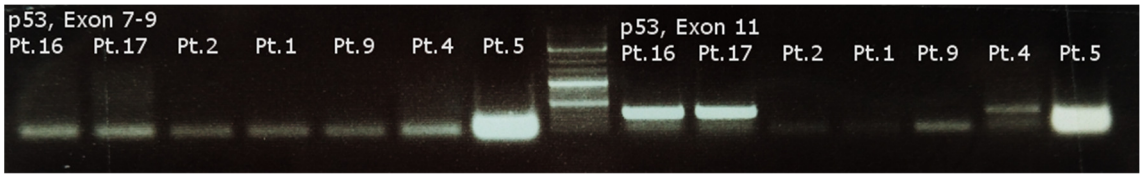

Figure 3.11: Agarose gel electrophoresis of exon 7-9 and 11 of *p53*. Not labeled in the middle: molecular weight marker.

In patient 17, amplification and sequencing of exons 5, 6, 10 and 11 were successful but showed no mutations. In patient 16, in addition to those four exons, exon 4 was sequenced but the results were unremarkable. In patient 4, exons 10 and 11 and in patient 5, exon 11 was sequenced but showed no mutations. In contrast to the slight bands visible by gel electrophoresis, sequencing of all exons of *TP53* in patients 1, 2 and 9 were unsuccessful. Ultimately, no *TP53* mutation was identified.

3.4 Multiplex Ligation-dependent Probe Amplification

3.4.1 Controls

Prior to the testing of the somatic tumor DNA, several controls were run previously to assess the functionality of the custom MLPA. Most of the controls were completely unremarkable as for example shown here (figure 3.12).

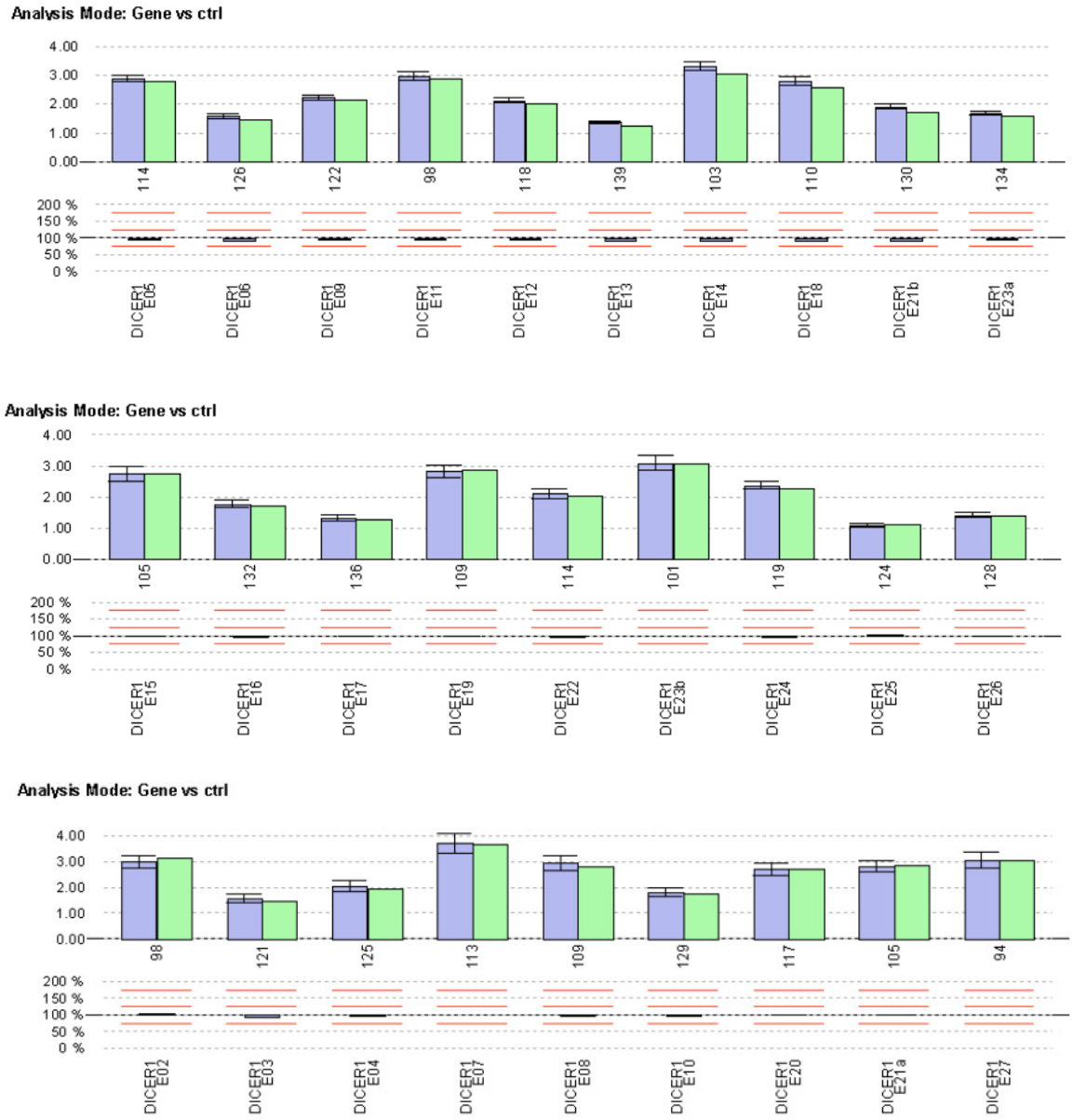

Figure 3.12: *DICER1* MLPA of a control patient. The MLPA shows no abnormality compared to the controls.

The controls and their mean gene dose are on the left in light blue while the healthy control is on the right in green. Overall there are only minimal variations and therefore no deletion or duplication is detected. Some of the controls also showed variations in part of the gene or even the complete gene. MLPA was repeated for those controls resulting usually in confirmation than rather in a change of the result.

The control illustrated in figure 3.12 was run multiple times and in one case, even though the intra- and intersample controls all were normal, there was a relative gene dose reduction of less than 50% detected in five exons in one of the mixes:

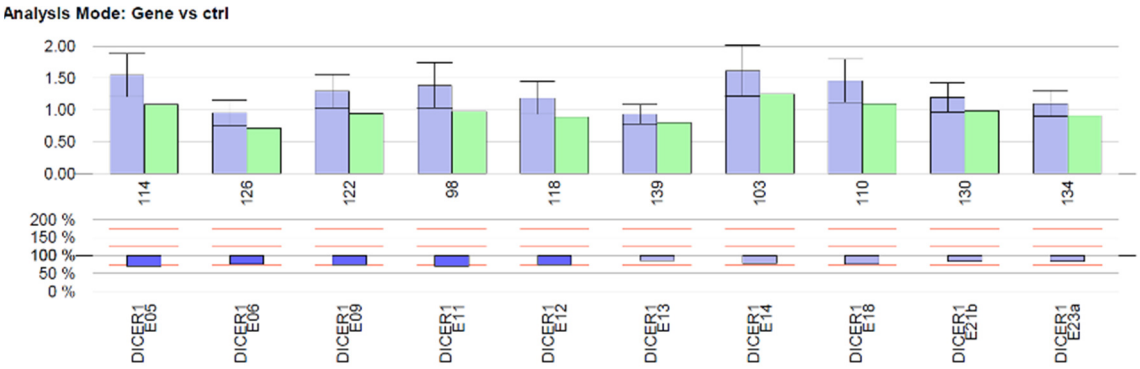

Figure 3.13: *DICER1* MLPA of a control patient. The illustration is showing a relative gene dose reduction of exons 5, 6, 9, 11 and 12 compared to the controls and therefore is marked as a deletion.

As seen in the illustration above in figure 3.13 there is a general reduction of gene dose and especially in exons 5, 6, 9, 11 and 12. This test result was not seen in the other *DICER1* mixes. The amount of gene dose reduction is small compared to other deletions and would not be considered significant.

In another genomic DNA control, the MLPA showed a deletion in the complete *DICER1* gene, exemplary shown here in figure 3.14.

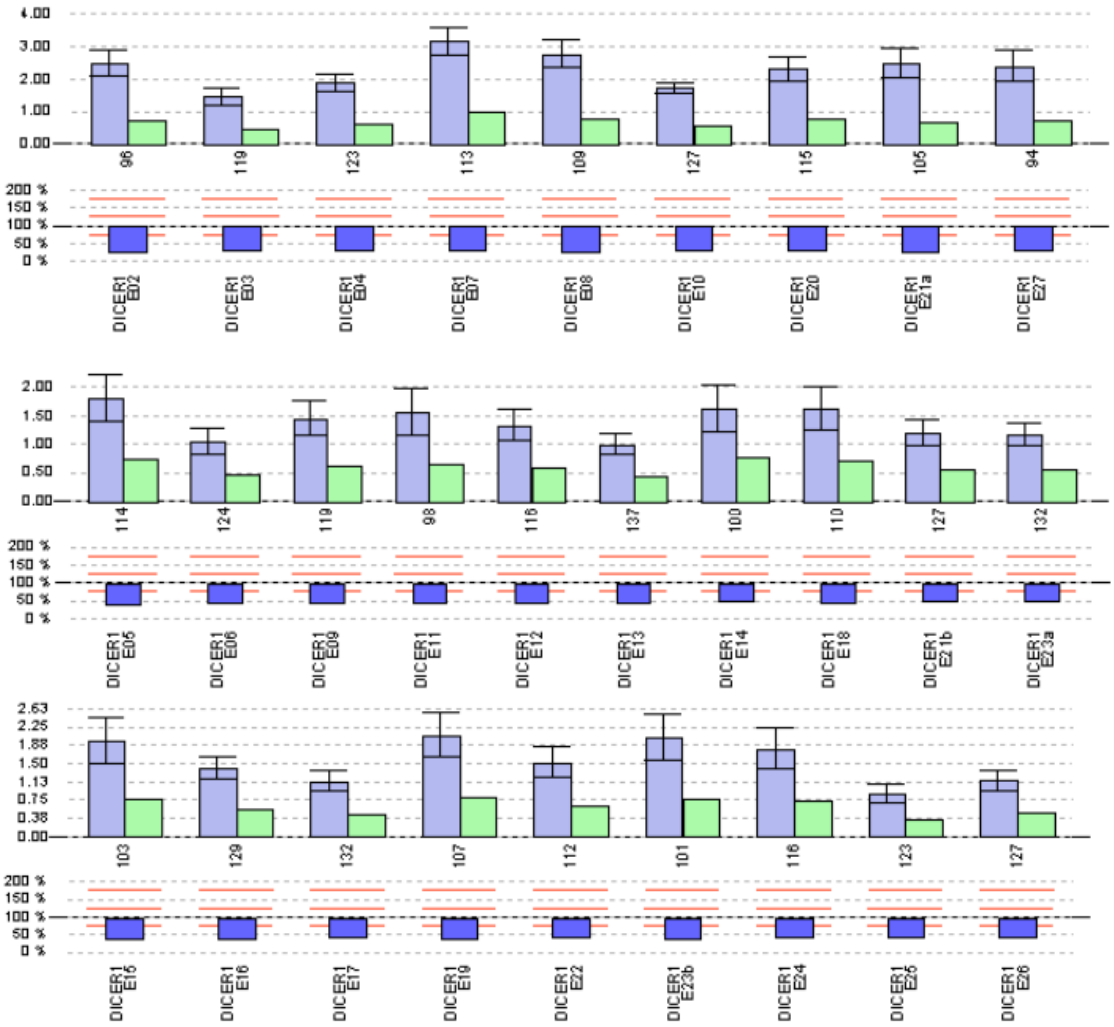

Figure 3.14: *DICER1* MLPA of a healthy control patient. It shows a deletion in all *DICER1* exons compared to the gene dose of the controls.

This control DNA was tested three times and always yielded the same result. For this patient there was no known genetic defect or history of disease. It is possible though that this control patient does have a deletion which was previously not known. Due to the heterogeneity of the results Sabbaghian et al. 2014 were contacted. They initially developed the synthetic MLPA for *DICER1* in collaboration with MRC Holland. In their paper they reported a patient which showed a deletion of exon 21 of *DICER1*. They provided a sample of the genomic DNA of that patient to test the validity of the MLPA. The MLPA confirmed the sole deletion of exon 21. The deletion of exon 21 of *DICER1* also had the advantage that, due to the size of exon 21, it was divided between two of the

three *DICER1*-MLPA mixes. Both mixes showed a significant reduction in gene dose, seen in figure 3.15.

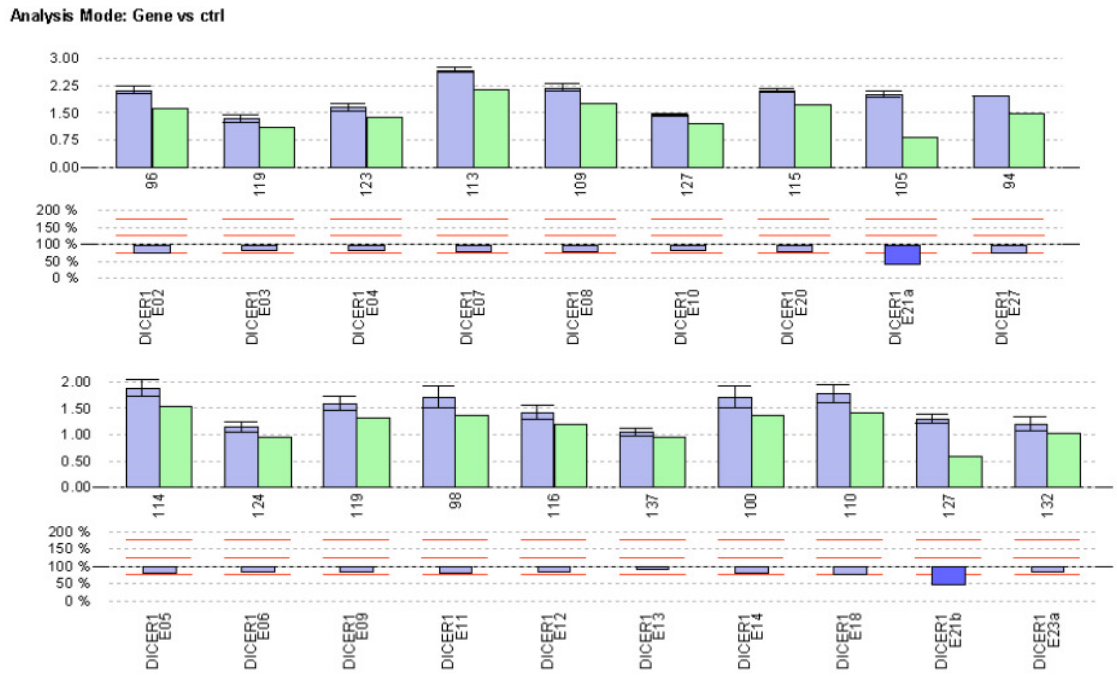

Figure 3.15: *DICER1* MLPA of a positive control from Sabbaghian et al. 2014. Both parts of exon 21 i.e. E21a and E21b show a reduction of more than 50% compared to the controls. This finding is consistent with a heterozygous deletion.

3.4.2 Patients

Due to lack of genomic DNA in patient 18 a germline MLPA was not performed.

3.4.2.1 Patient 12: Germline and family members

The germline MLPA of patient 12 showed a significant reproducible deletion of *DICER1* in all exons.

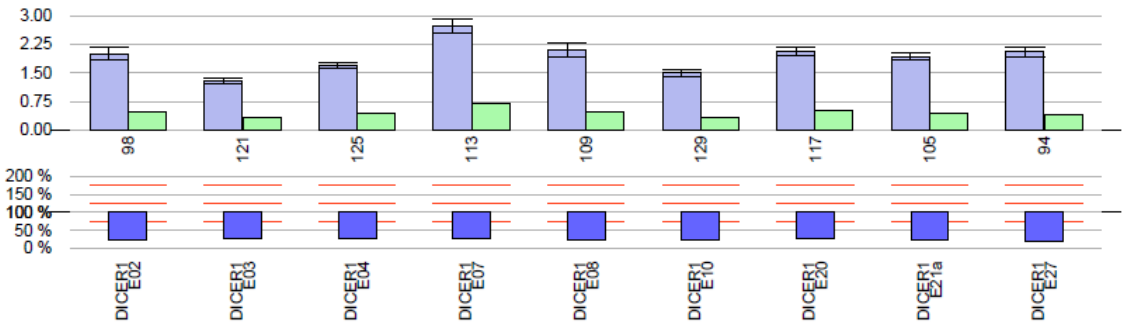

Figure 3.16: *DICER1* MLPA of patient 12. As represented above, there is a significant gene dose reduction of well over 50% compared to the controls. These deletions were found in all *DICER1* exons.

What is shown exemplary in figure 3.16 could also be seen in the other mixes and therefore all exons of *DICER1*. There was a gene dose reduction of more than 50% compared to the controls. This suggests a heterozygous germ line deletion of *DICER1* in patient 12. Because the MLPA is only designed to look for *DICER1* it does not provide any further information on the actual size of the deletion. The MLPA of the parents (i.e. patients 19 and 20) were normal which means that there is most likely a heterozygous de novo germline deletion in patient 12. Fittingly, analysis of somatic DNA from the pleuropulmonary blastoma also confirmed the deletion by MLPA.

The father of patient 12 had a history of seminoma and did not show a deletion of *DICER1* in the MLPA. In light of these results, there is no indication that the seminoma emerged due to a deletion in the germline *DICER1* gene.

3.4.2.2 Pleuropulmonary blastoma

Out of all 18 pleuropulmonary blastoma derived genomic DNA cases which were tested via MLPA, none was unremarkable. Patient 6 and patient 12 showed a heterozygous deletion of all *DICER1* exons respectively.

In another group of seven patients, only deletions and in one patient only duplications next to non-amplified exons were found. Patients 1, 3, 4, 5, 7, 11, 13, 15, and 17 only showed deletions while patient 8 only showed duplications, sometimes even multiple copies of the respective exons. The remaining patients (2, 9, 10, 14, 16 and 18) had a combination of non-amplified exons, deletions and duplications. Table 3.5 summarizes the results for patients in which the MLPA showed just one type of alteration i.e. either deletions or duplications.

Patient	1	3	4	5	7	8	11	13	15	17
Exon										
2										
3										
4										
5										
6										
7										
8										
9										
10										
11										
12										
13										
14										
15										
16										
17										
18										
19										
20										
21-1										
21-2										
22										
23-1										
23-2										
24										
25										
26										
27										

Table 3.5: *DICER1* MLPA results of patients 1, 3, 4, 5, 7, 8, 11, 13, 15, 17. These patients only showed either deletions or duplications. Background colors: Light grey = deletion; transparent = normal, black = duplication.

Table 3.6 shows the results for the patients in which deletions as well as duplications were identified in a single patient:

Patient	2	9	10	14	16	18a
Exon						
2						
3						
4						
5						
6						
7						
8						
9						
10						
11						
12						
13						
14						
15						
16						
17						
18						
19						
20						
21-1						
21-2						
22						
23-1						
23-2						
24						
25						
26						
27						

Table 3.6: *DICER1* MLPA results of patients 2, 9, 10, 14, 16 and 18a. These patients showed deletions as well as duplications in *DICER1*. Light grey = deletion; transparent = normal, black = duplication.

Inconsistent results in the control groups were found as stated above. However, in most patients the results were reproducible. The positive control patient showed exactly the same result which was found in the original paper indicating the reliability of the assay. Furthermore, a deletion of *DICER1* was found in the germ line in patient 12. Although overall the MLPA results from the tumors are quite heterogeneous, only two of the eighteen patients had a complete *DICER1* deletion and one of these was patient 12, confirming the deletion in the germline. As already stated, the family members did not carry the deletion.

The MLPA results from the tumors except of patients 6 and 12 do not show a conclusive pattern. There seem to be largely deletions although duplications – sometimes even with multiple copies – do not seem to be unusual. However, some controls indicate that these results might not be totally reliable. Due to the size of exons 21 and 23 they were split up for the MLPA and in some patients only parts of the exon were found to be deleted or duplicated. It is important to note that the safety mechanisms (inter- and intrasample controls) were normal and did not indicate any procedural or methodical error. Adjusting controls and repeating the MLPAs in cases with sufficient genomic material did not change the results significantly. Also, patient 18a is one of the patients showing quite inhomogeneous results. Sanger sequencing however was successful and confirmed two de novo mutations. This was also the tumor which was stored the shortest time, leaving less chance to disintegrate and be damaged by storage methods like formalin-fixation or temperature. This confirms, that the tumor DNA of patient 18 had a sufficient quality for testing but still showed deletions and duplications in the tumor.

3.5 OncoScan® (not part of this thesis)

To further determine the size of the deletion detected by MLPA, FFPE DNA as well as germline genomic DNA of patient 12 were send to the laboratory of human genetics of the university of Kiel where a DNA microarray was performed. In this analysis the deletion in the *DICER1* gene was confirmed. Figure 3.17 (A) shows the germline deletion on chromosome 14 covering the same area in which *DICER1* is found while figure 3.17 (B) shows the somatic deletion. The deletion is marked by the red background color.

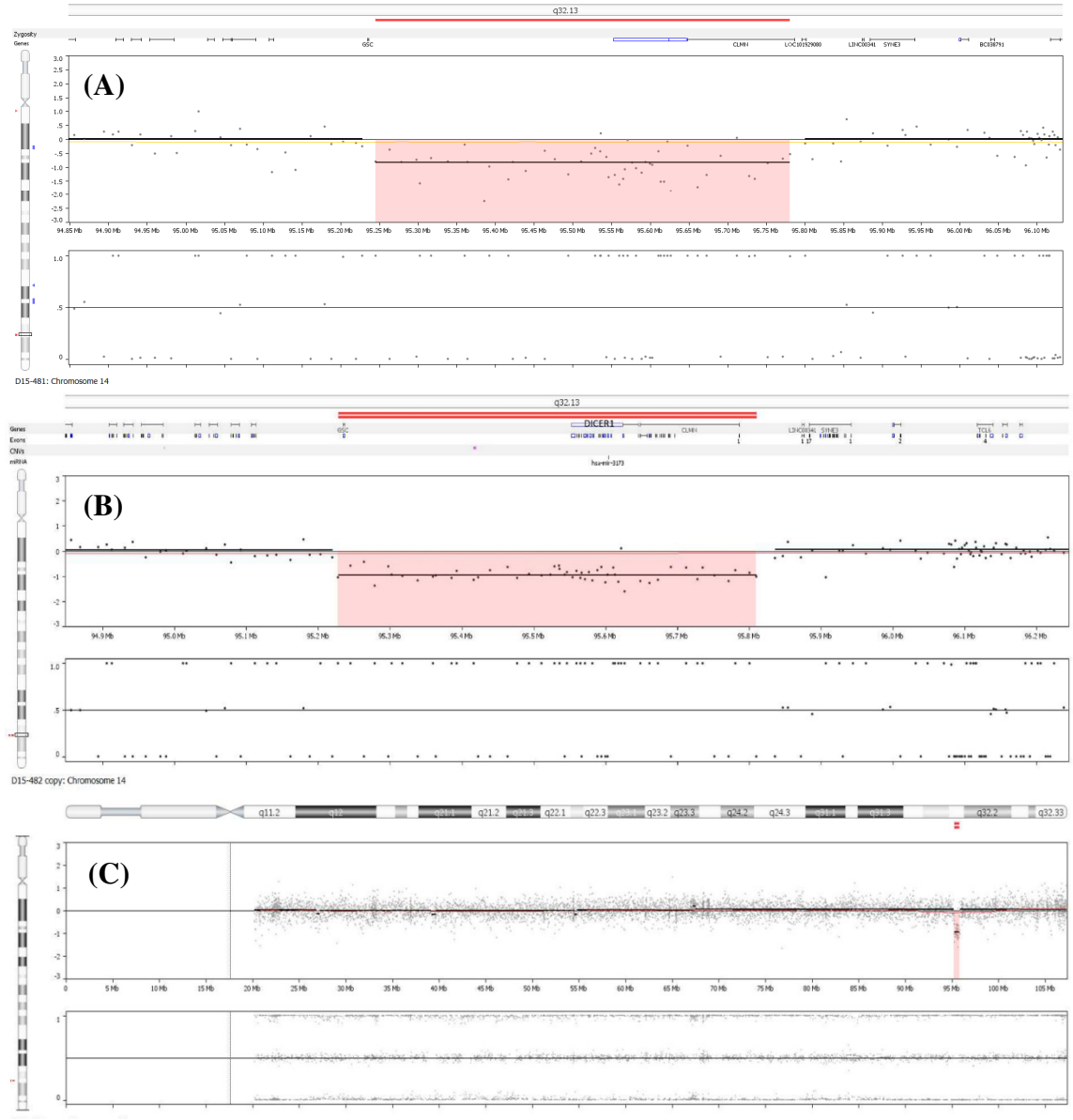

Figure 3.17: OncoScan® results from patient 12. (A) Region of interest of germline chromosome 14. (B) Region of interest of the somatic chromosome 14 from the pleuropulmonary blastoma of patient 12 showing the deletion in area q32.13 including *DICER1*. (C) Overview of the somatic chromosome 14. Point mutation and smaller deletions or duplications are not detected.

Figure 3.17 (C) gives an overview of the entire chromosome 14. The deleted area stretches well over the *DICER1* region.

The deletions in germline and somatic DNA are practically identical and span over 582kb in the tumor. Slight differences in length of the deletion are most likely the result of the poor quality of the germline DNA. As seen in figure 3.17 (C) there are no other significant deletions or duplications in chromosome 14. In the germline DNA no other abnormalities were detected. However, several deletions and duplications were found in the tumor itself. Especially in chromosomes 1, 8 and 15 several deletions as well as duplications were found. The sole deletion on chromosome 17 includes the entire locus of the tumor suppressor gene *TP53,* which is associated with a number of cancers and has been implicated with the miRNA-driven regulation of *DICER1* (see chapter 4.5). The 77Mb deletion on chromosome 10 includes the region for *PTEN* (Phosphatase and tensin homolog) which is on 10q23.31 (Online Mendelian Inheritance in Man (OMIM) #601728). *PTEN* is a prominent tumor suppressor gene and associated with various pathologies like Cowden syndrome and Lhermitte-Duclos syndrome. Other copy number variations include tumor suppressor genes *WT1* on cytogenic location 11p13 (OMIM) #607102) and *SUFU* (suppressor of fused, OMIM #607035) on locus 10q24.32. Also deleted is *Calmin* - Calponin-like transmembrane domain protein which is found in several different tissues in mice (OMIM #611121).

An overview of all the changes in the somatic DNA of patient 12 that were detected in the OncoScan® is given table 3.7.

Chromosome	**Region**	**Event**	**Length**	**Cytoband**
Chromosome 1	chr1:754,192-2,835,692	Loss	2081501	p36.33 - p36.32
	chr1:32,228,004-75,179,129	Loss	42951126	p35.2 - p31.1
	chr1:75,214,441-76,383,511	Gain	1169071	p31.1
	chr1:76,424,440-87,185,292	Loss	10760853	p31.1 - p22.3
	chr1:87,207,800-96,343,511	Gain	9135712	p22.3 - p21.3
	chr1:96,389,187-97,233,912	Gain	844726	p21.3
	chr1:97,250,022-97,819,405	Gain	569384	p21.3
	chr1:97,832,498-102,014,568	Gain	4182071	p21.3 - p21.2

	chr1:109,392,837-112,075,948	Gain	2683112	p13.3 - p13.2
	chr1:112,082,365-112,927,912	Gain	845548	p13.2
	chr1:159,285,991-249,212,878	Gain	89926888	q23.2 - q44
Chromosome 3	chr3:148,853,477-197,852,564	Gain	48999088	q24 - q29
Chromosome 4	chr4:119,086,650-188,921,355	Gain	69834706	q26 - q35.2
	chr4:188,932,202-189,313,568	Gain	381367	q35.2
	chr4:189,333,660-190,915,650	Gain	1581991	q35.2
Chromosome 6	chr6:169,723,097-170,913,051	Loss	1189955	q27
Chromosome 7	chr7:152,561,613-159,118,443	Loss	6556831	q36.1 - q36.3
Chromosome 8	chr8:172,417-2,092,803	Gain	1920387	p23.3
	chr8:2,119,247-2,780,241	Gain	660995	p23.3 - p23.2
	chr8:2,783,388-3,324,749	Gain	541362	p23.2
	chr8:3,325,727-5,461,753	Gain	2136027	p23.2
	chr8:5,474,720-11,857,317	Gain	6382598	p23.2 - p23.1
	chr8:11,859,080-13,771,888	Gain	1912809	p23.1 - p22
	chr8:13,791,808-29,490,608	Gain	15698801	p22 - p12
	chr8:52,102,658-52,774,812	Loss	672155	q11.21 - q11.23
	chr8:53,506,883-61,101,162	Gain	7594280	q11.23 - q12.1
	chr8:61,120,869-74,919,912	Gain	13799044	q12.1 - q21.11

	chr8:74,928,092-79,911,851	Gain	4983760	q21.11 - q21.12
	chr8:79,918,665-91,108,548	Loss	11189884	q21.12 - q21.3
	chr8:91,113,477-92,531,120	Gain	1417644	q21.3
	chr8:92,554,952-93,698,134	Gain	1143183	q21.3 - q22.1
	chr8:93,721,099-94,477,479	Gain	756381	q22.1
	chr8:94,491,914-95,459,348	Loss	967435	q22.1
Chromosome 10	chr10:58,250,201-135,434,303	Loss	77184103	q21.1 - q26.3
Chromosome 11	chr11:192,764-26,684,617	Loss	26491854	p15.5 - p14.2
	chr11:26,694,842-31,272,156	Gain	4577315	p14.2 - p13
	chr11:31,289,597-39,289,766	Gain	8000170	p13 - p12
Chromosome 14	**chr14:95,227,957-95,810,070**	**Loss**	**582114**	**q32.13**
Chromosome 15	chr15:20,161,372-23,631,360	Gain	3469989	q11.1 - q11.2
	chr15:23,631,810-30,367,255	Gain	6735446	q11.2 - q13.2
	chr15:30,967,896-32,029,693	Loss	1061798	q13.2 - q13.3
	chr15:32,051,488-32,515,100	Gain	463613	q13.3
	chr15:32,925,226-42,981,806	Loss	10056581	q13.3 - q15.2
	chr15:61,879,564-78,606,913	Gain	16727350	q22.2 - q25.1
	chr15:78,617,913-102,397,317	Gain	23779405	q25.1 - q26.3
Chromosome 17	chr17:400,959-11,761,675	Loss	11360717	p13.3 - p12
Chromosome 18	chr18:12,842-12,031,516	Loss	12018675	p11.32 - p11.21
Chromosome 19	chr19:13,204,835-15,336,930	Gain	2132096	p13.2 - p13.12
	chr19:15,341,617-16,713,332	Gain	1371716	p13.12 - p13.11

	chr19:16,724,314-20,218,177	Gain	3493864	p13.11 - p12
Chromosome 20	chr20:29,519,156-62,912,463	Gain	33393308	q11.21 - q13.33

Table 3.7: OncoScan® results from the pleuropulmonary blastoma DNA. Deletions and duplications are localized and their respective length is given. Most of the changes are found in chromosomes 1, 8 and 15. Chromosome 14 is highlighted because *DICER1* is localized on the q-arm of chromosome 14 in region q32.13.

A visual representation is shown in figure 3.18.

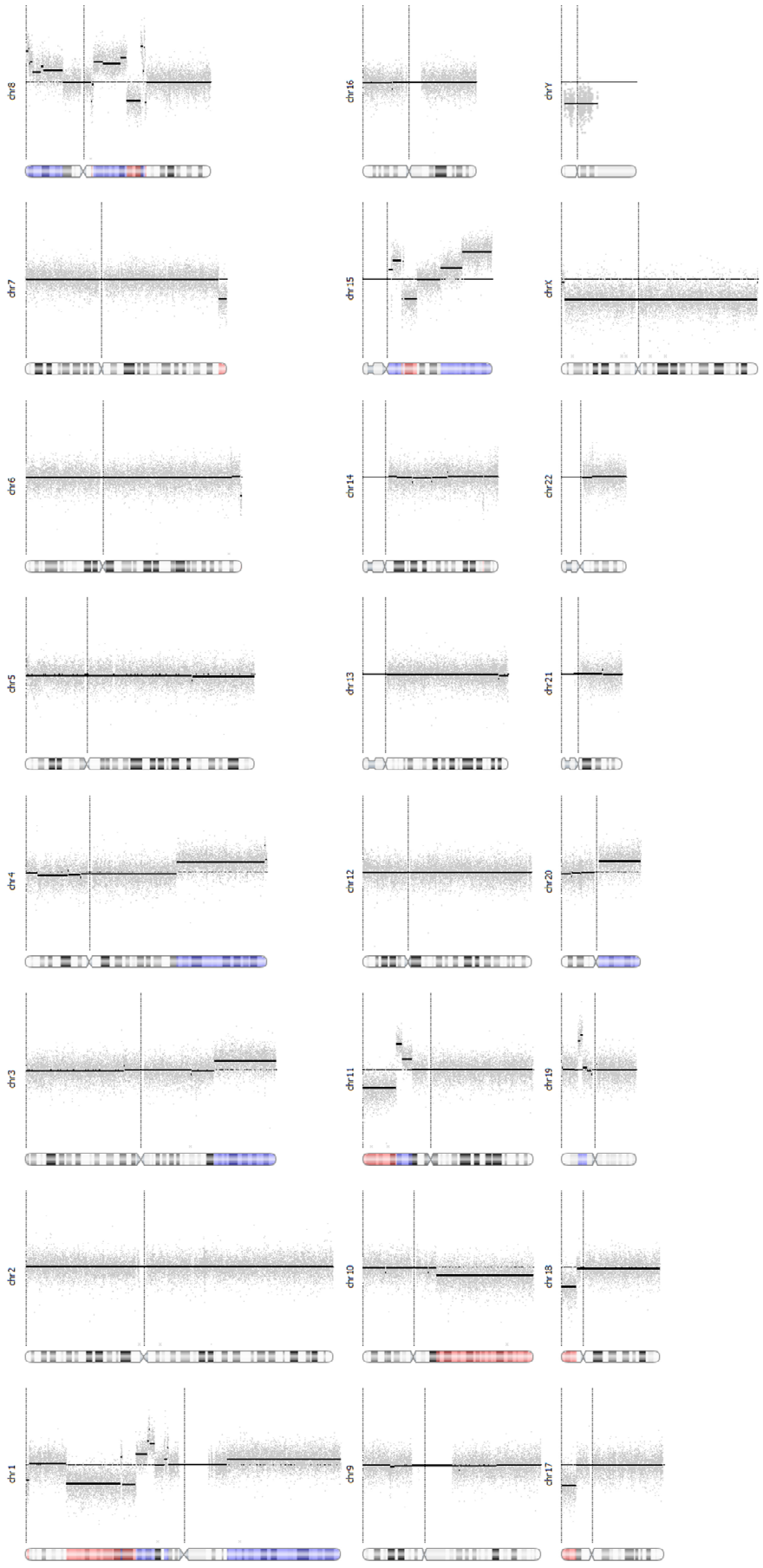

Figure 3.18: Corresponding results from table 3.7. OncoScan® results showing the chromosomes of the pleuropulmonary blastoma. The blue colored regions on the arms of the chromosomes are duplications while the red coloration determines a deletion.

4 Discussion

In this thesis 18 cases of pleuropulmonary blastoma were examined including germline DNA and DNA of family members when available. Mainly PCR, Sanger sequencing and multiplex ligation-dependent probe amplification were used. Nine mutations were found in a total of six patients. Additionally, a large de novo deletion on chromosome 14q including the *DICER1* locus was detected. There are missense mutations, deletions, duplications and splice-site mutations. Due to the fact that only in patients 12 and 18 additional germline material was available for testing, it was not possible to determine if the origin of the mutations from the other patients stem from germline or somatic cell line that is the tumor itself. The splice site mutation c.1510-1G>A discovered in patient 18 was found in germline and tumor, but was not found in the family members. It is therefore most likely a de novo germline mutation. The father of patient 12, who had a history of seminoma, did not show the germline deletion which is in line with recent findings that seminoma is not part of the *DICER1*-Syndrome (Sabbaghian et al. 2013).

The history of the pleuropulmonary blastoma and *DICER1* is relatively short. PPB was first described 1988 and the association with *DICER1* was made only 2009. *DICER1* itself is known since 2001. Several mutations in patients with pleuropulmonary blastoma and other *DICER1*-Syndrome associated pathologies have been published. In the available literature, from the nine mutations found in the 18 cases in this thesis four have previously

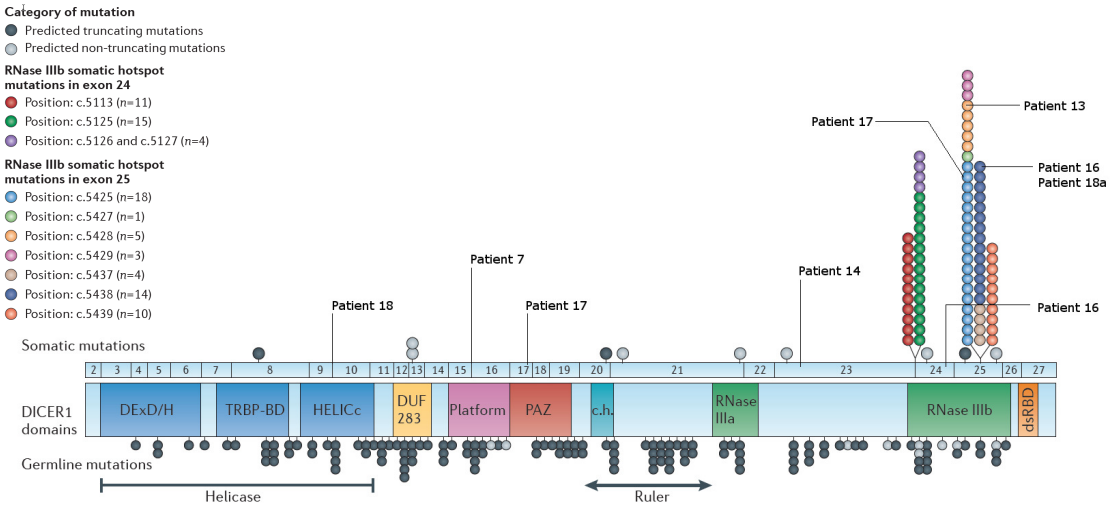

Figure 4.1: Somatic and germline *DICER1* mutations after Foulkes et al. 2014 matched with findings in this thesis. The mutations shown in this illustration are not only from pleuropulmonary blastomas but also other pathologies like cystic nephroma, Wilms tumor, or familial multinodular goiter.

been described in the literature: c.5428G > T, c.5438A > G (patients 16 and 18), c.5425G > A and c.5299delC (Foulkes et al. 2014, Brenneman et al. 2015 (revised 2018)).

In 2014 Foulkes et al. reviewed published cases showing germline and somatic mutations in tumors associated with *DICER1*. There are certain mutations which are commonly found in pleuropulmonary blastoma somatic DNA. They seem to occur especially in exon 24 and exon 25 which are coding for a RNase IIIb domain. Because of the abundance of these mutations in this domain they are called *hotspot mutations*. Figure 4.1 was originally published by Foulkes et al. 2014 and was modified to now contain the mutations found in this thesis. The four mutations that were already published are hotspot mutations, while the other mutations have not been reported so far (according to LOVD v.2.0. – Leiden Open Variation Database 10/2018; http://www.lovd.nl/2.0/ and current published research). Only for patient 18 it is proven that the mutation c.5438A > G is of somatic origin and the splice site mutation is a de novo germline mutation. However, in the other cases it is very likely that the hotspot mutations are of somatic origin as well due to the high prevalence of these mutations in tumors.

Most likely due to the poor quality of the FFPE and somatic DNA, in more than half of the patients, no mutation was found, probably due to unsuccessful sequencing.

Examination via multiplex ligation-dependent probe amplification showed a de novo germline deletion of *DICER1* in patient 12 which was also confirmed in the pleuropulmonary blastoma MLPA. Complete deletions of *DICER1* have been described previously only in one PPB case. Deletions of single exons however have been described in rare cases (Sabbaghian et al. 2014, Brenneman et al. 2015 (revised 2018)). In addition to patient 12, there was also patient 6 who showed a deletion of the entire *DICER1* gene. This deletion could also be present in the germline. Subsequent analysis of patient 12 via DNA microarray revealed a large deletion spanning over 580 kilobases in the tumor which was practically identical to the germline deletion. Slight differences in the size of the deletions are presumably the result of impunities and poor quality of the germline DNA.

The analysis of the residual patients by MLPA showed complex patterns of deletions and duplications and did not allow any meaningful interpretation. The custom MLPA with synthetic oligonucleotides showed the expected result in most cases. Conclusive results

were found for example in patient 12 in germline and tumor, the positive control with an exon 21 deletion or in several normal controls. As reported by Sabbaghian et al., it is possible that there is a deletion of one or more exons among the patients but due to the vast changes in the tumor DNA and lacking germline material it is not possible to differentiate between germline and tumor. The lack of germline material also is a consequence of the rarity of the tumor. The cases were collected over almost three decades and no germline material was available for current research. As a diagnostic method the *DICER1* MLPA presented itself to be a helpful tool. Unfortunately, there seems to be a limited reliability of this method which may be attributed to the fact the tumor material was paraffin embedded, mixed with unbuffered formalin (between 10 – 40%) and stored for many years leading to a significant decrease in DNA and tissue quality. As an additional method to screen for deletions or duplications in pleuropulmonary blastoma patients it can be helpful.

As clear as the association between PPB and *DICER1* seems to be, the mechanisms and involved genetics that lead to the development of the tumor are not as clear yet. The ideas and the understanding of their interaction have changed throughout recent history while still not being definite.

4.1 Tumor suppressor genes and oncogenes

Beforehand, two terms have to be explained (Rassow et al. Duale Reihe Biochemie, P.514): Tumor suppressor gene (TSG) and oncogene. The former is a gene, whose protein products prevent the development of a tumor by regulation of physiological cell division. TSGs are often recessive. In case a recessive gene gets damaged on both alleles, for example by a mutation or any other molecular genetic process, it will stop having its inhibitory effect. Then, the potential for cancer in the affected patient is increased. Prominent examples of TSGs are the *retinoblastoma gene* (Rb) and *p53*-gene. The latter is a gene which, when transcribed and translated, in a great manner will cause tumor growth. So called proto-oncogenes are responsible for cell growth and differentiation through signaling pathways. They are genes that through different ways can become oncogenes. Translocations, point mutations, gene amplification and other mechanisms

are responsible for the transformation into an oncogene. Oncogenes are characterized by a dominant pattern of inheritance. N-myc, kras, abl-translocation or HER2/neu are well-known examples of oncogenes.

The so called 20/20 rule was recently postulated by Vogelstein and colleagues in order to distinguish between TSG and oncogene. It states, that of the recorded mutations in TSGs >20% lead to inactivation of the gene while >20% of the mutations in oncogenes are missense mutations which occur in recurrent positions (Vogelstein et al. 2013, Foulkes et al. 2014).

Multiple copy number variations were detected in patient 12, including loss of *PTEN*, *SUFU* and gain of *WT1,* which are all tumor suppressor genes.

4.2 Finding the mechanism

DICER1 was discovered as a contributing factor for tumorigenesis of PPB by Hill and colleagues in 2009. Firstly, they found that normally differentiated epithelium in tumor material lacked DICER1 in immunohistochemical staining. Secondly, they established, that neoplastic mesenchymal cells were DICER1-positive. They postulated, that a new unknown mechanism involving miRNA-regulated diffusible growth factors or messengers were causing the faulty differentiation of the mesenchymal cells (so called '*non-cell-autonomous cancer initiation*'). It was noted in the literature by Foulkes and colleagues in 2014 that the available immunohistochemical staining methods might not have proven as reliable yet and might need further evaluation (Foulkes et al. 2011, Murray et al. 2014). This is also supported by the fact that other studies concluded that a complete loss of DICER1 seems to be incompatible with survival (Bernstein et al. 2003, Wienholds et al. 2003).

A different hypothesis for the tumor development was *DICER1* functioning as a *haploinsufficient tumor suppressor gene* (Kumar et al. 2009). Haploinsufficiency describes a state in which one of the two alleles that are usually found in a genome is either inactivated or deleted. This means of the two alleles in a diploid genome only one

is working properly. Tumor suppressor genes have a generally recessive nature meaning not both alleles are mandatory to exhibit its designed function.

Previously it was explained that approximately 72% of patients with PPB have a germline mutation. For this group of patients this hypothesis would mean that their lacking of a second functioning allele leads to vulnerability regarding tumor growth. For patients with only somatic mutations in the tumor this local susceptibility would lead to the tumor development.

This theory was supported by mice studies which showed that mice lacking one *Dicer*-allele developed a K-ras mediated lung tumor and retinoblastoma. These mice also had a better outcome and less frequent occurrence of tumors when they had no *DICER1* at all or a normal biallelic *DICER1* expression (Kumar et al. 2009, Lambertz et al. 2010, Slade et al. 2011, Bahubeshi et al. 2011). The lack of loss-of-heterozygosity (LOH, the inactivation of the second allele when the first allele is already inactivated) also supported this theory of *DICER1* as a *non-traditional TSG* (Rio Frio et al. 2011). Additionally, sequencing of the tumor material showed no additional mutations of the retained *Dicer1* allele in mice (Kumar et al. 2009) and somatic mutations were deemed not important (Slade et al. 2011). In this thesis however somatic mutations as well as germline mutations were found, hence biallelic changes. Haploinsufficient tumor suppressor genes have been suggested in other diseases as well like CUX1 or Nf1 in leukemias (McNerny et al. 2013, Koenigsmann et al. 2009).

Based on the studies of mice, it is thought that a complete loss of *DICER1* is not compatible with life and leads to early abortions (Bernstein et al. 2003, Wienholds et al. 2003). The reason is the elementary involvement of *DICER1* in essential steps of the regulation of large parts of the genome.

Nevertheless, some authors believe that the second mutation is does not cause a loss of suppressive effect but rather an *oncogenic* action due to an unfavorable miRNA profile (for *DICER1*-related ovarian cancers: Heravi-Moussavi et al. 2012).

As more and more reports of somatic *DICER1* mutations were documented, the possibility arose that PPBs might be caused by the so called *two-hit-hypothesis*. This concept describes the inactivation of genes and was described by Knudson in 1971. A

first hit (a mutation) occurs on one allele and after a variable timespan a second hit occurs on the second allele. The first hit may occur in the affected patient but can also be inherited from the parents. The consequence of this two-step process for a TSG is an inactivation, a so-called loss-of-function (LOF) and an increased risk for neoplasms. A common example for this mechanism is the *APC*-gene in colon carcinoma (familial adenomatous polyposis coli, FAP).

4.3 The modified two-hit-hypothesis

The previous considerations in section 4.2 imply, that *DICER1* is a special case regarding the two-hit hypothesis. Firstly, the second hits, which are usually missense mutations, occur in PPB patients in the tumor. Secondly, most of these mutations are found in the earlier described *hotspot regions*. The hotspot regions are located in exons that are coding for the RNase IIIb domain. The detected variants are no loss-of-function mutations in the traditional sense. Typically, these missense mutations occur in one of five amino acids (Brenneman et al. 2015 (revised 2018), Schultz et al. 2014). The affected mutation sites are either part of, or, in vicinity of the metal binding sites for Mn^{2+} or Mg^{2+}. These ions are required for the intramolecular dimerization of DICER1 (Zhang et al. 2004, Takeshita et al. 2007, Heravi-Moussavi et al. 2014).

Tumors apart from the *DICER1*-spectrum, that are considered to be caused by the traditional two-hit-hypothesis, may have mutations in any exon causing a loss-of-function. The newly described pattern seen in PPB, is also found in other tumors of the *DICER1* spectrum, including thyroid carcinomas and Sertoli-Leydig cell tumors. The impact of the effect on RNase III domains will be addressed in chapter 4.3.1.

Three patients in this project had two mutations. Analysis of the peripheral blood and tumor DNA of patient 18 revealed, that one of the mutations was a germline mutation (splice site mutation c.1510-1G>A). The other mutation was of somatic origin.

Due to lack of material, poor quality and fragmentation of DNA, complete testing was only possible in four patients (14, 16, 17 and 18). For instance, patient 12 had a large de novo germline deletion, but sequencing of the genomic DNA from the tumor was not

successful. Therefore, it still is possible that remainder of the patients had germline and/or somatic mutations, which were not detected.

4.3.1 Hotspot mutations and consequences of RNase III domain mutations

The somatic mutations, especially those in the hotspot regions, affect the RNase III domains of *DICER1* and most frequently the RNase IIIb domain. In the literature, the following five hotspots have been reported so far (Heravi-Moussavi et al. 2012, Seki et al. 2014, Foulkes et al. 2014, Brenneman et al. 2015 (revised 2018)):

E1705
D1709
D1810
E1813
G1809

Pleuropulmonary blastoma and Sertoli-Leydig tumor patients often have decreased levels of the 5p miRNA strand (22nt strand) and normal or increased levels of the 3p miRNA (18nt strand) strand, compared to healthy individuals. They also have a retention of loop sequences, which are still attached to the 5p miRNA. This has been shown several times e.g. by Heravi-Moussavi et al. 2012, Gurtan et al. 2012 and Pugh et al. 2014.

These analyses also indicated, that a mutation in an exon coding for the RNase IIIb domain leads to the decrease of 5p strands from the miRNA duplex, while a mutation in the RNase IIIa domain leads to a decrease of 3p strands. This allows the deduction, that the RNase IIIb domain is responsible for the cleavage of the 5p arm from the stem loop. The RNase IIIa domain on the other hand cleaves the 3p arm of the hairpin loop of the miRNA (Gurtan et al. 2012). Therefore, there is a convincing association between the respective RNase III domains and the 5p and 3p strands. In vivo mice studies showed a global reduction of miRNA processing in mice with PAZ domain mutations. Walker A motif mutations in the helicase domain however, led to no change in the miRNA profile (Gurtan et al. 2012). Some patients with PAZ mutations presented with MNG (Rio Frio et al. 2011, Murray et al. 2014).

A non-functional RNase IIIb domain is unable to cleave the 5p arm from the stem loop. Therefore, the 5p arm stays attached to the stem and remains in the cytoplasm, being

degraded subsequently, causing the reduction of 5p levels. 3p levels were also found to be upregulated compared to normal (fetal) lung tissues (Seki et al. 2014). However, this observation was not seen in all studies, as some show normal levels of the 3p arm miRNA (Anglesio et al. 2013). The opposite occurs when RNase IIIa is affected.

The normal or upregulated 3p arm levels in RNase IIIb-mutated cells imply, that there must be some residual *DICER1* activity in the tumor and there is no complete loss of miRNA processing in the cell (Heravi-Moussavi et al. 2012). As described earlier, only one of the miRNA duplex strands goes on to interact with mRNA. The other one is degraded (figure 1.2). The somatic *DICER1* mutations in the PPB are found predominantly in the RNase IIIb domain, leaving two possibilities. Either (1) *DICER1*, albeit mutated, is still able to execute some of its function, i.e. RISC loading or cleaving 5p/3p arms of the stem loop. Or, (2) that the other ('inert') strand also serves a yet unknown function (Heravi-Moussavi et al. 2012). For instance, the 'inert' strand could be involved in cell regulation and maintenance.

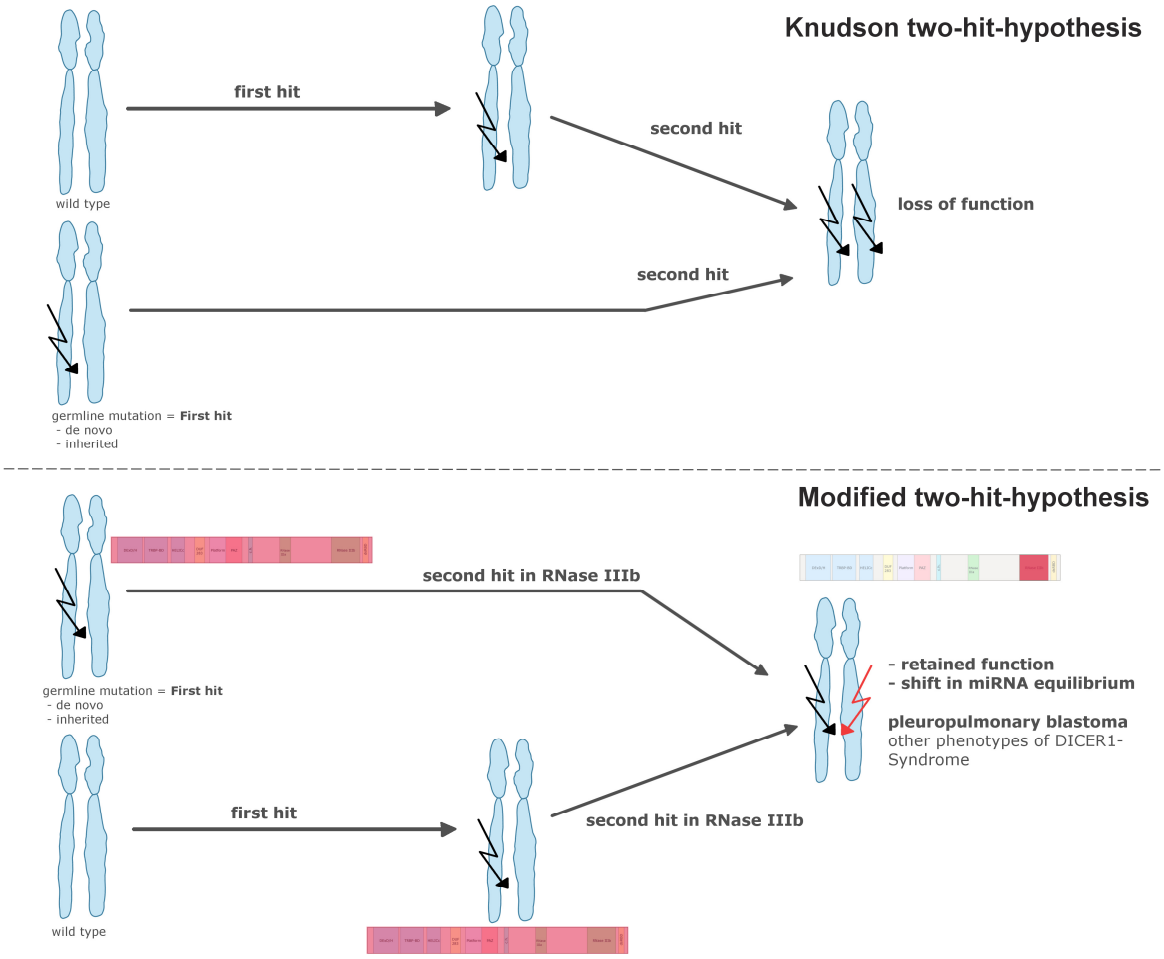

Figure 4.2: Comparison between the traditional two-hit-hypothesis by Knudson and the modified hypothesis of *DICER1* associated genesis of the pleuropulmonary blastoma. The red highlighting in the schematic *DICER1* gene represents the possible locations of a mutation. The black and red arrows indicate the affected allele.

It is unknown, whether the increase of 3p levels might be a compensational mechanism or a consequence of deregulation. The function of the 5p arm attached to the stem loop is also unknown. It might not have any remaining functional activity at all (Stewart et al. 2014).

The changes in miRNA profiles might be of use for future serum screening before, during and after treatments of PPB patients (Murray et al. 2014, Schultz et al. 2014). This issue will be addressed in chapter 4.6.

In this thesis, five of the nine mutations affected the RNase IIIb domain. In patient 16, even both mutations are located in this specific domain. In other studies, also the majority

of mutations also affected RNase IIIb (Brenneman et al. 2015 (revised 2018), Foulkes et al 2014). Only single mutations were reported for the RNase IIIa domain (Seki et al. 2014, Heravi-Moussavi et al. 2012, Foulkes et al. 2014). This rarity of mutations could mean, that RNase IIIa is important for the cell and its homeostasis. It could also mean, that the mechanism causing the mutations, favors the RNase IIIb domain for some, yet unknown, reason. The lack of RNase IIIb activity and the retained function of RNase IIIa could create a new equilibrium, which selects 3p miRNA and causes the oncogenic potential of a *DICER1* mutation in the RNase IIIb domain. The effect could be a continuous stimulation of proliferation, which increases the potential for cancer (Heravi-Moussavi et al. 2012).

Recently, it was shown that some hotspot mutations in exon 25 of *DICER1* actually do not lead to predicted change in the translated protein. Missense mutations c.5429A>G, c.5429A>T and c.5438A>G lead to an exon 25 skipping in vitro, but with *DICER1* still translated (Wu et al. 2013, Foulkes et al. 2014). C.5428G>T seems to create a cryptic splice site with *DICER1* truncation (Foulkes et al. 2014). A reason why this cryptic splice site occurs is not yet known. c.5438A>G was found in patients 18 and 16, while c.5428G>T was detected in patient 13.

Summarizing, there is an interesting conflict regarding cancer fitness. On one hand, tumor growth apparently depends on a somatic mutation in the second allele. On the other hand, the mutation must not completely inactivate the rest of *DICER1* function, because this would completely halt cell proliferation and function (see chapter 4.3.2). The miRNA star strand, which is derived from the RNase IIIa domain cleavage from the hairpin loop, might be a key event facilitating tumor growth.

4.3.2 Germline Mutations

The germline loss-of-function mutations are more common than the five hotspot mutations, which ultimately initiate tumor development. Furthermore, in contrast to the hotspot mutations, they are not accumulated in a particular area (Heravi-Moussavi et al. 2012). In this thesis, only one of the mutations could represent a germline event (patient 18). It was not in the RNase III domains but a splice site mutation of exon 10. So far, no

connection between the location of a germline mutation and the location of second hit mutation has been made. This points to a random distribution of the mutations (Foulkes et al. 2014).

So far, no RNase IIIb *germline* hotspot mutation has been found. Such a mutation is most likely incompatible with life. Brenneman et al. found a subset of patients, that harbors mosaic RNase IIIb hotspot mutations. These patients have a very high chance of developing any of the *DICER1*-related pathologies. Additionally, the disease in these patients manifests much earlier in life than in other germline-mutated patients. Intestinal polyps and intestinal intussusception might be previously unknown manifestations related to these mosaic mutations.

Two cases reported in the literature had intragenic deletions. The deleted exons were exon 21 (Sabbaghian et al. 2014) and exon 24 (Brenneman et al. 2015 (revised 2018)).

The large de novo deletion of patient 12 is a finding matching a recently described case from 2018. Here, a male pediatric patient had a 5.8 Mbp deletion, including the *DICER1* gene locus. The patient developed *DICER1*-Syndrome with cystic nephroma, ciliary body medulloepithelioma, cerebral sarcoma and PPB type I/Ir (de Kock et al. 2018).

Summarizing previous observations, germline mutations, including insertions and deletions, are regular findings in *DICER1*-Syndrome patients. Certainly, the combination between loss-of-function germline mutations and localized, protein function retaining somatic mutations seems to be a new concept, which has not been described in the literature previously (Foulkes et al. 2014).

4.3.3 Assessment and exceptions

To this point, the modified two-hit hypothesis seems to be a valid hypothesis for *DICER1*. A lot of evidence, including this project, points into this direction. It still remains unknown, what the mechanism for patients without germline mutations is. Some of these patients were recently shown to have two somatic mutations. One mutation causes the loss-of-function mutation (first hit) and the other missense mutation interferes with

normal RNase IIIb function (Pugh et al. 2014). Therefore, as in other tumors, a lack of a germline mutation is still consistent with a pleuropulmonary blastoma.

Due to this fact, Brenneman et al. (2015 (revised 2018)) suggested, that non-mosaic biallelic somatic *DICER1* mutations causing PPB are *sporadic* (*non-syndromic*) cases of the disease. These patients cannot be subsumed under the term *DICER1*-Syndrome. They do not have a positive family history and do not suffer from any of the other pathologies like cystic nephroma, thyroid alterations or cERMS, which are commonly found in *DICER1*-Syndrome. The reason is a lack of a *DICER1*-mutation distributed throughout various tissues of the body. Hence, PPB in sporadic cases is caused by local, tissue specific somatic mutations. The prognosis of the pleuropulmonary blastoma in syndromic and non-syndromic patients is the same.

To complicate matters, the modified two-hit-hypothesis does not seem to apply to all tissues. There are reports of *DICER1* working as a TSG in pineoblastomas (de Kock et al. 2014) without the retention of *DICER1* function (see chapter 4.3.1). According to one hypothesis, in some tissues a single hotspot RNase IIIb mutation is enough to cause tumor growth, even when one unaffected allele is present (Klein et al. 2014, Brenneman et al. 2015 (revised 2018)). Although sufficient sequencing of all exons and flanking introns of the thyroid carcinoma was possible, no additional mutation was detected in patient 12.

4.3.4 Effect on tumor cells and clinical presentation

DICER1 plays an important part in gene regulation. For this reason, it is surprising, that the clinical features are (mostly) extremely rare tumors. One would expect a general increase in neoplasms and much more common tumors than PPB, cERMS, and others. This is clinically not the case. Therefore, at least regarding tumor growth, *DICER1* does not seem to be as important as other genes like *TP53* (Slade et al. 2011).

4.3.4.1 Importance of *DICER1* for tumor cells

Causes for the clinical presentation mentioned above may be the importance of *DICER1* for life and viable cells. For instance, complete inactivation of *DICER1* in tumors led to significant reduction in growth and progression in prostate cancer (Zhang et al. 2014).

Additionally, floxed mice with completely knocked-out *Dicer1* have generally a better prognosis than mice with just one knocked-out *Dicer1* allele. Although tumor cells are uncoupled from the normal cell cycle regulation, they still seem to strongly depend on the existence of Dicer1 for survival. (Kumar et al. 2009). Normal tissue as well as tumor tissue follows a positive selection on functioning DICER1. These tissues rely on a retained function of DICER1, otherwise there is no tissue proliferation (Foulkes et al. 2014).

4.3.4.2 Disease onset

Most *DICER1*-associated conditions occur in pediatric patients. There seems to be a limited period of time, in which this vulnerable group of patients is susceptible to newly acquired somatic mutations. Therefore, the second hit seems to be developmental stage-dependent. This explains, why many *DICER1* related pathologies occur in early life (Bahubeshi et al. 2011). The low probability of these somatic mutations might also account for the reduced penetrance of *DICER1*-Syndrome (Brenneman et al. 2015 (revised 2018)). In the presence of a germline hotspot mutation on the other hand, only an additional loss-of-function mutation in the somatic tissue is required for the development of a neoplasm. The probability for such an event is much higher than a mutation in the RNase IIIb domain.

4.3.4.3 Penetrance and context specificity

The age dependence of the tumors may also explain the reduced penetrance. Due to so-called context specificity, the second hit only leads to neoplastic change, when it occurs at a certain time, in particular tissues and cell types (Heravi-Moussavi et al. 2012, Schultz et al. 2014, Brenneman et al. 2015 (revised 2018)). The chance of developing *DICER1*-related-tumors when organs are already terminally developed, is significantly decreased (Bahubeshi et al. 2010). Notably, there are cases in which some of the tumors occurred in adult patients (e.g. a patient with a PPB at the age of 36 (Hill et al. 1999)). All tissues undergo some cell turnover during normal stasis and a *DICER1* hotspot mutation might still occur during that process.

Contributing factors for the perception of a reduced penetrance might be subclinical findings, which are typically not screened for. There are data, that about 87% of 'healthy' *DICER1* mutation carriers have thyroid nodules and even 43% have lung cysts (Brenneman et al. 2015 (revised 2018)). Compared to mosaic germline mutations, patients carrying non-mosaic germline LOF mutations have a higher chance of tumor development during life.

Penetrance does not seem to vary with different germline mutations in-between families. However, there are very few families, which have a higher occurrence of MNG (Foulkes et al. 2014). The reduced penetrance is still a clinical challenge for practitioners and pediatric patients. One reason is, that exposure to x-radiation should be kept at a necessary minimum.

It should be noted, that although some tissue types favor the somatic *DICER1*-mutations, *DICER1* is only a major contributor in *some* pathologies like PPB or cystic nephroma. (Slade et al. 2011). Different germline *DICER1* mutations do not favor specific tumors. For instance, the young female patient (see section 1.2.4.1) had several tumors in different tissues. All of the known *DICER1* tissues might be affected throughout a family or even a single patient.

4.4 LOH and *DICER1* in non-syndromic tumors: Conflicting results?

4.4.1 Loss of heterozygosity

Loss of heterozygosity (LOH) is seen in cases of *DICER1*-related pineoblastoma (de Kock et al. 2014, Sabbaghian et al. 2014). For pleuropulmonary blastoma however, no LOH was reported so far. The second mutated allele of *DICER1* in PPB is still active and functioning, while a mutation in the germline causes a loss-of-function for the first allele (Bahubeshi et al. 2011, Heravi-Moussavi et al. 2012). Interestingly, pineoblastomas also show no RNase IIIb mutations (de Kock et al. 2014). This means, that some specific tissue relations are not discovered yet and other mechanisms might be involved.

Discovering LOH in a *DICER1*-related tumor indicates, that opposing previous findings in mice, a complete loss does seem possible in a viable tumor (Sabbaghian et al. 2012).

Furthermore, a complete loss of *PTEN* (phosphatase and tensin homologue) and loss of *DICER1* led to continued growth of cancer of the ovaries (Kim et al. 2012).

4.4.2 *DICER1* and non-syndromic tumors

DICER1 plays a role in (so far) non-syndromic tumors as well (Heravi-Moussavi et al. 2012). For instance, downregulated levels of *DICER1* are a negative prognostic parameter in pulmonary adenocarcinoma and ovarian cancer (Karube et al. 2005, Merritt et al. 2008, Kumar et al. 2009, Lambertz et al. 2010). Interestingly, overall increased levels have been seen in prostate cancer analysis. On the other hand, lower levels reduced the time to recurrence and correlated with a poorer outcome of these patients. Inactivation of one *DICER1* allele (hemizygous loss) in prostate cancer raises the invasive- and aggressiveness of the tumor in mice (Zhang et al. 2014). This dosage aspect of *DICER1,* adds to the tissue specific notion of this gene.

In precancerous lung lesions DICER1 was upregulated, while in some forms of the advanced tumors decreased levels were found (Chiosea et al. 2007). In other cancers like oral cancers and acute myeloid leukemia, an overexpression has been determined, with mixed associations regarding outcome (Martin et al. 2009, Jakymiw et al. 2010, Chiosea et al. 2007).

These conflicting results are yet to be explained. It might be the expression of unknown biological processes but also be due to technical difficulties (Foulkes et al. 2014). Generally, DICER1 is often essential for tumor growth, but too much functioning DICER1 decreases the malignancy of the tumor.

Multiple studies showed, that *DICER1* alteration impairs ds-DNA break repair by affecting *DICER1*- and *DROSHA*-dependent small RNAs (Wei et al. 2012, Tang et al. 2012, Francia et al. 2012). Besides the reasons already discussed, this could be an additional factor in the mechanism of tumor development.

4.5 Other factors in the pathogenesis of PPB: *TP53*, TRBP, Drosha

TP53 is an important tumor suppressor gene and checks the integrity of the DNA. It arrests the cell cycle, when DNA is damaged and then initiates apoptosis (programmed cell death). Being one of the most important TSGs, it is estimated that *TP53* is involved in the genesis of about 50% of tumors (Rassow et al. Duale Reihe Biochemie, P. 516). Pugh et al. found *TP53* alterations in 13 of 15 cases (2014). Much lower rates of *TP53* mutations have been described in other works (e.g. 5/12 patients, Seki et al. 2014). Patient 12 showed no mutations by Sanger sequencing. The OncoScan® revealed a deletion on chromosome 17p of 11,3Mb in the somatic DNA, which includes the gene locus of *TP53* (17p13.1).

TP53 also regulates miRNA processing (Suzuki et al. 2014). *DICER1* is regulated itself by miRNA (let-7), which in-turn is controlled by *TP53* (Seki et al. 2014, Lujambio et al. 2012). In pancreatic cancer, there appears to be a regulatory loop between *DICER1* and *TP53*. Here, an inactivation of *DICER1* increases the activity of *TP53* (Wang et al. 2012). It is not known, if this mechanism is involved in the pathogenesis of pleuropulmonary blastoma.

TRBP is a cofactor of DICER1 encoded by *TARBP2*. In colon cancer with microsatellite instability (MSI), Melo and colleagues found mutations, that truncated the translated protein. They showed, that the miRNA DICER1-pathway is disrupted, when *TARBP2* harbors a loss-of-function mutation. Once *TARBP2* is reintroduced, miRNA function is restored and tumor growth is halted. This shows that there might lie a therapeutic potential for cancer treatment within miRNA regulation and repair of the DICER1 pathway (Melo et al. 2009).

DGCR8, Drosha and Argonaute are involved in the same pathway as DICER1. A mutation in one of their coding genes could show the same effect as a mutation in *DICER1* itself (Sabbaghian et al. 2014). *DROSHA* RNase IIIb mutations are found in 12% of Wilms' Tumors (Torrezan et al. 2014).

Activation of the RAS-pathway could be an additional step in the development of PPB (Pugh et al. 2014). Trisomies like trisomy 8, loss of chromosomes 10 and 17 as well as

cases with 19q13 translocations have been documented in PPB (Seki et al. 2014, Pugh et al. 2014).

In patient 12, there are many copy number alterations in chromosome 8 but no trisomy 8. The impact of these alterations is not fully understood yet.

4.6 MiRNA serum screening: A possible diagnostic and therapeutic approach

The effects of mutations in the RNase IIIa and IIIb domains are of considerable clinical interest. The serum levels of their respective products (3p and 5p arms) have been studied in patients with PPB. MiRNA 125-3p and 125-2-3p were chosen. The level of both markers in a patient with PPB were significantly higher at time of diagnosis compared to healthy individuals, including relatives. After surgery and chemotherapy however, the serum miRNA levels normalized (Murray et al. 2014). These markers are stable and resistant to degradation (Bailey et al. 2014). It is unknown, why cells release miRNA into the plasma. It might be through cell-decay of the degenerating or necrotic tissue. It might also be active secretion or passive leakage of the neoplastic cell, to maintain a tumor-viable environment.

Serum miRNA profiles are promising biomarkers for the monitoring of PPB-patients. This includes treatment, surveillance, but also screening of susceptible patients carrying a *DICER1* germline mutation (Murray et al. 2014). Biomarkers may help to reduce x-ray exposure, especially in pediatric patients. Changes in miRNA expression, particularly decreased levels of miRNA have been detected and suggested for diagnosis and treatment for a wide range of other cancers as well (Lu et al. 2007, Gaur et al. 2007).

As discussed in section 4.3.1, DICER1 tumor cells might have a stronger dependence on 3p arms, compared to normal cells. If this is the case, a possible therapy could work through an anti-3p mechanism. This would cause a decrease in 3p arms and therefore a shift in environment within the cell, which could be unfavorable for the tumor cells (Pugh et al. 2014).

5 Summary

The pleuropulmonary blastoma is a very rare malignancy of childhood, but is still the most common pediatric lung tumor. It is an aggressive neoplasm and part of the newly discovered *DICER1*-Syndrome. This syndrome is characterized by mutations in the *DICER1* gene and a wide variety of clinical phenotypes. In this thesis, molecular genetic examinations of the so far largest German patient collective were performed. The methods used, included PCR, Sanger sequencing, multiplex ligation-dependent probe amplification and OncoScan® (the latter not part of this thesis).

In six patients, a total number of nine mutations and a large deletion spanning the entire *DICER1* gene locus were detected. Of the nine mutations, four had not been described in the literature. It was determined, that splice site mutation c.1510-1G>A of patient 18 and the large *DICER1* gene deletion of patient 12 were de novo germline mutations, predisposing these individuals to the *DICER1*-Syndrome. The deletion was detected by MLPA and could be specified to a size of 582kb by OncoScan®. Such a deletion has only been published once in a patient with PPB before. Five mutations were located on the RNase IIIb domain of *DICER1*. This domain contains hotspot regions for *DICER1*-Syndrome mutations. The distribution of the nine mutations, is in line with the so-called modified two-hit-hypothesis. Here, usually a germline *DICER1* mutation predisposes to a greater risk of disease, which is later induced by somatic mutations. There is a retained function of DICER1, when there are hotspot *DICER1* mutations in PPB. The mutations affect the processing of miRNA strands by DICER1 and are part of RNA interference (RNAi). A new equilibrium of the miRNA strands is thought to be a cancerogenous trigger of PPB. The exact mechanisms are not understood so far.

Upon diagnosis of PPB, subsequent PCR and Sanger studies should be performed to look for *DICER1* mutations. In germline negative cases, a screening for mosaicism and biallelic somatic mutations should follow. Analysis for copy-number-variations by MLPA can be added, when no germline mutation was found. However, the routine use of MLPA is hindered, since currently no commercial *DICER1*-kit is available and the use of synthetic oligonucleotides is required. A thorough patient and extended family history, with a focus of known *DICER1*-Syndrome phenotypes should be taken. Because of the autosomal-dominant pattern, the risk of inheritance to later generations is increased.

Depending on the type of mutation, the risk of further disease is also increased. These aspects should be addressed in a genetic counseling of the patient and family.

An enrollment in the International PPB Registry is strongly recommend, when a *DICER1*-Syndrome is suspected or confirmed, to help advancing disease-specific research and to be able to profit from latest studies regarding screening and therapy.

6 German summary

Das Pleuropulmoblastom (PPB) ist ein insgesamt sehr seltener, aber dennoch der häufigste pädiatrische Lungentumor. Dieser aggressive Tumor ist eine mögliche Ausprägungsform des kürzlich beschriebenen *DICER1*-Syndroms, welches noch eine Vielzahl anderer Phänotypen hervorrufen kann. In dieser Arbeit wurde das bisher größte deutsche PPB-Patientenkollektiv molekulargenetisch mittels PCR, Sanger Sequenzierung, Multiplex ligation-dependent probe amplification sowie OncoScan® (letzteres war nicht Teil dieser Arbeit) untersucht.

Insgesamt wurden bei sechs Patienten neun Mutationen sowie eine große Deletion, die den Genlokus des *DICER1* Gens umfasst, identifiziert. Vier der neun Mutationen wurden bisher nicht in der Literatur beschrieben. Die Deletion wurde mittels MLPA detektiert und zeigte im OncoScan® eine Größe von 582kb. Eine *DICER1* umfassende Deletion wurde bisher erst bei einem weiteren PPB-Patienten beschrieben. Sowohl die Splicevariante c.1510-1G>A von Patient 18 als auch die Deletion von Patient 12 stellen de novo Keimbahnmutationen dar, welche diese Patienten zum *DICER1*-Syndrom prädisponieren. Fünf Mutationen waren in der RNase IIIb Domäne von *DICER1* lokalisiert. In dieser Domäne finden sich *hotspot regions* für *DICER1*-Syndrom Mutationen. Die in dieser Arbeit gefundenen neun Mutationen passen zum Verteilungsmuster der sogenannten modifizierten 2-Treffer-Hypothese. Dabei haben die Betroffenen eine Keimbahnmutation sowie eine im Verlauf erworbene somatische Mutation, die oft die RNase IIIb Domäne betrifft, und zu keinem vollständigen Funktionsverlust von DICER1 führt. Die Mutationen beeinflussen die miRNA-Biosynthese, die Teil der RNA-Interferenz (RNAi) ist. Möglicherweise entsteht ein neues Gleichgewicht verschiedener miRNA-Stränge, die letztlich für die Entstehung des PPB mitverantwortlich sind. Hierbei sind jedoch noch nicht alle Aspekte abschließend erforscht.

Im Falle einer PPB-Diagnose sollten weitere molekulargenetische Untersuchungen mit PCR und Sanger Sequenzierungen in Hinblick auf *DICER1*-Mutationen erfolgen. Falls sich keine Keimbahnmutation findet, sollten Untersuchungen auf Mosaike und biallelische somatische Variationen angeschlossen werden. Mittels MLPA können Deletionen sowie Duplikationen festgestellt werden. Allerdings gibt es kein kommerziell

erwerbbares *DICER1*-kit, so dass synthetische Oligonukleotide verwendet werden müssen. Ferner sollte eine ausführliche Patienten- und Familienanamnese in Hinblick auf bekannte *DICER1*-Syndrom-Phänotypen erfolgen. Aufgrund des autosomal-dominanten Vererbungsmusters ist das Risiko für Folgegenerationen erhöht, allerdings ist die Penetranz reduziert. Je nach genetischer Konstellation besteht ein Risiko für weitere Erkrankungen aus dem *DICER1*-Spektrum. Diese Aspekte sollten den Betroffenen im Rahmen einer genetischen Beratung erläutert werden.

Alle Patienten mit einem vermuteten oder gesicherten *DICER1*-Syndrom, sollten beim *International PPB Registry* angebunden werden. Die dort gesammelten Daten sind sowohl elementar für die weitere Erforschung dieses seltenen Syndroms, als auch für die dazugehörige Diagnostik und Therapie.

7 Literature

Adzhubei IA, Schmidt S, Peshkin L, Ramensky VE, Gerasimova A, Bork P, Kondrashov AS, Sunyaev SR (2010) A method and server for predicting damaging missense mutations. Nat Methods 7(4):248-249.

Adzick NS (2003) Management of fetal lung lesions. Clin Perinatol. 30(3):481-92.

Alvarez-Garcia I, Miska EA (2005) MicroRNA functions in animal development and human disease. Development. 132(21):4653-62.

Anglesio MS, Wang Y, Yang W, Senz J, Wan A, Heravi-Moussavi A, Salamanca C, Maines-Bandiera S, Huntsman DG, Morin GB (2013) Cancer-associated somatic *DICER1* hotspot mutations cause defective miRNA processing and reverse-strand expression bias to predominantly mature 3p strands through loss of 5p strand cleavage. J Pathol. 229(3):400-9.

Bahubeshi A, Bal N, Rio Frio T, Hamel N, Pouchet C, Yilmaz A, Bouron-Dal Soglio D, Williams GM, Tischkowitz M, Priest JR, Foulkes WD (2010) Germline *DICER1* mutations and familial cystic nephroma. J Med Genet. 47(12):863-6.

Bahubeshi A, Tischkowitz M, Foulkes WD (2011) miRNA processing and human cancer: *DICER1* cuts the mustard. Sci Transl Med. 3(111):111ps46.

Bailey S, Raby KL, Coleman N, Murray MJ (2014) Serum microRNA screening for *DICER1*-associated pleuropulmonary blastoma. Pediatr Blood Cancer. 61(12):2329-30.

Bartel DP (2009) MicroRNAs: target recognition and regulatory functions. Cell. 136(2):215-33.

Bernstein E, Caudy AA, Hammond SM, Hannon GJ (2001) Role for a bidentate ribonuclease in the initiation step of RNA interference. Nature. 409(6818):363-6.

Bernstein E, Kim SY, Carmell MA, Murchison EP, Alcorn H, Li MZ, Mills AA, Elledge SJ, Anderson KV, Hannon GJ (2003) Dicer is essential for mouse development. Nat Genet. 35(3):215-7.

Bohnsack MT, Czaplinski K, Gorlich D (2004) Exportin 5 is a RanGTP-dependent dsRNA-binding protein that mediates nuclear export of pre-miRNAs. RNA. 10(2):185-91.

Boman F, Hill DA, Williams GM, Chauvenet A, Fournet JC, Soglio DB, Messinger Y, Priest JR (2006) Familial association of pleuropulmonary blastoma with cystic nephroma and other renal tumors: a report from the International Pleuropulmonary Blastoma Registry. J Pediatr. 149(6):850-854.

Brenneman M, Field A, Yang J, Williams G, Doros L, Rossi C, Schultz KA, Rosenberg A, Ivanovich J, Turner J, Gordish-Dressman H2, Stewart D10, Yu W, Harris A, Schoettler P, Goodfellow P, Dehner L, Messinger Y, Hill DA (2015, revised 2018) Temporal order of RNase IIIb and loss-of-function mutations during development determines phenotype in pleuropulmonary blastoma / *DICER1* syndrome: a unique variant of the two-hit tumor suppression model. F1000Res. 4:214.

Carthew RW (2006) Gene regulation by microRNAs. Curr Opin Genet Dev. 16(2):203-8.

Chiosea S, Jelezcova E, Chandran U, Luo J, Mantha G, Sobol RW, Dacic S (2007) Overexpression of Dicer in precursor lesions of lung adenocarcinoma. Cancer Res. 67(5):2345-50.

Delahunt B, Thomson KJ, Ferguson AF, Neale TJ, Meffan PJ, Nacey JN (1993) Familial cystic nephroma and pleuropulmonary blastoma. Cancer. 71(4):1338-42.

de Kock L, Sabbaghian, Druker, Weber, Hamel, Miller, Choong, Gottardo, Kees, Rednam, van Hest, Jongmans, Jhangiani, Lupski, Zacharin, Bouron-Dal Soglio, Huang, Priest, Perry, Mueller, Albrecht, Malkin, Grundy, Foulkes (2014) Germ-line and somatic *DICER1* mutations in pineoblastoma. Acta Neuropathol. 128(4): 583–595.

de Kock L, Geoffrion D, Rivera B, Wagener R, Sabbaghian N, Bens S, Ellezam B, Bouron-Dal Soglio D, Ordóñez J, Sacharow S, Polo Nieto JF, Guillerman RP, Vujanic GM, Priest JR, Siebert R, Foulkes WD (2018) Multiple *DICER1*-related tumors in a child with a large interstitial 14q32 deletion. Genes Chromosomes Cancer. 57(5):223-230.

Desmet FO, Hamroun D, Lalande M, Collod-Beroud G, Claustres M, Beroud C. Human Splicing Finder: an online bioinformatics tool to predict splicing signals. Nucleic Acid Research, 2009.

Dishop MK, McKay EM, Kreiger PA, Priest JR, Williams GM, Langston C, Jarzembowski J, Suchi M, Dehner LP, Hill DA (2010) Fetal lung interstitial tumor (FLIT): A proposed newly recognized lung tumor of infancy to be differentiated from cystic pleuropulmonary blastoma and other developmental pulmonary lesions. Am J Surg Pathol. 34(12):1762-72.

Doros LA, Rossi CT, Yang J, Field A, Williams GM, Messinger Y, Cajaiba MM, Perlman EJ, A Schultz K, Cathro HP, Legallo RD, LaFortune KA, Chikwava KR, Faria P, Geller JI, Dome JS, Mullen EA, Gratias EJ, Dehner LP, Hill DA (2014) *DICER1* mutations in childhood cystic nephroma and its relationship to *DICER1*-renal sarcoma. Mod Pathol. 27(9):1267-80.

Ferrari A, Bisogno G, De Salvo GL, Indolfi P, Perilongo G, Cecchetto G; Italian Study on Rare Tumours in Paediatric Age (TREP); Associazione Italiana Ematologia Oncologia Pediatrica (AIEOP) (2007) The challenge of very rare tumours in childhood: the Italian TREP project. Eur J Cancer. 43(4):654-9.

Filipowicz W, Bhattacharyya SN, Sonenberg N (2008) Mechanisms of post-transcriptional regulation by microRNAs: are the answers in sight?. Nat Rev Genet. Feb;9(2):102-14.

Foulkes WD, Bahubeshi A, Hamel N, Pasini B, Asioli S, Baynam G, Choong CS, Charles A, Frieder RP, Dishop MK, Graf N, Ekim M, Bouron-Dal Soglio D, Arseneau J, Young RH, Sabbaghian N, Srivastava A, Tischkowitz MD, Priest JR (2011). Extending the phenotypes associated with *DICER1* mutations. Hum Mutat. 32(12):1381-4.

Foulkes WD, Priest JR, Duchaine TF (2014) *DICER1*: mutations, microRNAs and mechanisms. Nat Rev Cancer. 14(10):662-72.

Fraire, A.E., Cagle, P.T., Irwin, R.S., Mody, D.R., Ernst, A., Blackmon, S.H., Allen, T.C., Dishop, M.K. (2010) Atlas of Neoplastic Pulmonary Disease, Springer, 7 - 12.

Francia S, Michelini F, Saxena A, Tang D, de Hoon M, Anelli V, Mione M, Carninci P, d'Adda di Fagagna F (2012) Site-specific DICER and DROSHA RNA products control the DNA-damage response. Nature. 488(7410):231-5.

Friedman RC, Farh KK, Burge CB, Bartel DP (2009) Most mammalian mRNAs are conserved targets of microRNAs. Genome Res. 19(1):92-105.

Gaur A, Jewell DA, Liang Y, Ridzon D, Moore JH, Chen C, Ambros VR, Israel MA (2007) Characterization of microRNA expression levels and their biological correlates in human cancer cell lines. Cancer Res. 67(6):2456-68.

Gurtan AM, Lu V, Bhutkar A, Sharp PA (2012) In vivo structure-function analysis of human Dicer reveals directional processing of precursor miRNAs. RNA. 18(6):1116-22.

Harris KS, Zhang Z, McManus MT, Harfe BD, Sun X (2006) Dicer function is essential for lung epithelium morphogenesis. Proc Natl Acad Sci U S A. 103(7):2208-13.

Heravi-Moussavi A, Anglesio MS, Cheng SW, Senz J, Yang W, Prentice L, Fejes AP, Chow C, Tone A, Kalloger SE, Hamel N, Roth A, Ha G, Wan AN, Maines-Bandiera S, Salamanca C, Pasini B, Clarke BA, Lee AF, Lee CH, Zhao C, Young RH, Aparicio SA, Sorensen PH, Woo MM, Boyd N, Jones SJ, Hirst M, Marra MA, Gilks B, Shah SP, Foulkes WD, Morin GB, Huntsman DG (2012) Recurrent somatic *DICER1* mutations in nonepithelial ovarian cancers. N Engl J Med. 366(3):234-42.

Hill DA, Sadeghi S, Schultz MZ, Burr JS, Dehner LP (1999) Pleuropulmonary blastoma in an adult: an initial case report. Cancer. 85(11):2368-74.

Hill DA, Dehner LP (2004) A cautionary note about congenital cystic adenomatoid malformation (CCAM) type 4. Am J Surg Pathol. 28(4):554-5.

Hill DA, Jarzembowski JA, Priest JR, Williams G, Schoettler P, Dehner LP (2008) Type I pleuropulmonary blastoma: pathology and biology study of 51 cases from the international pleuropulmonary blastoma registry. Am J Surg Pathol. 32(2):282-95.

Hill DA, Ivanovich J, Priest JR, Gurnett CA, Dehner LP, Desruisseau D, Jarzembowski JA, Wikenheiser-Brokamp KA, Suarez BK, Whelan AJ, Williams G, Bracamontes D, Messinger Y, Goodfellow PJ (2009) *DICER1* mutations in familial pleuropulmonary blastoma. Science. 325(5943):965.

Hogervorst FB , Nederlof PM, Gille JJ, McElgunn CJ, Grippeling M, Pruntel R, Regnerus R, van Welsem T, van Spaendonk R, Menko FH, Kluijt I, Dommering C, Verhoef S, Schouten JP, van't Veer LJ, Pals G (2003) Large genomic deletions and duplications in the BRCA1 gene identified by a novel quantitative method. Cancer Res. 63(7):1449-53.

Jakymiw A, Patel RS, Deming N, Bhattacharyya I, Shah P, Lamont RJ, Stewart CM, Cohen DM, Chan EK (2010) Overexpression of dicer as a result of reduced let-7 MicroRNA levels contributes to increased cell proliferation of oral cancer cells. Genes Chromosomes Cancer. 49(6):549-59.

Karube Y, Tanaka H, Osada H, Tomida S, Tatematsu Y, Yanagisawa K, Yatabe Y, Takamizawa J, Miyoshi S, Mitsudomi T, Takahashi T (2005) Reduced expression of Dicer associated with poor prognosis in lung cancer patients. Cancer Sci. 96(2):111-5.

Khan AA, El-Borai AK, Alnoaiji M (2014) Pleuropulmonary blastoma: a case report and review of the literature. Case Rep Pathol. 2014:509086.

Klein S, Lee H, Ghahremani S, Kempert P, Ischander M, Teitell MA, Nelson SF, Martinez-Agosto JA (2014) Expanding the phenotype of mutations in *DICER1*: mosaic missense mutations in the RNase IIIb domain of DICER1 cause GLOW syndrome. J Med Genet. 51(5):294-302.

Kim J, Coffey DM, Creighton CJ, Yu Z, Hawkins SM, Matzuk MM (2012) High-grade serous ovarian cancer arises from fallopian tube in a mouse model. Proc Natl Acad Sci U S A. 109(10):3921-6.

Knudson AG Jr. (1971) Mutation and cancer: statistical study of retinoblastoma. Proc Natl Acad Sci U S A. 68(4):820-3.

Koenigsmann J, Rudolph C, Sander S, Kershaw O, Gruber AD, Bullinger L, Schlegelberger B, Carstanjen D (2009) Nf1 haploinsufficiency and Icsbp deficiency synergize in the development of leukemias. Blood. 113(19):4690-701.

Kumar MS, Pester RE, Chen CY, Lane K, Chin C, Lu J, Kirsch DG, Golub TR, Jacks T (2009) *Dicer1* functions as a haploinsufficient tumor suppressor. Genes & Development. 23(23):2700-4.

Lau PW, Guiley KZ, De N, Potter CS, Carragher B, MacRae IJ (2012) The molecular architecture of human Dicer. Nat Struct Mol Biol. 19(4):436-40.

Lambertz I, Nittner D, Mestdagh P, Denecker G, Vandesompele J, Dyer MA, Marine JC (2010) Monoallelic but not biallelic loss of *Dicer1* promotes tumorigenesis in vivo. Cell Death Differ. (4):633-41.

Lee YS, Nakahara K, Pham JW, Kim K, He Z, Sontheimer EJ, Carthew RW (2004) Distinct roles for Drosophila Dicer-1 and Dicer-2 in the siRNA/miRNA silencing pathways. Cell. 117(1):69-81.

Lu J, Getz G, Miska EA, Alvarez-Saavedra E, Lamb J, Peck D, Sweet-Cordero A, Ebert BL, Mak RH, Ferrando AA, Downing JR, Jacks T, Horvitz HR, Golub TR (2005) MicroRNA expression profiles classify human cancers. Nature. 435(7043):834-8.

Lujambio A, Lowe SW (2012) The microcosmos of cancer. Nature. 482(7385):347-55.

MacSweeney F, Papagiannopoulos K, Goldstraw P, Sheppard MN, Corrin B, Nicholson AG (2003) An assessment of the expanded classification of congenital cystic adenomatoid malformations and their relationship to malignant transformation. Am J Surg Pathol. 27(8):1139-46.

Maniataki E, Mourelatos Z (2005) A human, ATP-independent, RISC assembly machine fueled by pre-miRNA. Genes Dev. 19(24):2979-90.

Manivel JC, Priest JR, Watterson J, Steiner M, Woods WG, Wick MR, Dehner LP (1988) Pleuropulmonary blastoma. The so-called pulmonary blastoma of childhood. Cancer. 62(8):1516-26.

Martin MG, Payton JE, Link DC (2009) Dicer and outcomes in patients with acute myeloid leukemia (AML). Leuk Res. 33(8):e127.

McNerney ME, Brown CD, Wang X, Bartom ET, Karmakar S, Bandlamudi C, Yu S, Ko J, Sandall BP, Stricker T, Anastasi J, Grossman RL, Cunningham JM, Le Beau MM, White KP (2013) CUX1 is a haploinsufficient tumor suppressor gene on chromosome 7 frequently inactivated in acute myeloid leukemia. Blood. 121(6):975-83.

Melo SA, Ropero S, Moutinho C, Aaltonen LA, Yamamoto H, Calin GA, Rossi S, Fernandez AF, Carneiro F, Oliveira C, Ferreira B, Liu CG, Villanueva A, Capella G, Schwartz S Jr, Shiekhattar R, Esteller M (2009) A TARBP2 mutation in human cancer impairs microRNA processing and DICER1 function. Nat Genet. 41(3):365-70.

Merritt WM, Lin YG, Han LY, Kamat AA, Spannuth WA, Schmandt R, Urbauer D, Pennacchio LA, Cheng JF, Nick AM, Deavers MT, Mourad-Zeidan A, Wang H, Mueller P, Lenburg ME, Gray JW, Mok S, Birrer MJ, Lopez-Berestein G, Coleman RL, Bar-Eli M, Sood AK Dicer, (2008) Drosha, and outcomes in patients with ovarian cancer. N Engl J Med. 359(25):2641-50.

Messinger YH, Stewart DR, Priest JR, Williams GM, Harris AK, Schultz Yang J, Doros L., Rosenberg PS, Hill DA, Dehner LP (2015) Pleuropulmonary Blastoma: A Report on 350 Central Pathology–Confirmed Pleuropulmonary Blastoma Cases by the International Pleuropulmonary Blastoma Registry. Cancer. 121(2): 276–285.

Miller SA, Dykes DD, Polesky HF (1988) A simple salting out procedure for extracting DNA from human nucleated cells. Nucleic Acids Res. 16(3):1215.

Miniati DN, Chintagumpala M, Langston C, Dishop MK, Olutoye OO, Nuchtern JG, Cass DL (2006) Prenatal presentation and outcome of children with pleuropulmonary blastoma. J Pediatr Surg. 41(1):66-71.

Murray MJ, Bailey S, Raby KL, Saini HK, de Kock L, Burke GA, Foulkes WD, Enright AJ, Coleman N, Tischkowitz M (2014) Serum levels of mature microRNAs in *DICER1*-mutated pleuropulmonary blastoma. Oncogenesis. 3:e87.

Priest JR, Watterson J, Strong L, Huff V, Woods WG, Byrd RL, Friend SH, Newsham I, Amylon MD, Pappo A, Mahoney DH, Langston C, Heyn R, Kohut G, Freyer DR, Bostrom B, Richardson MS, Barredo J, Dehner LP (1996) Pleuropulmonary blastoma: a marker for familial disease. J Pediatr. 128(2):220-4.

Priest JR, McDermott MB, Bhatia S, Watterson J, Manivel JC, Dehner LP (1997) Pleuropulmonary blastoma: a clinicopathologic study of 50 cases. Cancer. 80(1):147-61.

Priest JR, Magnuson J, Williams GM, Abromowitch M, Byrd R, Sprinz P, Finkelstein M, Moertel CL, Hill DA (2007) Cerebral metastasis and other central nervous system complications of pleuropulmonary blastoma. Pediatr Blood Cancer. 49(3):266-73.

Priest JR, Williams GM, Hill DA, Dehner LP, Jaffé A (2009) Pulmonary cysts in early childhood and the risk of malignancy. Pediatr Pulmonol. 44(1):14-30.

Pugh TJ, Yu W, Yang J, Field AL, Ambrogio L, Carter SL, Cibulskis K, Giannikopoulos P, Kiezun A, Kim J, McKenna A, Nickerson E, Getz G, Hoffher S, Messinger YH, Dehner LP, Roberts CW, Rodriguez-Galindo C, Williams GM, Rossi CT, Meyerson M, Hill DA (2014) Exome sequencing of pleuropulmonary blastoma reveals frequent biallelic loss of TP53 and two hits in *DICER1* resulting in retention of 5p-derived miRNA hairpin loop sequences. Oncogene. 33(45):5295-302.

Rassow, Heuser, Netzker, Deutzmann, Duale Reihe Biochemie (2012) 3rd edition, Georg Thieme.

Rio Frio T, Bahubeshi A, Kanellopoulou C, Hamel N, Niedziela M, Sabbaghian N, Pouchet C, Gilbert L, O'Brien PK, Serfas K, Broderick P, Houlston RS, Lesueur F, Bonora E, Muljo S, Schimke RN, Bouron-Dal Soglio D, Arseneau J, Schultz KA, Priest JR, Nguyen VH, Harach HR, Livingston DM, Foulkes WD, Tischkowitz M (2011) *DICER1* mutations in familial multinodular goiter with and without ovarian Sertoli-Leydig cell tumors. JAMA. 305(1):68-77.

Sabbaghian N, Hamel N, Srivastava A, Albrecht S, Priest JR, Foulkes WD (2012) Germline *DICER1* mutation and associated loss of heterozygosity in a pineoblastoma. J Med Genet. 49(7):417-9.

Sabbaghian N, Bahubeshi A, Shuen AY, Kanetsky PA, Tischkowitz MD, Nathanson KL, Foulkes WD (2013) Germ-line *DICER1* mutations do not make a major contribution to the etiology of familial testicular germ cell tumours. BMC Res Notes. 6:127.

Sabbaghian N, Srivastava A, Hamel N, Plourde F, Gajtko-Metera M, Niedziela M, Foulkes WD (2014) Germ-line deletion in *DICER1* revealed by a novel MLPA assay using synthetic oligonucleotides. Eur J Hum Genet. 22(4):564-7.

Sanger F, Nicklen S, Coulson AR (1977) DNA sequencing with chain-terminating inhibitors. Proc Natl Acad Sci U S A. 74(12):5463-7.

Saxena A, Tabin CJ (2010) miRNA-processing enzyme Dicer is necessary for cardiac outflow tract alignment and chamber septation. Proc Natl Acad Sci U S A. 107(1):87-91.

Schaaf, Zschocke, Basiswissen Humangenetik (2013) 2nd edition, Springer.

Seki M, Yoshida K, Shiraishi Y, Shimamura T, Sato Y, Nishimura R, Okuno Y, Chiba K, Tanaka H, Kato K, Kato M, Hanada R, Nomura Y, Park MJ, Ishida T, Oka A, Igarashi T, Miyano S, Hayashi Y, Ogawa S, Takita J (2014) Biallelic *DICER1* mutations in sporadic pleuropulmonary blastoma. Cancer Res. 74(10):2742-9.

Schouten JP, McElgunn CJ, Waaijer R, Zwijnenburg D, Diepvens F, Pals G (2002) Relative quantification of 40 nucleic acid sequences by multiplex ligation-dependant probe amplification. Nucleic Acids Res. 30(12):e57.

Schultz KA, Yang J, Doros L, Williams GM, Harris A, Stewart DR, Messinger Y, Field A, Dehner LP, Hill DA (2014) *DICER1*-pleuropulmonary blastoma familial tumor predisposition syndrome: a unique constellation of neoplastic conditions. Pathol Case Rev. 19(2):90-100.

Schultz KA, Harris A, Williams GM, Baldinger S, Doros L, Valusek P, Frazier AL, Dehner LP, Messinger Y, Hill DA (2014) Reply: Serum microRNA screening for *DICER1*-associated pleuropulmonary blastoma. Pediatr Blood Cancer. 61(12):2331-2.

Schultz KAP, Williams GM, Kamihara J, Stewart DR, Harris AK, Bauer AJ, Turner J, Shah R, Schneider K, Schneider KW, Carr AG, Harney LA, Baldinger S, Frazier AL, Orbach D, Schneider DT, Malkin D, Dehner LP, Messinger YH, Hill DA (2018) *DICER1* and Associated Conditions: Identification of At-risk Individuals and Recommended Surveillance Strategies. Clin Cancer Res. 24(10):2251-2261.

Slade I, Bacchelli C, Davies H, Murray A, Abbaszadeh F, Hanks S, Barfoot R, Burke A, Chisholm J, Hewitt M, Jenkinson H, King D, Morland B, Pizer B, Prescott K, Saggar A, Side L, Traunecker H, Vaidya S, Ward P, Futreal PA, Vujanic G, Nicholson AG, Sebire N, Turnbull C, Priest JR, Pritchard-Jones K, Houlston R, Stiller C, Stratton MR, Douglas J, Rahman N (2011) *DICER1* syndrome: clarifying the diagnosis, clinical features and

management implications of a pleiotropic tumour predisposition syndrome. J Med Genet. (4):273-8.

Stamatiou K, Polizois K, Kollaitis G, Dahanis S, Zafeiropoulos G, Leventis C, Lambou T (2008) Cystic nephroma: a case report and review of the literature. Cases J. 1(1):267.

Stewart DR, Messinger Y, Williams GM, Yang J, Field A, Schultz KA, Harney LA, Doros LA, Dehner LP, Hill DA (2014) Nasal chondromesenchymal hamartomas arise secondary to germline and somatic mutations of *DICER1* in the pleuropulmonary blastoma tumor predisposition disorder. Hum Genet. 133(11):1443-50.

Stuppia L, Antonucci I, Palka G, Gatta V (2012) Use of the MLPA assay in the molecular diagnosis of gene copy number alterations in human genetic diseases. Int J Mol Sci. (3):3245-76.

Suzuki HI, Yamagata K, Sugimoto K, Iwamoto T, Kato S, Miyazono K (2009) Modulation of microRNA processing by p53. Nature. 460(7254):529-33.

Takeshita D, Zenno S, Lee WC, Nagata K, Saigo K, Tanokura M (2007) Homodimeric structure and double-stranded RNA cleavage activity of the C-terminal RNase III domain of human dicer. J Mol Biol. 374(1):106-20.

Tang KF, Ren H (2012) The role of dicer in DNA damage repair. Int J Mol Sci. 13(12):16769-78.

Tokumaru S, Suzuki M, Yamada H, Nagino M, Takahashi T (2008) let-7 regulates Dicer expression and constitutes a negative feedback loop. Carcinogenesis. 29(11):2073-7.

Torrezan GT, Ferreira EN, Nakahata AM, Barros BD, Castro MT, Correa BR, Krepischi AC, Olivieri EH, Cunha IW, Tabori U, Grundy PE, Costa CM, de Camargo B, Galante PA, Carraro DM (2014) Recurrent somatic mutation in DROSHA induces microRNA profile changes in Wilms tumour. Nat Commun. 5:4039.

Vogelstein B, Papadopoulos N, Velculescu VE, Zhou S, Diaz LA Jr, Kinzler KW (2013) Cancer genome landscapes. Science. 339(6127):1546-58.

Wang HW, Noland C, Siridechadilok B, Taylor DW, Ma E, Felderer K, Doudna JA, Nogales E (2009) Structural insights into RNA processing by the human RISC-loading complex. Nat Struct Mol Biol. 16(11):1148-53.

Wang X, Zhao J, Huang J, Tang H, Yu S, Chen Y (2012) The regulatory roles of miRNA and methylation on oncogene and tumor suppressor gene expression in pancreatic cancer cells. Biochem Biophys Res Commun. 425(1):51-7.

Wei W, Ba Z, Gao M, Wu Y, Ma Y, Amiard S, White CI, Rendtlew Danielsen JM, Yang YG, Qi Y (2012) A role for small RNAs in DNA double-strand break repair. Cell. 149(1):101-12.

Wienholds E, Koudijs MJ, van Eeden FJ, Cuppen E, Plasterk RH (2003). The microRNA-producing enzyme *Dicer1* is essential for zebrafish development. Nat Genet. 35(3):217-8.

Wilson RC, Doudna JA (2013) Molecular mechanisms of RNA interference. Annu Rev Biophys. 42:217-39.

Wu MK, Sabbaghian N, Xu B, Addidou-Kalucki S, Bernard C, Zou D, Reeve AE, Eccles MR, Cole C, Choong CS, Charles A, Tan TY, Iglesias DM, Goodyer PR, Foulkes WD (2013) Biallelic *DICER1* mutations occur in Wilms tumours. J Pathol. 230(2):154-64.

Yi R, Qin Y, Macara IG, Cullen BR (2003) Exportin-5 mediates the nuclear export of pre-microRNAs and short hairpin RNAs. Genes Dev. 17(24):3011-6.

Zhang H, Kolb FA, Jaskiewicz L, Westhof E, Filipowicz W (2004) Single processing center models for human Dicer and bacterial RNase III. Cell. 118(1):57-68.

Zhang B, Chen H, Zhang L, Dakhova O, Zhang Y, Lewis MT, Creighton CJ, Ittmann MM, Xin L (2014) A dosage-dependent pleiotropic role of Dicer in prostate cancer growth and metastasis. Oncogene. 33(24):3099-108.

Websites:

https://www.ppbregistry.org/ - The International Pulmonary Blastoma/DICER1 Registry

https://www.omim.org/ - Online Mendelian Inheritance in Man (OMIM)

https://www.amboss.com/de - Amboss

http://www.lovd.nl/2.0/ - Leiden Open Variation Database

http://www.ensembl.org – Genome Browser

https://blast.ncbi.nlm.nih.gov/Blast.cgi - BLAST - Basic Local Alignment Search Tool (NCBI National Center for Biotechnology Information, Bethesda, USA)

http://www.internationalgenome.org - 1000 Genomes Project

http://www.cancergenome.nih.gov - Cancer Genome Atlas consortium

https://cancer.sanger.ac.uk/cosmic - COSMIC, Catalogue of Somatic Mutations in Cancer

8 Appendix

8.1 Devices and materials

Device, material, procedure	Type	Manufacturer	Location
Agarose	1,2%	Biozym Scientific GmbH	Hessisch Oldendorf, Germany
Caps	Domed Cap Strips	Sarstedt	Nümbrecht, Germany
Centrifuge	Hettich EBA 12R, Rotana 96R	Andreas Hettich GmbH & Co.KG	Tuttlingen, Germany
Direct Blood PCR	Phusion Blood Direct PCR Kit	Thermo Fisher Scientific	Massachusetts, USA
Distilled Water	Aqua ad iniectabilia	B.Braun	Melsungen, Germany
DNA extraction	QIAamp DNA Blood Mini Kit	Qiagen	Hilden, Germany
DNA gel extraction	Ultrafree-DA centrifuge unit	Merck, Millipore	Massachusetts, United States
DNA measurement	Qubit® 2.0 Fluorometer	Invitrogen, Thermo Fisher	Waltham, Massachusetts, United States
DNA measurement	Qubit® dsDNA BR Assay Kit	life technologies	Oregon, USA
DNA purification	Cycle-pure Kit	VWR peqlab	Pennsylvania, USA
DNA sizing	GeneRuler DNA Ladder Mix	Thermo Fisher Scientific	Massachusetts, USA
Ethanol	96 – 100%	Merck, Millipore	Massachusetts, United States
Ethidium bromide	0.1 µl/ml	Sigma-Aldrich	Missouri, USA

Gel Documentation Imaging	E-Box VX2	Vilber Lourmat Deutschland GmbH	Eberhardzell, Germany
Migration chamber with microtiter combs	PerfectBlue™ Wide Format Gel System Maxi ExW	Peqlab	Erlangen, Germany
MLPA	SALSA MLPA kit	MRC Holland	Amsterdam, Netherlands
$MgCl^2$		Thermo Fisher Scientific	Massachusetts, USA
Nucleus acid staining	Roti®-Safe-GelStain	Carl Roth GmbH	Karlsruhe, Germany
Oligonucleotides	PCR primer	Metabion international AG	Planegg/Steinkirchen, Germany
Oligonucleotides	MLPA probes	Integrated DNA Technologies	Iowa, United States
PCR	DreamTaq Green PCR Master Mix	Thermo Fisher Scientific	Massachusetts, USA
PCR	GoTaq® G2 Green Master Mix	Promega	Wisconsin, USA
Pipettes		Gilson	Ohio, United States
Pipette tips	Biosphere Filter tips 10µl, 100µl, 200µl, 1250µl type Eppendorf/Gilson	Sarstedt	Nümbrecht, Germany
Purification	DyeEx 96 Kit	Merck Millipore	Massachusetts, United States
Restriction digestion	Exonuclease I	Thermo Scientific	Massachusetts, USA

Restriction digestion	Thermosensitive Alkaline Phosphatase	Thermo Scientific	Massachusetts, USA
Sequencing	BigDye® Terminator V3.1 Ready Reaction Mix	Thermo Scientific	Massachusetts, USA
Sequencing	BigDye® Terminator 5x Sequencing Buffer Mix V1.1	Thermo Scientific	Massachusetts, USA
Sequencing tubes	PCR-Ketten/Multiply®	Sarstedt	Nümbrecht, Germany
Sequencer	ABI-Prism 3130 Genetic Analyzer	Applied Biosystems	California, United States
Thermal cycler	TGradient T1 Thermoblock	Biometra	Göttingen, Germany
Tris Acetate-EDTA-Buffer	1x	life technologies	Oregon, USA
Tumor purification and preparation	QIAamp® DNA FFPE Tissue Kit and Deparaffinization Solution	Qiagen	Hilden, Germany
UV-Transilluminator	60-ECM-20.M	Peqlab	Erlangen, Germany
Thermo Fast 96 PCR Plates	0,2ml Tube Plate 96 Well Multiply®	Sarstedt	Nümbrecht, Germany
Vortex		Heidolph	Schwabach, Germany
Whole Genome Amplification	GenomePlex® Complete Whole Genome Amplification (WGA) Kit	Sigma-Aldrich	Missouri, USA

8.2 Tools and software

Program	**Manufacturer**
Allele ID version 7.7	PREMIER Biosoft, Palo Alto, California, USA
GIMP 2.8 - GNU Image Manipulation Program	Open source
Microsoft Excel 2013	Microsoft
Microsoft Power Point 2013	Microsoft
Microsoft Word 2013	Microsoft
SeqPilot	JSI medical systems GmbH, Ettenheim, Germany
Sequence Scanner Software v2.0	Applied Biosystems, Thermo Fisher Scientific, USA

8.3 Oligonucleotides

8.3.1 DICER1

Exon	Forward primer (sense)	Reverse primer (antisense)	Size
2	TCAAATCCAATTACCCAGCAG	GCAATGAAAGAAACACTGGATG	358
3	TCTGCCAGAAGAGATTAAATGAG	TTTTGTAAATTTATTGGAGGACG	429
4	AAATCAGACAACCAAGGCTACAG	TTTTGGAGGATAACCTTGGAAC	390
5	TTTAATATTCATTCATTCATACACTGC	TTGTCGTCAAGACATGCTTTC	518
6	GAATTCTTACTCTTGCCCATTCC	TAGTGGCATTTCCACCAAAC	437
7	GAGCCGCATTAAGCATATTTTC	CCCACTGCTAACATTCTGGC	395
8	TCACATCACAACACAGGACG	AAATCCCAGTTAAACCCCAC	614
9	AAATCACTCTACAGCTACCTCATGG	TAAATCACCGTCGCCAAATC	820
10	TTCCTATGGATACAAAGAATAACAAAG	CATGTGTGTCAGAAATGACAGTTG	431
11	AACTTTTATTGCTGCACGATACTG	AGCAGGTTACTTTGGAGTACTGAAG	760
12	TGAACATGTAGATGACTACAAAAGC	TCACATTTCAAGTGCTCACC	777
13	AAGTGTTCATGGTGCATGATTC	TTTTACTAGGCAGGACTTTTAAAGATG	585
14	AAGCTGTGAATCGGAGAAAG	TTTGCAGTCCAGCTCATATTG	760
15	TCTAGTGGAGAAATAGAAGAGGCAC	TAAGAAGTGTCATGCCTCGG	468
16, 17	TTTTAGTAGAGACGAGGTTTCACC	GAAAGCATCATTTCTGTTCTGAAG	754
18	TTTGTGTGCAAAGCATCTCC	TGTAAAGGTGCCATTTAGCTTC	589
19	TTTGTGATATATTAATGGGCCAAG	ATTGCACTTGAGGGATTCTTACC	582

20	TCTCACTCCAACTGTTATGGCTTA	TTGGCCCATTAATATATCACA	776
21-1	GAGTACATTCATCGCTGGGC	AATTGCTGTTGCTCTCAGCC	508
21-2	ACTGCAAACCACTTTCAGGC	ACAAGCAGGAAATACCCGTG	501
22	AGAAATTTGCCTCCATCAAA	AAAGCATAGAATATGTGGGAATT	725
23-1	CAGGGCTTCCACACAGTCC	AACCCTTGCTTTTATTGAGTTTC	574
23-2	TACAAGGCCAACACGATGAG	AAACTGTGGTGTTGACACGG	571
24	TGCCGTCAGAACTCTGAAAC	TGTGGGGATAGTGTAAATGCTTC	403
25, 26	TGAACTTTTCCCCTTTGATG	TGGACTGCCTGTAAAAGTGG	450
27	TCTGCCTTCAATTCATTCCA	CCTGTCTGTCGGGGGTATG	448

8.3.2 TP53

Exon	Forward primer (sense)	Reverse primer (antisense)	Size
1	CGGCACCAGGTCGGCGAGAATCCTGACTC	CCCCAGCCCCAGCGATTTTCCCGAGCTG	405
2-4	GGAAGCCGAGCTGTCTCAGACACTGGC	CAGGAAGCCAAAGGGTGAAGAGGAATCCC	858
2-4	Internal sense: GACCTGGAGGGCTGGGGACCTGGAGG		
5-6	GCATGTTTGTTTCTTTGCTGCCGTCTTC	CAGGAGAAAGCCCCCCTACTGCTCACC	558
7-9	GGCCTCCCCTGCTTGCCACAGGTCTCC		
10	CTCAGGTACTGTGTATATAC	CTATGGCTTTCCAACCTAGGA	218
11	CCCGTTGTCCCAGCCTTAGGCCCTTC	GACAAAGCAAATGGAAGTCCTGGGTGC	328

8.3.3 Multiplex Ligation-dependent Probe Amplification - MLPA

Exon	FWD-Primer	LHS	RHS	REV-Primer	Fragment size
I-27	GGGTTCCCTAAGGGTTGGA	GTGGTGTCAGCTTATACATGGGACTCC	TGGCCTGAGAGTGCACACTAAATGC	TCTAGATTGGATCTTGCTGGCAC	**94**
I-2	GGGTTCCCTAAGGGTTGGA	TGCTTCCTCACCAATGGGTCCTTTCTTT	GGACTGCCATGGCAACAAGAAGCAATTC	TCTAGATTGGATCTTGCTGGCAC	**98**
I-21a	GGGTTCCCTAAGGGTTGGA	GTGAACTGCAGAACGTTGCTCAGCGAGTC	CCCTGGTAAGCTCCACGTTGAAGTTTCAGCAGAT	TCTAGATTGGATCTTGCTGGCAC	**105**
I-8	GGGTTCCCTAAGGGTTGGA	CTATCAGACTGTCGTGCCGTATTGGTAGTTCTGG	GACCCTGGTGTGCAGATAAAGTAGCTGGAATGA	TCTAGATTGGATCTTGCTGGCAC	**109**
I-7	GGGTTCCCTAAGGGTTGGA	CACTACTGCAGTATTGATACCTTTTGTTTCTTATGT	TAAAGGTATACTTCTCAGCCATGTGAGATTGTGGT	TCTAGATTGGATCTTGCTGGCAC	**113**
I-20	GGGTTCCCTAAGGGTTGGA	CATCCAATTCCAGCATCACTGTGGAGAAAAGCTGTTTGTCTCC	CCAGCATACTTTATCGCCTTCACTGCCTTTTG	TCTAGATTGGATCTTGCTGGCAC	**117**
I-3	GGGTTCCCTAAGGGTTGGA	CATGTTTCTAGGTTGAACTGCTTGAAGCAGCTCTGGATCAT	AATACCATCGTCTGTTTAAACACTGGCTCAGGGAAGAC	TCTAGATTGGATCTTGCTGGCAC	**121**
I-4	GGGTTCCCTAAGGGTTGGA	CAACAAGTGTCAGCTGTCAGAACTCATTCAGATCTCAAGGTTG	GGGAATACTCAAACCTAGAAGTAAATGCATCTTGGACAAA	TCTAGATTGGATCTTGCTGGCAC	**125**
I-10	GGGTTCCCTAAGGGTTGGA	CAACTTGGTGGTTCGTTTTGATTTGCCCACAGAATATCGATCC	TATGTTCAATCTAAAGGAAGAGCAAGGGCACCCATCTCTAATTA	TCTAGATTGGATCTTGCTGGCAC	**129**

Exon	FWD-Primer	LHS	RHS	REV-Primer	Fragment size
II-11	GGGTTCCCTAAGGGTTGGA	TATGTGTTGAGGCCTGACGATGGTGGT	CCACGAGTCACAATCAACACGGCCATTGG	TCTAGATTGGATCTTGCTGGCAC	**98**
II-14	GGGTTCCCTAAGGGTTGGA	CCAGTGTTCCAGGAAGACCAGGTTCCACGAAA	CGAAGGCAGTGCTACCCAAAAGCAGTTAG	TCTAGATTGGATCTTGCTGGCAC	**103**
II-18	GGGTTCCCTAAGGGTTGGA	GGGGCTTCAGAGATGACACTTGGATTGCACTTG	AGGGATTCTTACCAGACATCACTAGACATGCAGAG	TCTAGATTGGATCTTGCTGGCAC	**110**
II-5	GGGTTCCCTAAGGGTTGGA	GTTACTTATCACTGTCAGACATTAACCTTTTGGTGT	TTGATGAGTGTCATCTTGCAATCCTAGACCACCCCT	TCTAGATTGGATCTTGCTGGCAC	**114**
II-12	GGGTTCCCTAAGGGTTGGA	CTCATCTAGCTCCTAAATGCAGAACCCGAGAGT	TGCCTGATGGTACATTTTATTCAACTCTTTATCTGCCAATTAA	TCTAGATTGGATCTTGCTGGCAC	**118**
II-9	GGGTTCCCTAAGGGTTGGA	CTTATATCAGTAGCAATTTCATAACTGGACATGGCATTGG	GAAGAATCAGCCTCGCAACAAACAGATGGAAGCAGAATTC	TCTAGATTGGATCTTGCTGGCAC	**122**
II-6	GGGTTCCCTAAGGGTTGGA	GTGAAAATTGTCCATCATGTCCTCGCATTTTGGGACTAACT	GCTTCCATTTTAAATGGGAAATGTGATCCAGAGGAATTGGAAG	TCTAGATTGGATCTTGCTGGCAC	**126**
II-21b	GGGTTCCCTAAGGGTTGGA	CAATCCTGGACTTATTCTTCAGGCTTTGACTCTGTCAAACGCT	AGTGATGGATTTAACCTGGAGCGGCTTGAAATGCTTGGCGACTCC	TCTAGATTGGATCTTGCTGGCAC	**130**
II-23a	GGGTTCCCTAAGGGTTGGA	CCTCGTTTCAGACAAAAGACTGCATGCTGGCGAATGGCAAACTGGATG	AGGATTACGAGGAGGAGGATGAGGAGGAGGAGAGCCTGATGTGG	TCTAGATTGGATCTTGCTGGCAC	**134**

Exon	FWD-Primer	LHS	RHS	REV-Primer	Fragment size
III-23b	GGGTTCCCTAAGGGTTGGA	GAACCTTTCAGTGAGCTGTGCTGCTGCTT	CTGTGGCCAGTTCACGCTCTTCTGTATTGA	TCTAGATTGGATCTTGCTGGCAC	101
III-15	GGGTTCCCTAAGGGTTGGA	GCTCTATCCTCCTGAAGATACCACAAGATGC	TTTGGAATACTGACGGCCAAACCCATACCTCA	TCTAGATTGGATCTTGCTGGCAC	105
III-19	GGGTTCCCTAAGGGTTGGA	CCTTTAAGCAGTGCTGAGAAGAGGAAAGCCAAA	TGGGAAAGTCTGCAGAATAAACAGGTAATGAGTT	TCTAGATTGGATCTTGCTGGCAC	109
III-22	GGGTTCCCTAAGGGTTGGA	CTACCCAGCCGCATGGTGGTGTCAATATTTGATCC	CCCTGTGAATTGGCTTCCTCCTGGTTATGTAGTAAAT	TCTAGATTGGATCTTGCTGGCAC	114
III-24	GGGTTCCCTAAGGGTTGGA	CTCAGATTGTTACCAGCGCTTAGAATTCCTGGGAGATG	CGATTTTGGACTACCTCATAACCAAGCACCTTTATGAAG	TCTAGATTGGATCTTGCTGGCAC	119
III-25	GGGTTCCCTAAGGGTTGGA	GATATTTTTGAGTCGCTTGCTGGTGCCATTTACATGGATAGTGG	GATGTCACTGGAGACAGTCTGGCAGGTGTACTATCCCA	TCTAGATTGGATCTTGCTGGCAC	124
III-26	GGGTTCCCTAAGGGTTGGA	CTAATGATTCTGAAAAATATTTACACTGTGGTGTGCTGTTGTCAG	ATTTCTGTTTGTAATCTGATTGACTTCTCTTTTTTCCTTCT	TCTAGATTGGATCTTGCTGGCAC	128
III-16	GGGTTCCCTAAGGGTTGGA	CCACACTTTCCTGTGTACACACGCTCTGGAGAGGTTACCATAT	CCATTGAGTTGAAGAAGTCTGGTTTCATGTTGTCTCTACAAATGCTT	TCTAGATTGGATCTTGCTGGCAC	132
III-17	GGGTTCCCTAAGGGTTGGA	CTTTAAATTCATGGAAGATATTGAGAAGTCTGAAGCTCGCAT	AGGCATTCCCAGTACAAAGTATACAAAAGAAACACCCTTTGTTTTTAAATTA	TCTAGATTGGATCTTGCTGGCAC	136

9 Acknowledgements

I would like to especially thank Florian Oyen for his dedicated and inspiring support during the time in the laboratory of the PHO as well during the years while writing this thesis. Without him, this thesis would not have been the same. Additionally, I would like to express my gratitude towards my advisor, Prof. Dr. rer. nat. Schneppenheim, who gave me the opportunity to gather my first experience with scientific research and to work in his laboratory. I am very grateful for his guidance and support by sharing his tremendous knowledge. It was an honor to work with him and to be able to benefit from his years of experience in the field of science.

Most importantly, I would like to thank my long-lasting girlfriend Katharina Franke for supporting me through all the years of medical studies (including this thesis) and my work in the hospital. You have shown a degree of patience and understanding I have never experienced before. I have already learned more from you than I could have ever hoped for and I continue to look forward to everything that we will do in the future.

10 Curriculum vitae

Der Lebenslauf wurde aus datenschutzrechtlichen Gründen entfernt.

11 Affidavit

Ich versichere ausdrücklich, dass ich die Arbeit selbständig und ohne fremde Hilfe verfasst, andere als die von mir angegebenen Quellen und Hilfsmittel nicht benutzt und die aus den benutzten Werken wörtlich oder inhaltlich entnommenen Stellen einzeln nach Ausgabe (Auflage und Jahr des Erscheinens), Band und Seite des benutzten Werkes kenntlich gemacht habe.

Ferner versichere ich, dass ich die Dissertation bisher nicht einem Fachvertreter an einer anderen Hochschule zur Überprüfung vorgelegt oder mich anderweitig um Zulassung zur Promotion beworben habe.

Ich erkläre mich einverstanden, dass meine Dissertation vom Dekanat der Medizinischen Fakultät mit einer gängigen Software zur Erkennung von Plagiaten überprüft werden kann.

Unterschrift: .....